Development of a Growth Factor Delivery System

Giles T. S. Kirby, BSc(Hons)

Thesis submitted to The University of Nottingham
for the degree of Doctor of Philosophy

March 2014

I don't pretend we have all the answers.
But the questions
are certainly worth thinking about.

–Arthur C. Clarke

Abstract

Bone repair is not always a spontaneous process. In some cases, intervention is required. This can involve the use of autograft but requires donor tissue. As a consequence there is a potential lack of material and donor site morbidity. Current alternatives are limited. There is a need for synthetic alternatives with a similar efficacy to autograft. Growth factors are currently being explored to address this need. A limiting factor to growth factor approaches are safety concerns and high costs. Both these problems stem from the fact that growth factors have short *in vivo* half lives and are administered at supraphysiological levels to maximise the duration of effect. There is a strong need for a growth factor delivery system that can maintain therapeutic doses and restrict administration to a specific location. This is currently limited by the fragile nature of growth factors.

Microparticles were utilised. Microparticles were formed from poly(DL-lactic-co-glycolic acid) with a poly(ethylene glycol) based plasticiser. This provided a method to modulate protein release based on the specific polymer formulation. Protein release was assessed with a model protein. The biological activities of released growth factors were assessed. Microparticles were fabricated for the delivery of vascular endothelial growth factor (VEGF), platelet derived growth factor (PDGF) and bone morphogenetic protein-2 (BMP-2) for release at time points conducive with osteogenic regeneration. A method was developed and validated to combine these microparticles with a suitable scaffold material. These composite scaffolds were developed with the intention of assessing controlled release of growth factors in a bone segmental defect.

A method to fabricate microparticles with consistent size distributions and morphologies was developed. Formulations were tailored such that protein release from microparrticles could be from 2 days to 30 days. The biological activity of the released model protein was verified, as was the biological activity of released BMP-2. A method was devised to combine microparticles with a scaffold suitable for osteogenic regeneration of a segmental defect. This composite scaffold maintained a high level of porosity making it suitable for tissue ingress and growth factor diffusion.

This study addresses key limitations to growth factor therapies. The sustained release of growth factors has the potential to mitigate dose-induced toxic effects as well as maintain therapeutic concentrations for longer periods. The nature of the delivery system delivers localised growth factors minimising the risk of systemic dosing leading to adverse reactions. This microparticle technology has potential in developmental research research as well as clinical therapies.

Acknowledgements

I would like to thank my supervisors Professor *Kevin Shakesheff* and Associate Professor *Felicity Rose* for always making themselves available despite being very busy. Without their guidance this research would not have been possible. In addition, I would like to thank the post-doctoral researchers Doctor *Cheryl Rahman* and Doctor *Lisa White* for their assistance with collaborations and specific work packages.

Sections 2.4.1.3 to 2.4.2.4 (Pages 46 to 68) in Chapter 2 of this thesis were carried out in collaboration with Doctor *Lisa White* and Mrs *Helen Cox*. Each of us had equal involvement.

In the last three years I have worked with most members of the Tissue Engineering Group. I very much appreciate their assistance and willingness to help.

The funding for my research was provided by the Engineering and Physical Sciences Research Council (EPSRC) through the Doctoral Training Centre for Regenerative Medicine based between *Loughborough University*, *University of Keele* and *University of Nottingham*.

I would like to thank our collaborators at Queensland University of Technology in Brisbane, Australia[1][2] for permitting me to work in their laboratories during my visit and their continued support enabling us to carry out a large *in vivo* study.

I would like to also thank our collaborators at the University Hospital in Basel, Switzerland[3] for recent efforts regarding soft tissue angiogenesis and the use of my microparticles.

Last but not least I would like to thank my girlfriend, friends and family for supporting me in this endeavour.

[1] Dietmar Hutmacher, Regenerative Medicine Group
[2] Marie Woodruff, Biomaterials and Tissue Morphology Group
[3] Andrea Banfi & Veronica Sacchi, Department of Biomedicine

Abbreviations

αMEM	α-Minimum Essential Medium
BCA	Bicinchoninic acid
BMP-2	Bone Morphogenetic Protein-2
CMC	Carboxymethyl cellulose
cc	Cubic centimeter
CDI	1,1-carbonyldiimidazole
DCM	Dichloromethane
DCP	Dynamic compression plate
ELISA	Enzyme-linked immunosorbent assay
ECM	Extracellular matrix
FDA	Food and Drug Administration
FDM	Fused deposition modelling
GPC	Gel permeation chromatography
g	Grams
hMSC	Human mesenchymal stem cell
IHBI	Institute of Health and Biomedical Innovation
IGF-1	Insulin growth factor-1
$_pI$	Isoelectric point
kV	Kilovolts
mRNA	Messenger ribonucleic acid

μg	Micrograms
ml	Millilitres
mM	Milli molar
mg	Milligrams
NMR	Nuclear magnetic resonance
pNP	Para-nitrophenol
pNPP	Para-nitrophenyl phosphate
PBS	Phosphate buffered saline
PDGF	Platelet Derived Growth Factor
PLGA	Poly(DL-lactic-co-glycolic acid)
PEG	Polyethylene glycol
PTFE	Polytetrafluoroethylene
PVA	Polyvinyl alcohol
^{1}H NMR	Proton nuclear magnetic resonance
rpm	Revolutions per minute
THF	Tetrahydrofuran
TMS	Tetramethyl silane
UK	United Kingdom
VEGF	Vascular Endothelial Growth Factor
v/v	Volume per unit volume
w/o/w	Water in oil in water
w/v	Weight per unit volume

Contents

CHAPTER 1

Introduction

1.1 The Emergence of Tissue Engineering

> "Tissue engineering is an interdisciplinary field that applies the principles of engineering and the life sciences toward the development of biological substitutes that restore, maintain, or improve tissue function." [1]
> –*Langer, 1993*

Tissue engineering is a convergence of different disciplines. Tissue engineering draws on the successes from clinical medicine, engineering and science. The current driving force for developments in tissue engineering is a lack of transplants and a shortage of efficacious implants for human organ or tissue replacements.

Tissue engineering has become synonymous with regenerative medicine as the boundaries between replacement and repair become blurred.

1.2 Bone Physiology and Repair

1.2.1 Structure

Bone is a connective tissue with a number of important roles. Bone supports & protects organs, transfers forces, produces red and white blood cells, stores minerals, stores growth factors & fats and even has a role in sound transduction. Millions of years of evolution have led to mechanisms that allows bone to accomplish these tasks.

Bone can be divided into two main categories based on structure: Cortical and cancellous bone.

1.2.1.1 Cortical Bone

Cortical bone, also known as compact or dense bone, makes up the hard outer layer of bones. The porosity is relatively low, in the range 5–30 % [2]. Cortical bone is responsible for around 80 % or the bone mass in an adult human.

1.2.1.2 Cancellous Bone

Cancellous bone, also known as trabecular or spongy bone, has a very open porous network. This is essential since it contains blood vessels and bone marrow. Cancellous bone is responsible for the remaining 20 % of bone mass in an adult human.

1.2.2 Fracture Repair and Remodelling

Bone remodelling is an ongoing and dynamic process. In the 19^{th} century, *Julius Wolff* proposed that bone is deposited or resorbed in accordance with the stresses placed upon it. The results of this can be observed in weightlifters and astronauts [3]. This is known as Wolff's law.

1.2.2.1 Cell Types

Osteoblasts Osteoblasts are located on the surface of osteoid seams. They produce a protein mixture, osteoid, which contains mainly type 1 collagen. This osteoid later becomes mineralised so is the template for new bone development. Osteoblasts also produce hormones thought to help regulate processes. Osteoblasts are immature bone cells, once they become trapped within mineral they become osteocytes (bone cells).

Osteocytes Osteocytes are responsible for matrix maintenance. They help maintain calcium homoeostasis, form new bone and act as mechano-sensory receptors.

Osteoclasts Osteoclasts are responsible for bone resorption. They are located on the surface of bone in *Howship's lacunae* (resorption pits).

1.2.2.2 Fracture Repair

Fracture repair is a proliferative physiological process and generally spontaneous. Fracture healing consists of three main phases.

1. Reactive phase.
2. Reparative Phase.
3. Remodelling phase.

This process is outlined in Figure 1.1.

Reactive Phase Blood cells accumulate in tissues adjacent to the injury site. This forms a blood clot known as a hematoma. Within hours, cells within the hematoma degenerate and die as well as some cells outside the clot. Firbroblasts survive within this area and begin to replicate. This loose aggregation of cells develop small blood vessels, this is known as granulation tissue. This provides structure and nutrients to the site of repair.

Reparative Phase This phase begins days after fracture. Progenitor cells within the periosteum, proliferate and differentiate. The periosteal progenitor cells proximal to the fracture develop into chondroblasts and begin to form hyaline cartilage. Periosteal cells distal to the fracture become osteoblasts and begin to produce woven bone.

As this is taking place, fibroblasts within the granulation tissue develop into chondroblasts which also begin to form hyaline cartilage from within the granulation tissue.

Cartilagenous tissue continues to grow from each end of the fracture until it unites forming a hetrogeneous tissue known as a *soft callus*. This callus provides sufficient stability for blood vessels to begin to form.

Osteoblasts continue to lay down woven bone (which is quickly transformed into lamellar bone) until the soft callus is transformed into bone. Once the cartilagenous *soft callus* is completely transformed into a *hard callus*, fracture union is said to have occurred.

Remodelling Phase During the normal bone healing process, more hard callus is deposited than is needed. This results in a fracture that appears enlarged when viewed under X-ray. Osteoblasts and osteoclasts deposit and remove bone and over a number of years a normal shape is restored.

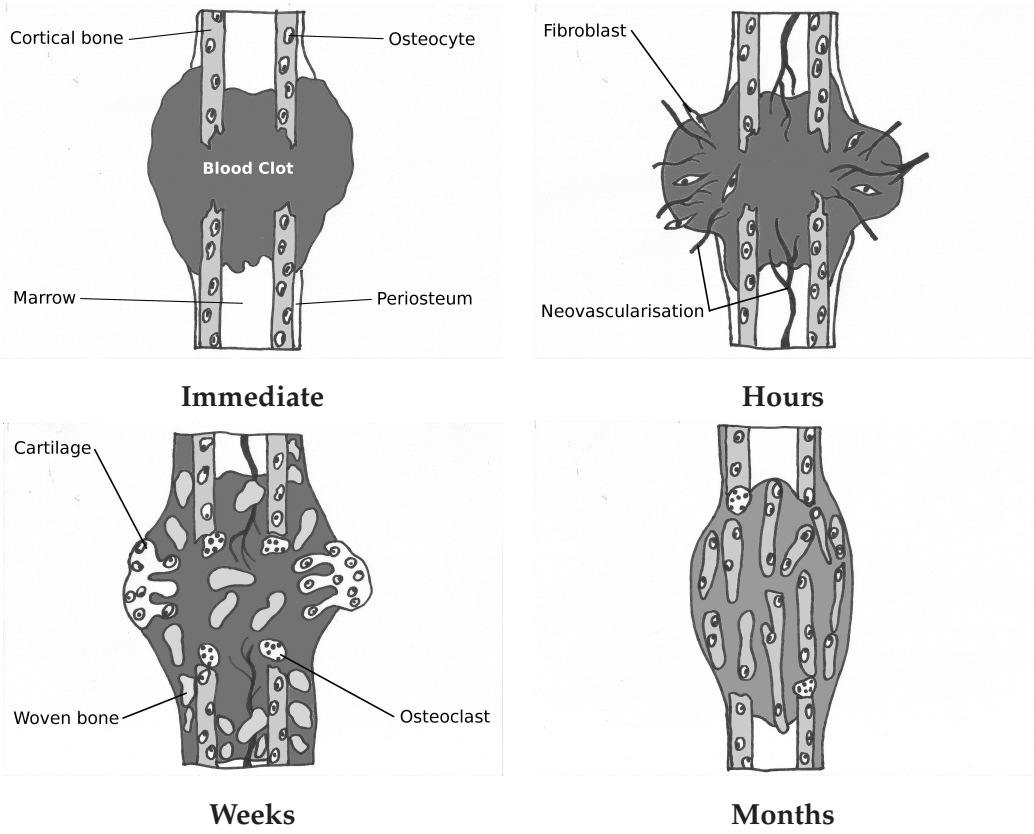

Figure 1.1: Schematic detailing the events during the course of a fracture repair. Very soon after the fracture a hematoma forms. Over the course of days, granulation tissue forms (reactive phase). From days to weeks woven bone begins to appear (reparative phase). The new bone is remodelled over months to years (remodelling phase). Original figure.

1.2.3 Fracture Repair Complications

Complications are generally in the form of delayed-union or non-union fractures. These conditions occur in 5–10 % of long bone fractures [4]. A delayed union fracture can be defined as when a fracture shows clinical or radiological signs of healing but fails to unite within an anticipated period of time [5]. A non-union fracture is defined as when the normal biological healing process has stopped without union occurring.

Non-union fractures can be divided into atrophic and hypertrophic non-unions. Hypertrophic non-union fractures show abundant callus formation without union and atrophic non-union fractures show little or no callus. These conditions are thought to be a result of an adverse mechanical environment or a failure of the biology, respectively [5]. It has been suggested that non-unions may result from characteristics of the fracture, iatrogenic factors or patient factors. It has even been shown that smoking has a detrimental affect on fracture healing [6].

1.2.4 Intervention Strategies

1.2.4.1 Normal Fracture Intervention

The nature of intervention is dependent on the nature and severity of a fracture. There are only ever three reasons to immobilise a fracture:

1. To prevent displacement or angulation of bone fragments.
2. To prevent movement that might interfere with union.
3. To relieve pain.

Intervention is generally kept to a minimum where possible and natural physiological processes are allowed to progress.

1.2.4.2 Non-union Fracture Intervention

Cases where physiological processes fail to achieve a suitable outcome require a greater degree of intervention. Hypertrophic non-union fractures are treated with rigid immobilisation as the problem is thought to be mechanical. Atrophic non-union fractures have limited treatment options. Fixation can be improved or the end-layer of bone could be removed to provide raw ends for healing. Another option in the use of bone grafts.

Bone grafts can be of four general types: Autologous, allogeneic, xenogenic or synthetic. Each have their own advantages and disadvantages. The principle of a successful graft is to provide osteoconduction, osteoinduction and (for autografts) osteogenesis. Bone grafting can be particularly effective since bone has the ability to completely regenerate due to ongoing remodelling.

Autografts Autologous bone grafts involve utilising bone obtained from the same individual recieving the graft. Autografts are currently considered the clinical gold standard. The best grafting success rates have been achieved with vascularised autografts [7]. Bone is harvested from a non-essential area such as the iliac crest. This method avoids issues of tissue rejection. Implanted tissue has osteogenic potential but additional operative sites are required for harvesting which can lead to pain and complications [8]. There is also a limited supply of tissue [9, 10].

Allografts Allogeneic bone grafts negate the need for a donor site, mitigating the associated complications. Allografts are obtained from cadavers and can be fresh, freeze dried or demineralised and freeze dried. Bone banks specialise in preparing these grafts. The failure rate of grafts from banked bone is higher than that of autografts and has been quoted at 20–35 % [11]. As with any allogeneic therapy there is always a risk of pathogenic infection.

Xenografts Xenogenic materials are less common and currently under evaluation. The most common source is bovine. Due to the pathogenic risks, xenogenic materials are deprotinated leaving a mineral structure that has a chemical composition and structure almost identical to human bone [12]. These materials are regarded as osteocompatible fillers [12].

Synthetic Grafts A variety of synthetic materials are used in orthopaedic surgeries. These can be broadly divided into two categories: Ceramics and polymers. Ceramics are by far the most common, these include glass ceramics [13, 14], calcium sulphate [15], calcium phosphate [16] and hydroxyapetite [17]. Polymeric alternatives are a relatively new option. The only commercial polymeric product graft at this time is HEALOS® (*DePuy Synthes*). This consists of cross-linked collagen coated with hydroxyapetite to improve biomimicry of the material structure.

Since these materials are not bone-derived, a mechanical property mismatch is a problem. This can lead to implant failure and tissue damage [18]. These materials lack

functionalities that encourage tissue integration and self-repair. Methods are currently under investigation that impart bio-functionality onto these otherwise inert synthetic materials [19, 20]. It is hoped that this research will lead to highly available bone graft substitutes with a high degree of long-term implantation success.

Here lies the niche to be exploited. Autografts, the clinical gold standard have good efficacy but limited availability, as do allografts. There is a growing need for synthetic materials with greater efficacy.

1.3 Growth Factors

One of the reasons autografts are thought to be so effective is that they contain the necessary signalling molecules required for repair and vascularisation [21]. These signalling molecules are known collectively as growth factors.

1.3.1 Overview

Growth factors are proteins that serve as signalling agents for cells. They play a key role in influencing and regulating cellular processes such as proliferation, differentiation and matrix synthesis. Recent advancements of recombinant protein technologies have increased the level of interest for using growth factors as therapeutic agents [22] particularly in bone engineering [23].

Growth factors act on cells by binding to specific surface receptors. This induces an intracellular signalling system to convey a message to the nucleus which then induces a biological response (Figure 1.2).

The most important growth factors for applications in bone regeneration include various Bone Morphogenetic Proteins (BMP's), Vascular Endothelial Growth Factor (VEGF), Platelet Derived Growth Factor (PDGF), Insulin-like Growth Factor (IGF), Fibroblast Growth Factor (FGF) and Transforming Growth Factor β (TGF-β) [20].

For the purpose of this thesis, three of these growth factors have been selected for study: VEGF, PDGF and one of the BMP's. The two important events during a fracture repair are neovascularisation and osteogenesis. VEGF and PDGF are thought to be crucial in the formation of successful vasculature [24], recent literature suggests the synergism of these growth factors to be important [25]. BMP's are the most well studied set of growth factors in bone regeneration. Unlike other growth factors, BMP's can be osteoinductive [26].

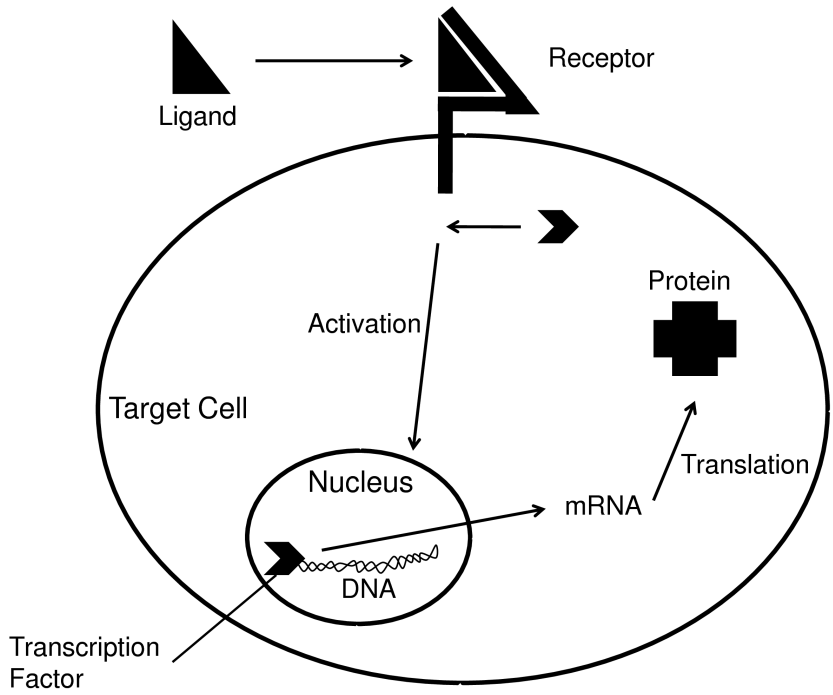

Figure 1.2: Diagramatic representation of how growth factors affect cell activity. The ligand (growth factor) binds to the extracellular domain of the receptor. The intracellular domain of the receptor then activates a signal transduction system. A transcription factor binds to the DNA and induces the expression of a new gene. Figure drawn by the author, Giles Kirby.

1.3.2 Bone Morphogenetic Protein

Bone morphogenetic proteins (BMP) are members of the TGF-β superfamily. The osteoinductive effect of these molecules was first observed in the mid 1960's. Dr. *Marshall Urst* demonstrated the induction of new ectopic bone from decalcified bone matrix [27]. BMP's have a powerful ability to induce orthotopic and ectopic new bone formation [28]. Of particular interest are BMP-2, BMP-4 and BMP-7 (Also known as Osteogenic Protein-1 (OP-1)). These molecules have been reported to have a strong efficacy in inducing bone formation [29–31].

Modern recombinant protein technology has allowed us to elucidate the effect and importance of specific proteins. BMP-2 was the first to show it could induce new bone and cartilage formation [32].

Bone morphogenetic proteins are intrinsically stable proteins due to their tightly-folded, disulphide stabilised structure. This makes them excellent candidates for therapeutic products. The stability of lyophilised BMP is thought to be in the order of years [23].

1.3.3 Vascular Endothelial Growth Factor

Vascular endothelial growth factor (VEGF) is thought to stimulate angiogenesis and vasculogenesis. It creates blood vessels during embryo development and during tissue repair. Over expression of VEGF is associated with tumours and much of our knowledge of VEGF comes from research into cancer. The structure of VEGF was determined in 1989 and published simultaneously by two groups studying what they thought to be different molecules [33–35]. One was looking at endothelial cell mitogenesis and the other, vascular permeability. The 6 isoforms of VEGF were later elucidated. Each isoform has a different number of amino acids due to alternative splicing of VEGF mRNA. These different isoforms (121, 145, 165, 183, 189 and 206) have differing levels of solubility and extra-cellular matrix (ECM) affinity.

1.3.4 Platelet Derived Growth Factor

The structure and function of Platelet derived growth factor (PDGF) is similar to that of VEGF hence they are both said to be in the PDGF/VEGF family [36]. PDGF, like VEGF, is composed of a disulphide linked polypeptide dimer. There are two forms of PDGF; *a* and *b*. This leads to three dimeric versions; *aa*, *bb* and *ab*. PDGF plays an important role in wound healing. This is seen from three different approaches: The effect of PDGF

on cell cultures, the presence of PDGF and PDGF receptors during wound healing and topical application of PDGF to healing wounds [37].

PDGF stimulates mitogenesis and chemotaxis of fibroblasts, endothelial and smooth muscle cells [38, 39]. This enhances stability of early vasculature and is thought to be crucial in generating stable vasculature [40].

1.3.5 Clinical Use

1.3.5.1 Platelet Derived Growth Factor

Diabetic ulcers seem an ideal candidate for angiogenic growth factors. This is a pathological environment and regeneration is inhibited by the ischemic nature. It seems logical that if we could induce angiogenesis, this might increase the rate of repair. In December of 1997 the U.S. Food and Drug Administration (FDA) granted approval for the use of REGRANEX® (becaplermin) gel for the treatment of diabetic foot ulcers. The active ingredient (becaplermin) is a form of PDGF-BB.

A clinical study in 1998 demonstrated that the healing rate for diabetic ulcers (in contrast to a negative control) was significantly higher [41] and a cost-effectiveness study in 2001 indicated that REGRANEX exhibited a '*favourable economic as well as clinical profile*' [42]. However at this early stage, there was no large clinical trials comparing REGARNEX to the clinical gold standards for treatment. History tells us that for a new healthcare product to become successful it must be more efficacious or cheaper (ideally both) than the clinical gold standard.

A randomised clinical trial was published in 2005 comparing REGRANEX to OASIS. The OASIS wound dressing consists of acellular porcine small-intestine submucosa. This graft significantly stimulates wound closure [43]. The results from this comparison indicated that the incidence of full thickness diabetic foot ulcer healing was significantly higher for groups treated with OASIS than REGRANEX (p=0.055) [44]. It should be noted that the sample size was too small for this result to be truly representative but the publication of this paper reflected badly on REGRANEX.

In 2008 the FDA issued a warning that there as an increased risk of death from cancer from patients who used three or more tubes of REGRANEX although the risk of new cancers was not increased. Due to reported '*commercial reasons*', REGRANEX was withdrawn from sale in the UK in June 2011. Currently epidemiological studies are ongoing to assess cancer risks.

REGRANEX did not employ any kind of controlled release and it is possible that

high doses (0.01 %) of PDGF-BB were systemically distributed throughout the body increasing cancer development. Importantly, this therapy indicated clinical benefit from an angiogenic growth factor therapy. If costs can be reduced and safety increased then this indicates a potential future for angiogenic growth factor therapies.

1.3.5.2 Bone Morphogenetic Protein

Currently preparations BMP-2 and BMP-7 are under clinical evaluation for use in spinal fusion. To date, two recombinant human bone morphogenetic protein (rhBMP) carrier systems have been approved by the FDA for clinical use. These are OP-1 (*Stryker*®) and InFUSE™ (*Medtronic*). These deliver BMP-7 and BMP-2 respectively. Both of these systems utilise a collagen carrier and supraphysiological concentrations of growth factor (around 1.5 mg per cc). This high level of BMP within these therapies has been an ongoing concern and in 2008 the FDA issued a public health notification regarding life-threatening complications associated with rhBMPs in cervical spine fusion. Use in spinal fusion has demonstrated similar efficacy to that of autografts [45].

BMP-2 is the most researched and published osteoinductive protein and InFUSE is also indicated for use in fresh tibial fractures, and oral maxillofacial bone grafting procedures. Spinal fusion models have consistently shown rhBMP-2 to be as good as (or better than) autogeneous bone [46, 47]. The success of a randomised clinical trial involving 279 patients [48] led to FDA approval of InFUSE in 2002. For nearly 9 years, industry sponsored studies reported the clinical benefits of rhBMP-2 in spinal surgeries but in 2011 a damning review was published [49]. Thirteen industry-sponsored reviews of rhBMP-2 safety and efficacy showed that there were no rhBMP-2 associated adverse events. It was found that these studies had potential methodological bias, specifically in reporting donor site pain.

As early as the year 2000 when initial lubmar fusion clinical trials were taking place [50, 51] it was clear that adverse events resulting from rhMBP-2 could not be well predicted. This is because the expression of BMP-2 is not limited to fracture inflammatory environments causing osteoinduction. It is present in other pathways including abnormal growth signalling pathways and the induction of an altered immune response [52, 53]. Accordingly, in 2002 the following was published in a review:

> 'Safety issues associated with the use of bone morphogenetic proteins in spine applications include the possibility of bony overgrowth, interaction with exposed dura, cancer risk, systemic toxicity, reproductive toxicity,

> immunogenicity, local toxicity, osteoclastic activation, and effects on distal organs.' [53]

The industry sponsored studies that followed failed to verify any of these risks.

In 2008 the FDA issued a public health notification of *'Life-threatening Complications Associated with Recombinant Human Bone Morphogenetic Protein in Cervical Spine.'*. This resulted from a number of independent reports noting complications from using rhBMP-2 in cervical spinal fusion. These included soft tissue swelling and a compromised airway [49, 54, 55].

These complications could be associated with theorised toxic dosing of BMP-2. They beg the question; was the dose of BMP too high? Once again, the therapeutic benefit of a growth factor therapy have been shown but complications have arisen potentially related to dosing.

1.4 Scaffolds

1.4.1 Overview

Scaffolds are used in tissue engineering approaches for a number of reasons. Scaffolds are space filling agents that can be used to deliver therapeutic molecules or cells. Scaffolds can also take on the role of the extracellular matrix (ECM), presenting necessary anchorage and stimuli so that cells perform as desired. The mechanical properties of the extracellular matrix is a crucial factor affecting cellular behaviour.

It has been suggested that to create functional equivalents for human tissue, tissue engineered solutions must recreate physical, mechanical and chemical properties of the native environment. In this way we can try to replicate the complex interactions between cells and their microenvironments that influence morphogenesis, function and regeneration [56, 57].

Extracellular matrix (ECM) not only provides structural support and protection for cells, it also contains physical, chemical and mechanical cues which influence cell behaviour. The ECM modulates cellular behaviour and in turn cells remodel the ECM. This is a complex and dynamic process. The ECM is highly hydrated and contains a number of soluble and insoluble factors. Concentration gradients within the ECM play an important role in chemotaxis [58, 59], morphogenesis and wound healing [60–62]. An ideal tissue engineered solution should attempt to replicate these features.

When attempting to repair a soft-tissue environment, a soft scaffold with simi-

lar mechanical properties is desired. For these applications hydrogels are often utilised [24, 63–67]. Hydrogels have been explored for their potential to deliver cells and therapeutic molecules.

Osseous tissue usually requires a stiffer scaffolds material to provide structural support and direct cell behaviour accordingly. Current grafting options are discussed in Section 1.2.4.2. Autografts intrinsically contain ideal combinations of cells and bioactive molecules. In addition, the cells have the potential to continue to deliver therapeutic levels of bioactive molecules conducive to physiological regeneration. In contrast synthetic alternatives are relatively inert. Attempts have been made to include bioactive molecules [19, 68] to increase efficacy of potential therapies but these types of grafts are poor delivery substrates for cellular therapy options. It seems that without the ability to deliver prolonged physiological levels of the correct growth factors, the efficacy of osteogenic scaffolds will remain limited.

1.4.2 The Future of Scaffolds in Bone Healing

Current synthetic grafting materials are generally ceramics and used as graft extenders. In this way they increase the bulk volume of an autograft, minimising the amount of material that requires harvesting. Modern chemical and fabrication techniques are being applied to biodegradable polymers (natural and synthetic) in the hopes of generating grafts and implants with more suitable mechanical and biological properties.

It is hoped that one day fully synthetic scaffolds with appropriate molecular cues will become clinical gold standards, negating the problems associated with autologous harvesting.

A collagen based material was the first clinical polymeric alternative (HEALOS®). This material is no worse than autologous grafting in lumbar spinal fusion [69]. In addition cellular infiltration into the porous structure has been demonstrated [70]. Since the degree of cross-linking can be modified, this affects porosity, cellular infiltration and ultimately mechanical strength can be tailored. This provides a far higher level of control over the final tissue than can be achieved with current methods.

Other polymers under investigation for use is bone repair are the aliphatic polyesters polycaprolactone (PCL), polymers of lactic acid (LA) and glycolic acid (GA) and the copolymer poly(lactic-co-glycolic acid) (PLGA). Lactic acid has two stereoisomers, giving rise to three forms of LA polymer: L-LA, D-LA and DL-LA. PLGA is of particular interest because by altering the ratios of monomers the degradation rate can be tuned

(Figure 1.3).

Porosity is one of the key factors for bone grafting. This is the means by which cells and nutrients infiltrate the scaffold and it is well known that the degree of porosity affects the rate of integration and the final volume of regenerated bone [72]. It has been suggested that an interconnected porosity greater than 75 % is required to facilitate adequate vascularisation and nutrient diffusion [73]. A number of methods have been explored to generate porous polymeric structures. These include supercritical foaming [73, 74], fused deposition printing [75, 76], salt leaching [77, 78] and various microparticle composites [79, 80].

It is hoped that by combining the correct materials, fabrication methods, bioactive molecules and maybe even cells, that synthetic scaffolds could exhibit regenerative efficacy greater than or equal to autografts.

1.4.3 Structural requirements

As important as issues such as porosity and biocompatibility are, it is important not to forget that this is only half the story when looking specifically at bone tissue engineering. The structural properties of these scaffolds are of utmost importance to support necessary load bearing and provide the right mechanical stimuli for bone regeneration.

A negative correlation between porosity and mechanical strength has been demonstrated [81, 82] so there will always need to be a compromise between porosity and mechanical strength for scaffolds aimed at different anatomical regions. It is accepted that the stiffness of a fracture fixation has an important influence on bone regeneration. A flexible fixation can lead to callus healing [83] or worse, nonunion [84]. It is also hypothesised that a degree of interfragmentory movement is needed as a stimulus for bone regeneration and this is a focus of current research [85, 86].

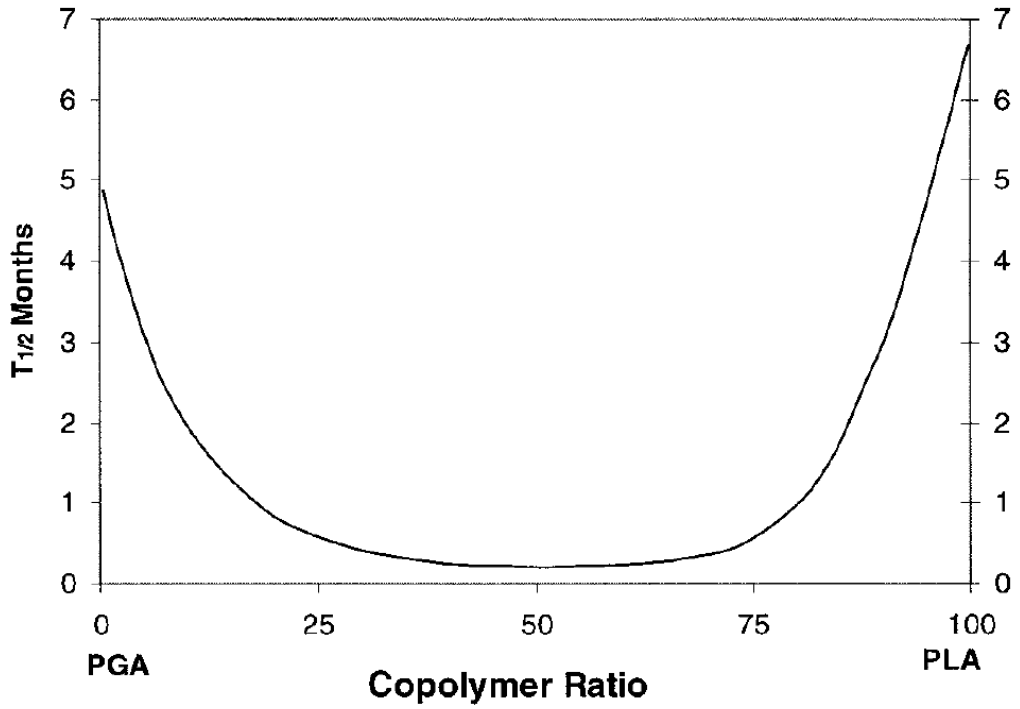

Figure 1.3: Half-life of PLA and PGA homopolymers and copolymers implanted in rat tissue [71].

1.5 Growth Factor Delivery from Microparticles

1.5.1 Overview

The purpose of a delivery system is to deliver a particular dose of something to a particular location at a specific time. The delivery of a bioactive molecule such as a growth factor can be done in several ways. The simplest way to deliver a growth factor involves simply injecting it as a solution into a site. Such approaches have shown significant effects. For example direct injection of fibroblast growth factor into porcine cardiac muscle increased the number of micro-vessels [87]. Although this direct approach can work in some cases there will always be clinical concerns over growth factor migration and toxicity at supraphysiological levels. Supraphysiological levels of growth factor are used to try and mitigate issues of a short half life (Table 1.1).

Clinical examples of this high dosing are Medtronics InFUSE™ and Strykers OP-1. Growth factors are generally thought to have an effect at concentrations in the order of picograms to nanograms. This is sufficient to generate a cellular response [88]. These systems deliver growth factors in the order of hundreds of micrograms to milligrams (per millilitre) in an attempt to prolong therapeutic levels. This has severe cost implications and will only extend the active dose by a matter of days.

A number of marketed formulations for therapeutic proteins utilise micro/nano particles/spheres (Table 1.2). These systems protect therapeutic proteins within polymeric matrices in an effort to maintain stability and/or increase the duration between administrations. It should be noted that none of these systems are designed specifically to administer proteins to a particular site of interest.

A number of growth factor delivery systems have been published for the purposes of tissue regeneration/repair, many based on microparticles. This section will focus on hydrophobic polymeric microparticles of lactic and glycolic acid. Polymers derived from D,L-lactic and glycolic acids are by far the most explored for the delivery of therapeutic proteins.

Poly(D,L-lactic-co-glycolic acid) (PLGA) is generally fabricated through the ring-opening polymerisation of lactide and glycolide cyclic dimers. PLGA has an extensive history of research and clinical use. The most well known use is sutures such as *Vicryl*®. PLGA is also used in grafts, implants, prosthetic devices and microparticles for drug delivery. PLGA is considered to be biocompatible, bioresorbable and non-toxic. PLGA (and other aliphatic polyesters) degrade mainly via hydrolytic mechanisms [89, 90]. It is possible that there is some enzyme catalysis taking place

in vivo [91] but the evidence is not convincing. Degradation products, lactic acid and glycolic acid, undergo degradation through the Krebs cycle to form harmless water and carbon dioxide [92, 93].

Growth Factor	Half-life
VEGF	50 minutes [94]
PDGF	2 minutes [95]
BMP-2	7–16 minutes [96, 97]

Table 1.1: Serum half-life of three growth factors of interest.

Drug	Trade name	Route	Application
Leuprolide acetate	Lupron depot®	3-month depot suspension	Prostate cancer
Recombinant human growth hormone	Nutropin depot®	Monthly s/c injection	Growth hormone deficiency
Goserelin acetate	Zoladex®	s/c implant	Prostate cancer
Octreotide acetate	Sandostatin LAR® depot	Injectable s/c suspension	GH supression anticancer
Triptorelin	Decapeptyl®	Injectable depot	LHRH agonist
Recombinant bovine somatropin	Posilac®	Oil based injection	To increase milk production in cattle

Table 1.2: Marketed formulations of proteins from biodegradable microparticles. Adapted from *Sinha et al* [98].

1.5.2 Growth Factor Stability

Growth factors are fragile. As well as the primary structure, many rely on complex secondary, tertiary and sometimes quaternary folding for their biological activity. This means that they are particularly susceptible to detrimental conditions present during micro-encapsulation and release.

In a physiological situation, growth factors are expressed by cells. The rapid expression and metabolism of growth factors ensures that the combinations and concentrations of growth factors are relevant to the changing physiological situation. Some experimental *in vivo* approaches have utilised transduced cells in order to up-regulate expression of particular growth factors [40]. This is a good tool to assess the effects of growth factors or even the effects of growth factor combinations but the level of dosing is relatively imprecise and this approach has too many safety concerns to become a clinical approach in the near future.

The FDA defines a stable pharmaceutical as one that deteriorates less than 10 % in two years [99]. Encapsulation of a growth factor within a delivery vehicle involves three stages in which the growth factor must remain stable: Fabrication, storage and release. Proteins can degrade by a number of mechanisms [100–106]. A lyophilised protein based therapeutic can remain stable for months or even years at ambient temperatures [107]. The stages with the highest potential for protein denaturation are during fabrication and release. These can involve aqueous/organic interfaces, temperature changes, agitation, hydrophobic surfaces, detergents or breakdown products from the degrading carrier system. Each of these must be addressed. The key to achieving release of a stable protein is understanding the conditions involved in a particular system.

One such approach achieved stable release of recombinant human growth hormone (rhGH) over a 1 month period [108]. Stability was achieved by complexing the rhGH with zinc. This reduced the solubility of the hormone thus its susceptibility to degenerative mechanisms. Although this approached worked, systems that rely on modification of the encapsulated active will always be dependent on the type and functionality of that active. To develop a system that is able to deliver multiple growth factors in multiple situations will require an approach that addresses the detrimental conditions independent of protein manipulation. This approach would have a greater number of applications.

An example of this approach has been to mitigate the acidic microenvironment within PLGA matrices. Acidity results from accumulation of lactic acid and glycolic acid

breakdown products. This acidic environment causes protein unfolding leading to aggregation as well as acid-catalysed hydrolysis [109]. Magnesium hydroxide ($Mg(OH)_2$) has been incorporated within the polymer to try and neutralise this damaging environment. This approach has shown a greater overall release of bovine serum albumin (BSA) [110] indicating reduced aggregations. This approach has proven effective at mitigating pH issues in several studies [111, 112], but the inclusion of salts could themselves be a risk factor leading to protein instability. Some proteins become unstable at high salt concentrations [113]. This may cause denaturation problems during a lyophilisation process.

An acidic micro-environment within PLGA microparticles may not even be an issue in certain situations. Degradation of larger PLGA devices tends to be hetrogeneous [90, 114, 115]. This is because the build up of acidic monomers in the core leads to an increased rate of hydrolysis through acid catalysis. The degradation of smaller devices such as microspheres under 300 µm appears to be more homogeneous [116]. As previously mentioned, the acidic microenvironment within degrading PLGA may be detrimental to protein activity but if the size of the delivery device is kept small enough then this issue could potentially be mitigated.

1.5.3 Microparticle Fabrication Techniques

1.5.3.1 Solvent Evaporation and Solvent Extraction

Single Emulsion As the name suggests, this process involves a single emulsification step and in the case of hydrophobic polymers, an oil-in-water (*o/w*) emulsion. The polymer is dissolved in an organic solvent that is immiscible with water. Dichloromethane (DCM) is the most commonly used. A lipophilic drug can then be also dissolved into the organic phase but for hydrophilic growth factors another technique must be used. A method that has shown to work with model proteins involves micronising the protein then dispersing it within the organic phase [117, 118]. This is referred to as a solid-in-oil-in-water (*s/o/w*) emulsion. The potential for higher entrapment efficiencies have been reported using this technique in preference of a double emulsion method.

This oil phase is emulsified within a larger aqueous phase. A surfactant such as poly(vinyl alcohol) (PVA) is generally used to stabilise this emulsion while the organic solvent either evaporates or is extracted by a leaching method. A stable emulsion is important for high entrapment efficiencies and regular particle morphology [119]. The result is a suspension of hardened polymer microparticles in an aqueous solution. The microparticles are collected by centrifugation, sieving or filtration. The microparticles

are then dried to produce a free-flowing product.

This process method favours lipophilic drugs such as steroids [93, 120]. Hydrophilic proteins have a tendency to diffuse into the aqueous phase resulting in low entrapment efficiencies. An approach to mitigate this issue is an oil-in-oil (*o/o*) technique. A water miscible solvent such as acetonitrile is used to dissolve the polymer as well as the the hydrophilic drug. This is then emulsified within a different oil. There are concerns that this environment could be damaging to fragile growth factors.

Double emulsion This method utilises two emulsification steps. This is a water-in-oil-in-water (*w/o/w*) method and is particularly suited for the encapsulation of hydrophilic molecules (such as growth factors) within a hydrophobic polymer (such as PLGA). A schematic of this process can be found in the methods chapter (Section 2.3.3, Page 40). The growth factor is dissolved in water (or a buffered solution) and this is emulsified within an organic phase that contains dissolved polymer. Once again, DCM is the most common solvent. This is the first emulsion step. The next emulsion step sees this *w/o* emulsion emulsified in a larger aqueous phase, once again a surfactant is often used to stabilise this emulsion while the organic solvent is extracted. The microparticles are then collected and dried.

This process is the most popular for the encapsulation of growth factors. A large number of parameters can be adjusted to influence growth factor release rates and entrapment efficiencies. The deleterious environments inherent to this process are also well documented. The most significant during the fabrication stage is the oil/water interface. This can cause denaturation of proteins and growth factors [103]. The most common approach is the inclusion of an excipient to competitively block the interface [102, 104, 121–123].

Emulsification Techniques Formation of an emulsion requires the combining of immiscible solvents. Common methods impart energy into the system in the form of shearing fluidic forces. Different emulsification techniques lead to different microparticle sizes, morphologies and polymer crystallinity. The most published methods are sonication, microfluidics, high pressure mixing and mechanical agitation such as stirrers, impellers and baffles.

1.5.3.2 Phase Separation (coacervation)

The word *coacervate* is derived from the Latin *coacervare*, meaning to assemble together or cluster. A coacervate is formed when a substance is pushed out of solution by another substance. For example the solubility of PLGA could be reduced by the addition of another component. This results in two phases: the polymer-containing coacervate and the supernatant. Typically poly(dimethylsiloxane) is added to PLGA dissolved in DCM. This forms the coacervate droplets [124]. These polymer droplets then coat the suspended drug/growth factor particles. The rate of addition of the precipitating agent directs the rate of polymer droplet formation. This should be done slowly so the polymer evenly coats the drug particles.

Since this process lacks any emulsion stabiliser, agglomeration of particles is a problem [93]. This process utilises harsh solvents. These could be damaging to growth factors or other fragile proteins.

1.5.3.3 Spray Drying

Spray drying involves mild conditions, it less dependent on the solubility of the drug and is considered easier to scale up [120, 125, 126]. The drug is dispersed within an organic solvent, containing the polymer. For hydrophilic compounds a *w/o* technique is sometimes used [127]. This mixture is sprayed into a warm, dry environment. The resulting microparticles can be collected and dried further.

This method has been used to encapsulate heparin, a relatively large hydrophilic glycosaminoglycan, into PLGA microparticles. The resulting microparticles were 2–5 µm in diameter and released heparin for up to 50 days *in vitro* [127].

A variation on this method is known as cryogenic atomization. This method involves spraying the polymer/drug emulsion and rather than being dried they are snap-frozen. The DCM is later extracted. This method has been used to encapsulate the model protein *ovalbumin* into hydrophobic polymers forming microparticles approximately 20 µm in diameter [128]. Western blot analysis verified that the released ovalbumin was active and this method is reported to achieve higher entrapment efficiencies than a double emulsion method [129].

1.5.4 Sterilisation

It is important that the microparticle product is sterile in order to carry out long-term release studies, *in vitro* or *in vivo* analysis. There are two ways to approach

this: Terminal sterilisation or aseptic manufacturing. Fabrication techniques such as sonication or microfluidic emulsion methods are particularly suited for sterile fabrication as they are enclosed. Other methods can be carried out in a sterile way but it can be difficult for laboratory-scale production. Standard sterilisation techniques are outlined (Table 1.3).

Steam and dry heat methods are not suitable for growth factor loaded PLGA microparticles because the relatively low T_g temperatures of PLGA could lead to particle deformation. Elevated temperatures may also contribute to growth factor denaturation. Gas sterilisation is a popular choice for thermoplastic polymers that are degradable by hydrolysis. However, there are concerns that any chemical sterilisation methods may leave residual sterilisation agent behind in harmful quantities. It is important that polymeric systems are adequately degassed and aerated following sterilisation with ethylene oxide [131].

Gamma irradiation is a popular choice for biomaterials and pharmaceuticals. It is a fast effective method with a high degree of penetration. If this technique is used for PLGA, the reduction of molecular weight should be considered (Figure 1.4). It has been shown that that gamma irradiation can cause radiolytic scission of PLGA [132, 133]. These shorter chains will have an increased hydrolytic degradation rate [134] therefore the potential for an increased rate of growth factor release.

A common approach for laboratory-scale biomaterials involves fabrication under a clean environment and ultraviolet irradiation [76]. This is suitable for non-clinical applications but the issue of sterility must be considered for any materials with potential for clinical translation.

Sterilisation technique	Advantages	Disadvantages
Steam (high pressure–120 °C-135 °C)	No toxic residues	Deformation of microparticles (temperature above T_g), hydrolytic degradation
Dry heat (160 °C-190 °C)	No toxic residues	Deformation of microparticles (temperature above T_g)
Radiation	High penetration, fast	Radiolytic scission of polymer and/or growth factor
Gas sterilisation (ethylene oxide)	Low temperature process	Long process due to degassing, residues are toxic

Table 1.3: Standard sterilisation techniques and their applicability to PLGA. Adapted from *Kyriacos et al, 1996* [130].

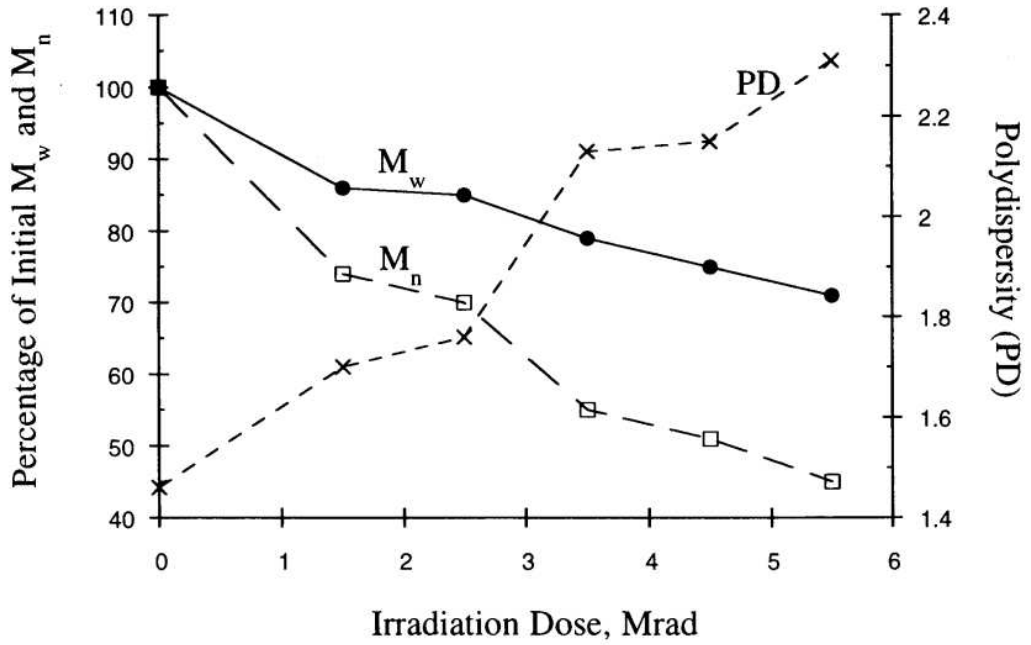

Figure 1.4: Effect of gamma sterilization on the molecular weight distribution of PLGA microparticles. Published by *Hausberger et al, 1995* [134].

1.5.5 Characterisation of Growth Factor Release

1.5.5.1 Release *in vitro*

The release of growth factors from microparticles is dependent on a number of formulation and processing variables. To estimate how these microparticles will perform *in vivo*, *in vitro* release studies are carried out. These studies can assess total protein release or the activity of some proteins. Total protein can be assessed colorimetrically using an assay such as the *Bradford assay* [135] or a *bicinchoninic acid* assay [136]. The activity of released proteins can be quantified enzymatically or using a structurally dependent assay such as an Enzyme-Linked Immunosorbent Assay (ELISA). Cellular assays can also be used to identify the activity and sometimes concentration of bioactive molecules by looking at certain markers expressed by the cells.

So that the protein release from microparticles will be representative of their behaviour *in vivo*, consideration must be paid to the intended *in vivo* site and the best way to recreate that in the laboratory. Generally, this involves physiological temperature, a buffer to maintain physiological *pH* and some kind of agitation. For a full review on how to obtain complete release from PLGA microparticles see *Gitea et al, 2008* [137].

1.5.5.2 Release *in vivo*

Assessment of *in vivo* release relies on measuring physiological responses to released cues in contrast to control conditions. Assessments like this in animal models are the only way to determine how a particular therapeutic biomaterial will perform clinically. Common measures of the repair of an osseous defect are radiography, biomechanical testing, micro computerised tomography and histological analysis [76]. In this way the mineral density/structure, mechanical strength and cellular presence/morphology can be assessed to give an indication of whether a particular technique was significantly better than another.

1.6 Aim

1.6.1 Scientific Need

The importance of angiogenesis during an osteogenic repair is well understood. The growth factors that enhance angiogenesis and osteogenesis are also well understood.

Current research is assessing various combinations of these growth factors during osseous repair. There is currently a lack of scientific data that assesses these growth factor combinations in large mammal models over the duration of a full fracture repair. There is also a lack of standardised, well defined systems to deliver different growth factors while addressing issues of denaturation and therapeutic dosing.

1.6.2 Aims of Thesis

This thesis aims to address two goals: To generate and validate a system for delivering growth factors and develop the materials and processes to a stage where they can be applied into an *in vivo* model.

1.6.2.1 Delivery System

The formation of a polymeric microparticle system for the delivery of growth factors is proposed. This will be formulated and fabricated in such a way as to protect un-released growth factor from hydrolytic and enzymatic degradation. The microparticles will modulate the duration and concentration of growth factor release and control the location of growth factor action. The system should also be applicable to multiple growth factors so the release kinetics should not be dependent on growth factor characteristics such as molecular weight and isoelectric point.

By protecting the un-released growth factor structure it is hypothesised that issues associated with a short *in vivo* half life can be mitigated. By extending growth factor half lives the therapy could impart a longer duration of biological activity, reduce the need for multiple administrations and potentially reduce the total amount of growth factor required to achieve a desired response. A controlled release system has the potential to minimise the total amount of growth factor required while conserving the therapeutic effect.

It is hoped that by maintaining a dose of growth factor in a therapeutic range, negative effects resulting from toxic concentrations can be avoided. The biomimicry of a therapeutic concentration of growth factor may also increase the efficacy of this type of system.

The targeted nature of a microparticle system aims to limit the location of action of released growth factors to a region of interest or repair. If systemic dosing can be avoided it is hoped that risks such as the cancer concerns over REGRANEX can be reduced.

It is hoped that one system that can be formulated to achieve different release profiles will be a viable option for clinical therapies. For example if a short and a long duration of release are required within a site then a mixture of microparticles will be far easier to store, manipulate and administer than composite therapy such as one involving the mixture of a hydrogel and a hydrophobic polymer device.

These needs will be addressed by combining different formulations of PLGA with a more hydrophilic plasticiser. This should provide a greater level of control over hydration rates than current approaches thus greater control over the release of growth factors. The microparticle fabrication process will be tailored to be robust and consistent and also to minimise environments damaging to growth factor structure and activity. The formulation will be augmented with an albumin stabiliser to help protect the growth factor structure and also to competitively block the deleterious *w/o* interface. The addition of an albumin excipient will also enable the concentration of growth factor within the microparticles to be adjusted but the ratio of PLGA to protein to remain the same (though adjustment of albumin levels). This keeps the process robust as it is suspected that changing the ratio of PLGA to protein could affect release rates.

1.6.2.2 Preparation for assessment *in vivo*

This microparticle delivery system will be developed with the intention of delivering a combination of angiogenic and osteogenic growth factors to a segmental defect model at levels and a duration similar to a physiological repair environment.

It is hypothesised that the induction of angiogenesis early during the repair process will lead to a more rapid and a more complete repair. If this is the case then this research could lead to the next generation of bone repair strategies delivering combinations of growth factors at physiological levels.

The microparticle growth factor delivery system will be used to tailor populations of microparticles to deliver VEGF, PDGF and BMP-2 accordingly. The release will be verified and microparticles will be combined with an osteoconductive and structurally supportive scaffold ready for future studies.

1.6.3 Objectives

The objectives required to achieve these goals can be broken down into three main strategies (corresponding with results chapters) and a series of sub-objectives.

1. Develop a polymeric system for growth factor release.
    - Fabricate PLGA microparticles with consistent size distributions.
    - Encapsulate model protein and assess encapsulation efficiency.
    - Assess release of protein under simulated physiological conditions.
    - Deduce how changes in formulation equate to protein release.
    - Assess the activity of a model protein.
    - Ensure replacement of the model protein with a growth factor has no significant effect on the release profile.
2. Verify the biological activity of released growth factor.
    - Culture cells *in vitro* in the presence of growth factor releasing microparticles.
    - Assess biological changes resulting from the released growth factor.
3. Implement this system to make it suitable for an *in vivo* model.
    - Select microparticle formulations to deliver growth in the required way.
    - Fabricate microparticles and validate the protein release.
    - Develop a method to combine the microparticles with a scaffold suitable for a segmental defect.

This thesis begins with the fabrication of microparticles. Can PLGA degradation be tailored such that protein can be released over just days or for a number of weeks?

CHAPTER 2

Results I: Microparticle fabrication

2.1 Introduction

This chapter details the selection, optimisation and characterisation of a polymeric growth factor release system. The main introduction outlined the clinical need for a growth factor delivery system and how PLGA was selected as a delivery candidate. A more hydrophilic co-polymer was selected as an adjunct to the PLGA. The purpose of this second polymer was to provide another method to modulate protein release. Increasing the ratio of the more hydrophilic polymer should increase the rate of water ingress into the polymer composite leading to increased protein diffusion through pores and micro-channels. It was also speculated that this water ingress would increase the rate of PLGA bulk degradation due to hydrolytic mechanisms. It has been demonstrated that polyethylene glycol (PEG) inclusion into PLGA microparticles has been able to modulate release profiles [138, 139]. A PLGA-PEG-PLGA triblock copolymer was selected for this purpose because of its documented biocompatibility [140] and use in delivery systems [66, 141, 142]. The surfactant nature of this copolymer was also considered, it has been shown that the PEG segmant promotes stability of proteins [143].

Microparticle fabrication using a double emulsion water-in-oil-in-water (*w/o/w*) solvent evaporation process has been well investigated for the encapsulation of hydrophilic molecules of interest within a hydrophobic matrix [144–146]. Our research group also has prior experience in this technique [147].

Model proteins are often used to develop and evaluate release systems of this nature. A well selected model protein should have similar physicochemical characteristics to the active protein of interest as well as a published method to assess the structural activity of the protein following encapsulation and release. Lysozyme was selected

in this instance because of its similar characteristics to the growth factors of interest (Table 2.3, Page 52). Lysozyme also has a well documented activity assay involving the kinetic breakdown of a bacterial cell wall (Section 2.3.5.4, Page 42).

The main disadvantage to the *w/o/w* double emulsion fabrication method is a potential for protein denaturation and aggregation during fabrication. The primary emulsion step requires an aqueous solution of protein to be dispersed within an organic solvent. This generates a water/solvent interface. It has been shown that lysozyme unfolds and aggregates as a result of this interface [103]. This issue must be addressed to ensure maximum biological activity of an encapsulated growth factor. A potential solution has been to include excipients with the active protein that are thought to competitively block the harmful interface [102, 104, 121–123]. Albumins have been shown to maintain stability during lyophilization [148], to increase encapsulation efficiency within the polymer [145] and reduce aggregates [105].

The goal of *in vitro* release from therapeutic formulations is to replicate (as accurately as possible) what the *in vivo* release will be. From this data we can then estimate optimum formulations and dosages. This is not a simple endeavour. There are a number of factors to consider. The release media used to assess protein release are generally buffered solutions that replicate a physiological pH. Most authors favour phosphate buffered saline (PBS, pH 7.4) at 37 °C. Unfortunately, few proteins are stable in these conditions. Lysozyme, for example, aggregates in these conditions [101, 149] whereas it can be stabilised in a glycine buffer (pH 2.5) and demonstrated complete release [101]. The pH of a release medium also affects the protein degradation rate; acidic conditions catalytically affect the degradation of the esters present in PLGA [150].

A system that can be used for the controlled release of multiple proteins with different rates requires a number of key considerations. Protein release is a combination of three factors:

1. **Burst release** – The release of surface bound protein (or protein near to the surface).
2. **Diffusion** – Mediated by microparticle hydration/swelling and the presence of micro-channels.
3. **Bulk degradation** – The release of physically entrapped protein resulting from polymer scission erosion.

Inclusion of PLGA-PEG-PLGA can be used to modulate water ingress affecting diffusion and hydrolytic degradation. In addition the monomer ratios of PLGA

provide control over bulk degradation rates with minimal effects on hydrophilicity. A *w/o/w* fabrication method simply requires that the protein be water soluble, so is applicable to many proteins/growth factors. Minimal denaturation of the encapsulated proteins is critical. The addition of an albumin carrier should provide competitive protection to the harmful water/oil interface. Release assessment (*in vitro*) must accurately mimic the conditions expected *in vivo* including any protein adsorption, aggregation or denaturation so that appropriate judgements can be made regarding a therapeutic dose.

This chapter also introduces another potential application for a growth factor releasing microparticle system. This system has potential in biomimicry of extracellular matrix (ECM) as well as elucidating the importance and role of growth factors at a basic science level.

Concentration gradients have been used in cell-biomaterial screening [151] and to study cell processes such as migration and angiogenesis [152]. Concentration gradients of angiogenic factors are important in angiogenesis and neovascularisation causing endothelial cell migration up a concentration gradient and the sprouting of microtubules [153, 154]. Such gradients are being explored to increase endothelial cell migration into scaffolds with the aim of minimising necrosis [155]. More long range growth factor gradients are thought to enable efficient functioning of bones [156].

A number of methods have been developed to create chemical concentration gradients [157]. Most methods produce relative concentrations between two solutions. These can either be:

- Different concentrations of the same species.
- Concentrations of different species.
- Both the above.

The simplest method to generate a concentration gradient relies on molecular diffusion through a medium. This requires a source and a sink so that molecules can be passively diffused [158, 159]. Diffusion can be time consuming so techniques are being developed to make the process easier such as microfluidic devices [160]. Given sufficient source and sink volumes, stable gradients can theoretically be maintained for days using passive diffusion techniques.

Microparticles as growth factor delivery vehicles are being explored for spatiotemporal applications but there is very little literature regarding the generation of defined gradients using microparticle delivery. Theoretically microparticles could be a large

source of growth factors and deliver a steady dose, this would enable the generation of stable gradients for long periods. This could more accurately mimic *in vivo* environments and be useful as both a tool to increase our understanding of cellular responses to gradients but also as a method to increase the biomimicry within tissue engineered constructs.

PLGA microparticles have been used alongside silk scaffolds to try and create a gradient of BMP-2 and Insulin Growth Factor-1 (IGF-1) to study osteochondronic differentiation of human Mesenchymal Stem Cells (hMSCs) [161]. Differentiation was observed using the silk scaffolds but not the PLGA microparticles in alginate. It is possible that the diffusion was too rapid. A system has been demonstrated with PLGA microparticles to deliver a concentration gradient of dye with future applications for growth factor delivery [162].

It is hypothesised that our well characterised microparticles may be well suited for this application.

2.2 Aims

The aim was to develop a robust protocol to fabricate microparticles with consistent size and morphology. This fabrication method had to be suitable for the incorporation of fragile growth factors with high entrapment efficiencies. These microparticles had to exhibit sustained release profiles over different durations depending on the particular formulation.

A novel PLGA / PLGA-PEG-PLGA polymer system was selected to provide control over water ingress. The novelty for this piece of research is to vary this polymer blend in such a way that sustained release of proteins can be executed for different periods of time. For longer-releasing formulations this involved a protein release 'hand off' from diffusion mediated release to bulk erosion mediated release. To highlight other potential uses of this system, other methods were briefly explored to deliver and utilise these microparticles. They have applications in soft tissue regeneration and the development of more advanced *in vitro* models.

2.3 Methods

2.3.1 Synthesis of PLGA-PEG-PLGA

Triblock copolymers of PLGA and PEG were prepared by a ring opening polymerisation of D,L-lactide and glycolide in the presence of PEG with a small amount of stannous octoate. The process was described by Zentner *et al* in 2001 [141] and adapted by Hou *et al* in 2008 [163]. Under a dry nitrogen atmosphere, polyethylene glycol 1500 (PEG) (*Sigma, CAS: 25322-68-3*) and Tin (II) 2-ethylhexanoate (*Sigma, CAS: 301-10-0*) were heated to 45 °C to bring the PEG to a molten state. This was allowed to equilibrate for 1 hour. Dimers of DL-lactide (*Lancaster synthesis, CAS: 95-96-5*) and glycolide (*PURAC, Netherlands*) were added to the reaction vessel. The temperature was maintained between 110 °C and 150 °C for 8 hours. The crude polymer was purified by dissolving in a minimum amount of cold ($2 - 8$ °C) deionised water then heating to 80 °C to precipitate the polymer. The water (containing dissolved unreacted monomers) was discarded. This process was repeated. The polymer was freeze dried and stored at -20 °C.

2.3.2 Characterisation of PLGA-PEG-PLGA

2.3.2.1 Gel Permeation Chromatography

Gel permeation chromatography is a type of size-exclusion chromatography that measures the size of molecules and is commonly used to analyse polymers. It provides data regarding the distribution of molecular mass in a given polymer sample. Notable arithmetic outputs are the weight average molecular weight (M_W) and the number average molecular weight (M_N). M_W is a calculation of average molecular weight that is generally biased towards higher molecular weight molecules whereas M_N is an arithmetic mean that is biased towards lower molecular weight molecules. In a perfect polymer with a single molecular mass, these averages would be equal. These two methods for estimating the average molecular weight allow us to assign a numerical value relating to the degree of molecular weight heterogeneity. This is known as the polydispersity index (PDI) or heterogeneity index and is calculated as shown in equation 2.3.1.

$$PDI = M_W / M_N \tag{2.3.1}$$

The PDI is a value greater than or equal to 1. As the PDI approaches 1, the degree of molecular weight heterogeneity decreases.

Analysis was carried out using a GPC instrument (*PL-GPC 120, Polymer Labs*) with differential refractometer detection. Tetrahydrofuran (THF) was utilised as an eluent and two columns (30 cm, *PolarGel-M*) were fitted in series and calibrated against polystyrene standards.

2.3.2.2 ^{1}H Nuclear Magnetic Resonance

Proton nuclear magnetic resonance (^{1}H NMR) spectroscopy is a method of identifying the environment and abundance of protium atoms. This allows for extrapolations of molecular structure and molecular ratios. The three important pieces of information obtained from NMR are the chemical shift (δ), the spin-spin coupling and the integration curve. A higher value of δ is caused by a deshielded protium caused by the withdrawal of electron density by adjacent atoms. Tables are available for common functional groups listing δ values. Spin-spin coupling is the result of the magnetic field of neighbouring atoms splitting the detection peak. This provides further information as to the structure of the molecule. The integration curve is the area under detection peaks and directly correlates with the abundance of particular protium environments within a sample. A typical NMR spectra for PLGA-PEG-PLGA is shown (Figure 2.1). The molecular structure of PLGA-PEG-PLGA is shown and indicated to illustrate how the peaks correspond to functional groups. From the integration values at these functional groups it is possible to calculate the ratio of lactide to glycolide and the ratio of PLGA to PEG.

Proton Nuclear Magnetic Resonance (NMR) spectra of PLGA-PEG-PLGA samples were obtained in deuterated chloroform ($CDCl_3$) using an NMR instrument (*DPX-300, Bruker*) at 400 MHz. A tetramethylsilane (TMS) signal was taken as the zero chemical shift. Number-average molecular weight, lactide to glycolide ratio and PLGA to PEG ratio were calculated by integrating the signals relating to each monomer – the CH and CH_3 pertaining to DL-lactide, the CH_2 of glycolide and the CH_2 of ethylene glycol (Figure 2.1).

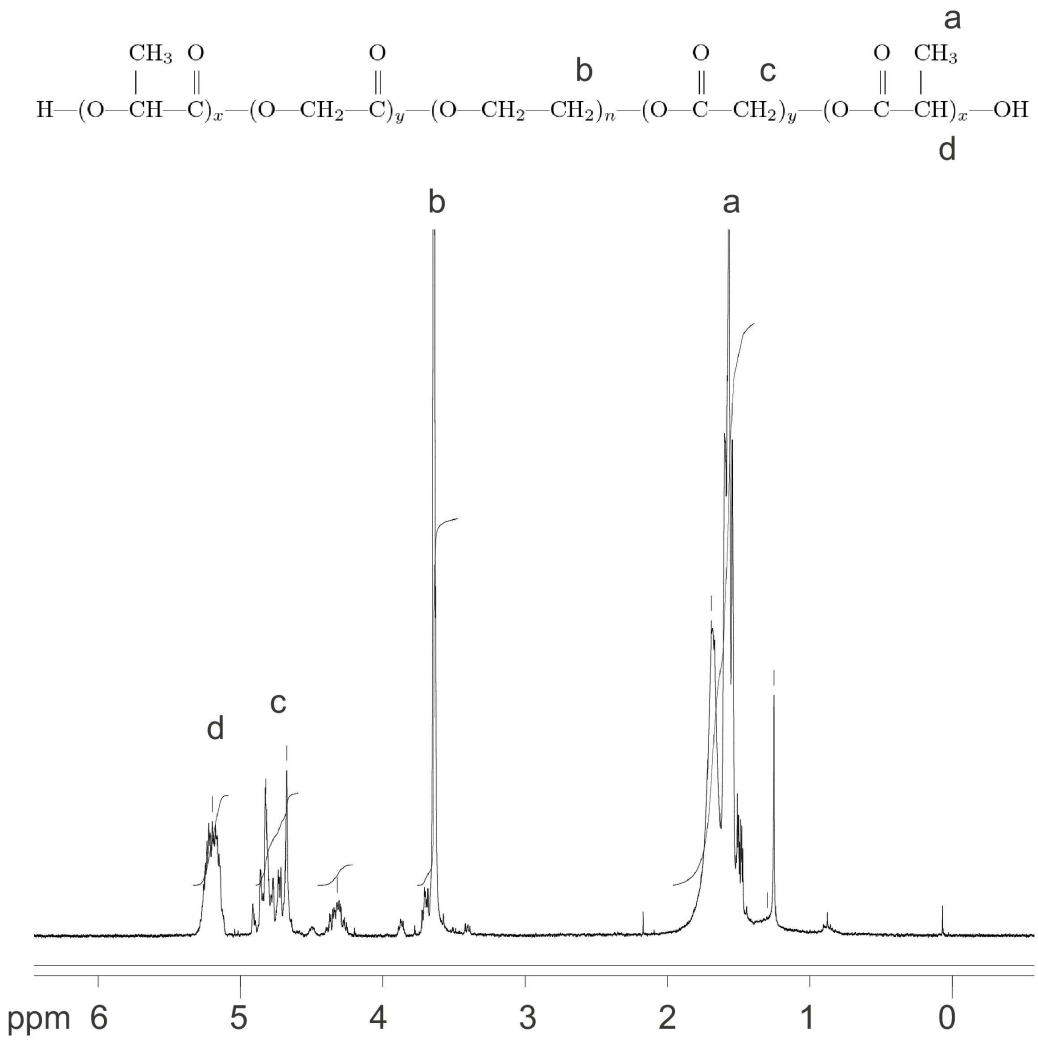

Figure 2.1: Representative ^{1}H NMR spectrum of PLGA-PEG-PLGA triblock copolymer.

2.3.3 Microparticle Fabrication

Microparticles were prepared using the well reported technique of double emulsion solvent evaporation. Briefly a w/o/w emulsion was formed consisting of the aqueous molecules of interest within an organic solvent containing dissolved polymer within an aqueous surfactant. This fabrication process is outlined in figure 2.2 on page 40. Specific details regarding the polymer can be found in table 2.1.

2.3.3.1 Vortex Method

Poly(DL-lactic-co-glycolic acid) (1.00 g) was dissolved in 5 ml dichloromethane (DCM) in a 25 ml scintillation vial forming the organic phase. A protein solution consisting of 10 mg protein in 100 µl deionised water was added to the organic phase and held on the vortex shaker at a 45 degree angle for 90 seconds forming the primary emulsion. This primary emulsion was added to 200 ml of 0.3% *w/v* polyvinyl alcohol in a 250 ml beaker while being stirred at 300 rpm. This produced the secondary emulsion.

After 4 hours the suspension of microparticles was filtered and washed with 2 l of deionised water using vacuum filtration and a 0.2 µm filter. The microparticles were transferred to a 20 ml centrifuge tube, snap-frozen using liquid nitrogen and then dried on a freeze dryer for 24 hours (until dry). Microparticles were vacuum sealed and stored at $-20\,^{\circ}\mathrm{C}$.

2.3.3.2 Homogenisation Method

Poly(DL-lactic-co-glycolic acid) (1.00 g) was dissolved in 5 ml dichloromethane (DCM) in a 30 ml PTFE jar forming the organic phase. A protein solution consisting of 10 mg protein in 100 µl deionised water was added to the organic phase and homogenised for 2 minutes at speed *A* forming the primary emulsion. This primary emulsion was added to 200 ml of 0.3% *w/v* polyvinyl alcohol in a 250 ml beaker and homogenised for a further 2 minutes at speed *B* forming the secondary emulsion. The beaker was then magnetically stirred with a 50 mm glass encased stirrer bar at 300 rpm for 4 hours.

The suspension of microparticles was filtered and washed with 2 l of deionised water using vacuum filtration and a 0.2 µm filter. The microparticles were transferred to a 20 ml centrifuge tube, snap-frozen using liquid nitrogen and then dried on a freeze dryer for 24 hours (until dry). Microparticles were vacuum sealed and stored at $-20\,^{\circ}\mathrm{C}$.

Homogeniser speed *A* and *B* were used to control the resulting microparticle size.

mole% lactide	mole% glycolide	Inherent viscosity (dl/g)	M_W (Da)	M_N (Da)	PDI
50	50	0.44	56,000	30,000	1.87
85	15	0.45	56,000	32,000	1.75

Table 2.1: Molecular data of the PLGA used for microparticles. This data was obtained from Lakeshore Biomaterials analytical report. Inherent viscosity was carried out in 0.5% *w/v* in chloroform at 30 °C. These two formulations are later referred to as PLGA 50:50 and PLGA 85:15

Speeds of 4,000 and 9,000 rpm (respectively) produced a modal particle size of $22 - 26$ µm and speeds of 2,000 and 2,000 rpm produced a modal size of $70 - 100$ µm. Lower homogenisation speeds failed to produce complete and homogeneous emulsions and higher speeds caused excessive foaming.

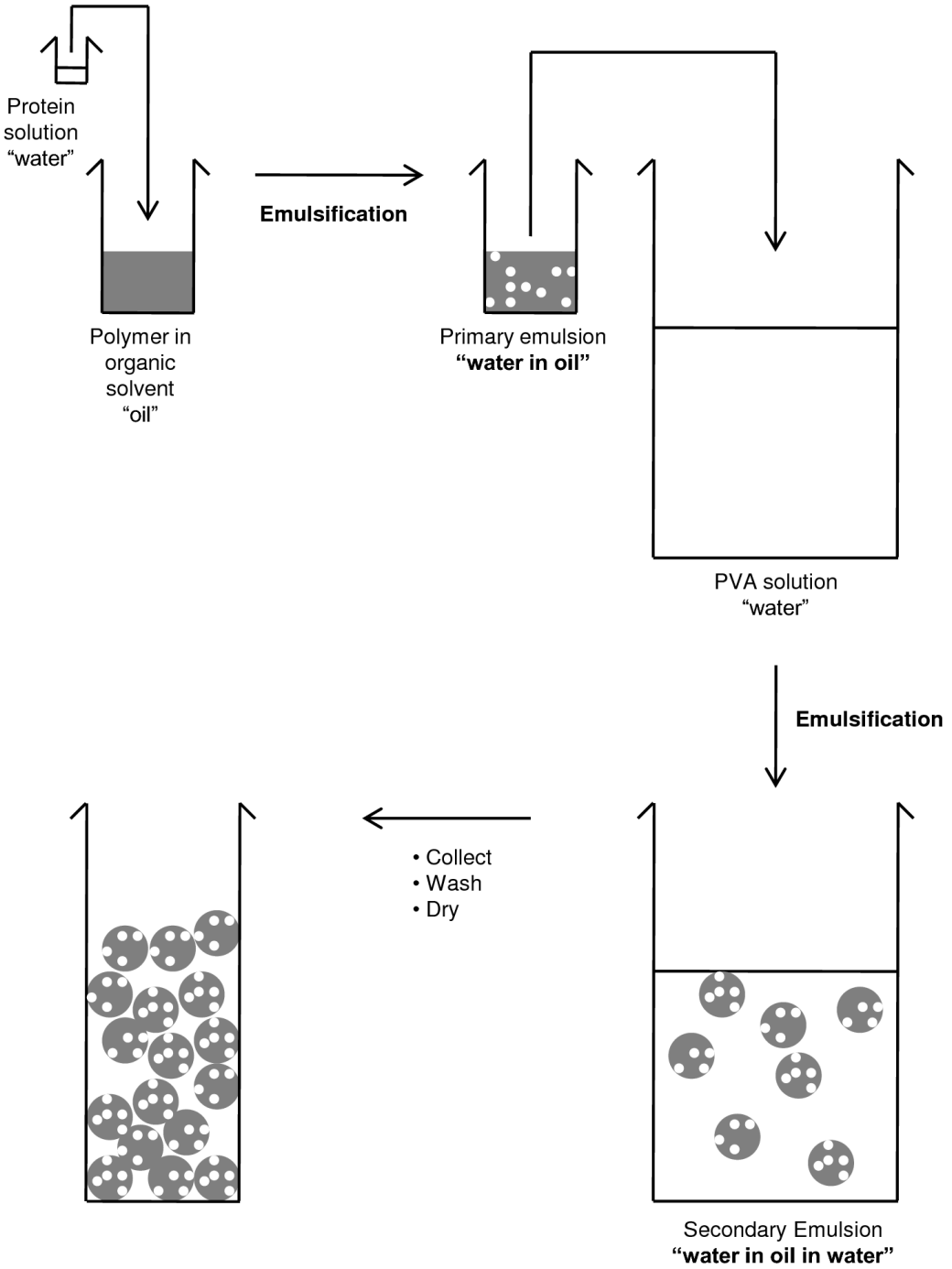

Figure 2.2: Schematic showing the double emulsion method of microparticle fabrication. This is the same method whether vortex or homogenisation is used to form the emulsions. This diagram is not to scale.

2.3.4 Microparticle Characterisation

2.3.4.1 Scanning Electron Microscopy

Microparticles were mounted on 12.7 mm SEM stubs (*Agar, G301*) and adhered using 12 mm adhesive carbon tabs (*Agar, G3347N*). Samples were sputter coated for 4.5 minutes using a Balzers SCD 030 gold sputter coater (*Balzders Union Ltd., Leichtenstein*) and imaged using a Jeol 6060LV variable pressure scanning electron microscope (*Jeol (UK) Ltd.*) with an accelerating voltage of 10 kV.

2.3.4.2 Size Analysis using Laser Diffraction

Microparticles were sized by laser diffraction using a Coulter LS230 (*Beckmann Coulter*) fitted with the optional hazardous fluids module. Background readings (water alone) were measured and subtracted and the software was loaded with the refractive index of water (The suspension fluid) and garnet (a mineral with similar optical charcteristics to PLGA). Samples of microparticles were suspended in double deionised water and gradually added to the Coulter module until an obscuration of 8-12% was indicated. Three 30 second runs were averaged and recorded.

2.3.5 Assessment of Protein Release From Microparticles

2.3.5.1 Assessment of Encapsulation Efficiency

Encapsulation of protein within the microparticles was determined using a method developed by *Sah et al* [164] and adapted by *Morita et al* [118]. Microparticles (10 mg) were incubated in dimethylsulphoxide (DMSO) (750 µl) at room temperature for 1 hour. A solution of sodium lauryl sulphate (0.02 %) in 0.2 N sodium hydroxide (2150 µl) was then added for a further hour. This resulted in a solution of polymer and protein. This was neutralised using dilute hydrochloric acid and the protein content was measured using a BCA protein assay (Section 2.3.5.3, Page 42). Appropriate controls (microparticles with no protein) were used.

2.3.5.2 Protein Release *in vitro*

Protein was released into phosphate buffered saline at 37 °C with agitation from an orbital stage set at 5 rpm. These conditions were selected to mimic *in vivo* environments as closely as possible. Initial release studies using model proteins were released

as follows. Dry microparticles (50 mg) were combined with PBS (3 ml) in a 15 ml centrifuge tube (*Greiner, 188261*). This was incubated on the orbital rocker and the PBS was sampled at regular intervals determined (in part) by the amounts of protein released and the detection limits of the assay. Sampling involved allowing the microparticles to settle then completely removing and replacing the PBS. Release supernatants were stored at $-20\,^{\circ}C$ prior to assaying.

Release studies for growth factor loaded microparticles were carried out on a smaller scale whereby dry microparticles (25 mg) were added to PBS (1.5 ml) in a 1.6 ml Eppendorf (*Sarstedt, 72.690*). Work within the group demonstrated that this reduction in scale had no significant effect on release characteristics (unpublished data).

2.3.5.3 Protein Quantification

Protein was quantified using a bicinchoninic acid (BCA) assay (*Thermo Scientific Pearce, 23335*). This assay colorimetrically quantifies peptide groups found within protein molecules [136]. Calibration solutions were custom made to be representative of the mixture of protein types within the samples and within the same dissolution medium as the samples, in this case PBS. Calibration plots were obtained for each individual microplate to account for differences in incubation times and plate anomalies. If measured protein concentrations were outsude the linearity of the assay (i.e. not within the calibration plot range) then the samples were appropriately diluted and the assay repeated. Each sample was assayed in triplicate. Unknown samples were compared against the calibration plot in the linear range of the assay. Least squares regression was used to calculate the equation of a trend line based on the calibration samples; this equation was used to obtain the concentration of unknown samples.

2.3.5.4 Quantification of Active Lysozyme

In 1922 Alexander Flemming first identified lysozyme through its destructive effect on a suspension of *Micrococcus lysodeikticus* [165]. Lysozyme breaks down the cell wall of *Micrococcus lysodeikticus* by lysing a 1,4 glycosidic bond. The rate of this enzymatic effect is dependent upon concentration of the lysozyme and the concentration of *Micrococcus lysodeikticus* can be determined by measuring the turbidity of the solution at 450 nm. [Nb, I may move this first bit into another chapter]A variation upon protocols published by Bezemer *et al* [166] and Sohier *et al* [167] was used. A suspension of *Micrococcus lysodeikticus* (*Sigma, M3770*) in water (2.3 mg/ml) was prepared, 100 µl

of which was added to 100 µl of release supernatant in a 96 well plate and the change in turbidity at 37 °C over one minute measured at 405 nm using a colorimetric plate reader (*Infinite M200, Tecan Uk Ltd.*). The change in turbidity of samples was compared to a calibration plot in the linear range of 0-25 µg/ml to obtain the lysozyme concentration.

2.3.6 Selection of a Hydrogel to Position Microparticles

A number of hydrogels were assessed as the patterning substrate. Suitable gels had to possess two key characteristics:

1. *Physical characteristics* that allowed positioning of microparticles without disrupting the structure of the gel (tearing) followed by rapid gelation to ensure the positioned microparticles stay in place.
2. *Chemical characteristics* that facilitate the diffusion of large molecules such as proteins with minimal binding or denaturation.

Both the physical and chemical characteristics also had to act together in a suitable way to allow cell attachment, proliferation and differentiation.

A novel method to functionalise agarose with gelatin was selected. This provided a substrate with the correct physical characteristics as well as the necessary cues for cell adhesion and proliferation (Appendix D, Page 125).

This hydrogel facilitated positioning of microparticles with a high degree of accuracy (Figure 2.16).

2.3.7 Micro-positioning of Microparticles

Microparticles were suspended in saline (0.9 %) and custom pulled glass capillaries were used to inject and manipulate microparticles as desired. Glass capillaries were coupled to a micro-injector (*CellTran vario, Eppendorf*) to give precise control over injection volumes. Accurate positioning was achieved using a micro-manipulator (*TransferMan NK2, Eppendorf*) and visualised with an inverted microscope (*DM IRB, Leica*).

2.3.8 Statistical Comparisons and Data Analysis

Statistical analyses were carried out using the software environment 'R' [168, 169] (version 2.10.1). Sample data was assessed for normality and variance using quantile-quantile plots and F-tests, respectively. Statistical methods were chosen accordingly.

Statistical significance was defined with a confidence interval of 95%. Comparisons with a p-value of less than 0.05 were considered significant. For certain graphical comparisons box plots were favoured over bar graphs as they are better for representing averages. Outliers (in normally distributed data) were defined as values that were $\geq$ 2.5 quantiles from the mode.

All data analysis was carried out on an i486-pc-linux-gnu platform running Ubuntu 10.04 LTS. OpenOffice.org (version 3.2.0) and Python^{TM} (version 2.6) were utilised to manage and process data.

2.4 Results and Discussion

2.4.1 Fabrication

2.4.1.1 Polymer formulation

Two different formulations of PLGA were chosen for assessment. Specific details of the formulations can be found in table 2.1 on page 39. These polymers were chosen because they have similar characteristics but different lactide to glycolide ratios. PLGA with a monomer ratio of 85:15 is known to have a slower degradation rate than 50:50 and both ratios have been documented for protein release [101, 170]. This difference in degradation rates was exploited in order to influence protein release.

PLGA-PEG-PLGA was used as an adjunct in the polymeric formulation in order to further modulate water ingress into the polymer matrix and allow further tuning of release characteristics.

2.4.1.2 PLGA-PEG-PLGA Characterisation

Synthesis of PLGA-PEG-PLGA is susceptible to batch-to-batch variation and long-term storage may lead to degradation and changes in polymeric characteristics. It was important to characterise each batch after synthesis as well as at later time points. Significant differences in the PLGA-PEG-PLGA structure could affect the polymers overall hydrophilicity thus affecting water ingress, hydrolytic degradation and protein release rates. Different overall chain length could also result in different physicochemical characteristics.

The GPC and NMR data for different batches of PLGA-PEG-PLGA are shown (Table 2.2). Each batch was assessed immediately after synthesis and at later intervals to evaluate changes over time.

The batches show inter-batch variation but to no greater extent than intra-batch variation. The discrepancies between batches appeared relatively small. Since no data was available regarding manufacturing tolerances of this process with respect to protein release it was decided that that this variation would be acceptable for initial studies. Protein release from microparticles fabricated using different triblock batches would be monitored for differences.

If we assume that hydrolytic degradation is the only breakdown method acting on the copolymer then we would expect to see a reduction in PLGA chain length over time and the ratios of monomers to remain the same. This reduction in chain length

	^{1}H NMR			GPC		
Batch A	M_N	% mole lactide	% mole glycolide	M_N	M_W	PDI
Mar 2011*	1577–1500–1577	83	17	2861	4590	1.60
Jun 2011	1706–1500–1706	71	29	2442	4022	1.65
Mar 2012	1695–1500–1695	75	25	2577	4539	1.76
Batch B						
Jun 2011*	1589–1500–1589	72	28	1874	3338	1.78
Mar 2012	1435–1500–1435	73	27	2632	3844	1.46
Batch C						
Jun 2011*	1428–1500–1428	70	30	2576	3960	1.54
Mar 2012	1653–1500–1653	75	25	3026	4582	1.51

Table 2.2: Proton NMR and GPC characterisation of PLGA-PEG-PLGA. Batches were assessed post synthesis and at later intervals. This table details three batches of copolymer; A, B and C. The dates indicate the date of assessment, the first date (*) being immediately after fabrication. The NMR M_N is in the format of the three polymer strings within PLGA-PEG-PLGA, the mass of PEG being known and the PLGA chains determined numerically. Literature commonly represents the data in this way.

would only be apparent in GPC data as it assesses complete chain lengths whereas NMR works under the assumption that *all* the monomers present are polymerised and numerical averaging produces a result based on the assumption that the chain length is monodisperse. It appears that there are polymer fragments and potentially un-reacted monomers in the mixture. This is why the number average molecular weight value differs between NMR and GPC techniques.

What we see from the data (Table 2.2) is that there appears to be no trend in the change of PLGA-PEG-PLGA chain length over time. The results appear variable. We deduce from this that the batch of polymer had a non-homogeneous bulk consistency so aliquots used for analysis differed to a greater extent than any overall change induced by degradation. This effect could potentially be mitigated in the future by the addition of a final mixing step. Similarly there is a slight variation of the lactide:glycolide ratio over time. This is also attributed to sampling variation.

2.4.1.3 Double emulsion microparticle fabrication

Microparticle fabrication within the group had previously been carried out using a vortex mixer to form the primary emulsion [147, 171]. It was initially apparent that

this method was variable as the degree of vortex achieved was dependent on the technique of the user. A comparison was carried out between the vortex method for emulsification and the use of a homogeniser which utilised a radial flow impeller imparting shear stress.

Representative batches of microparticles were formed using vortex and homogenisation methods. size distributions were assessed using laser diffraction (Figure 2.3).There is high degree of microparticle size variability exhibited my microparticles formed using the vortex method. In contrast the homogenisation method produced a more consistent size distribution. The size distribution of microparticles will affect microparticle surface area thus diffusion and degradation rates. Some studies exploit this releationship between surface area and drug diffusion rates to modulate release [146]. In order to achieve consistent microparticle physical characteristics it was decided that the homogenisation method would be utilised for all further fabrication.

Images of microparticles obtained using electron microscopy (Figure 2.4) show that after fabrication and lyophilisation the microparticles retain a regular spherical morphology. There are also few micro pores and no visible cracks in the microparticles. These are factors that could affect protein release as the initial release is dependant on protein release from, or near to, the surface of the microparticles. A greater surface area resulting from a porous structure would likely have a higher burst release. The SEM images qualitatively validate the sizing data obtained using laser diffraction. Assessment of these formulations indicated that the inclusion of this triblock copolymer has an influence on microparticle size. Increasing levels of PLGA-PEG-PLGA, decrease the average microparticle size. It is likely that the copolymer is stabilising the emulsion due to it's surfactant structure. This would result in more efficient emulsion generation and reduce the likelihood of micelles coalescing.

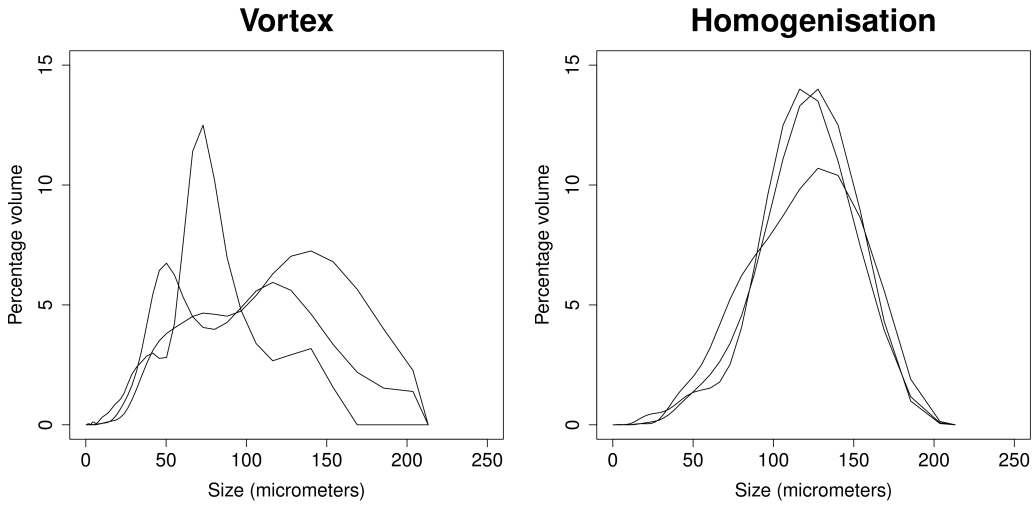

Figure 2.3: Size distributions of microparticles formed using the vortex method and the homogenisation method. Microparticles formed by vortex show a higher variability in size to those formed using the homogenisation method. Plots show the distribution of representative samples from three independent batches of microparticles. Microparticles were fabricated using the vortex method (2.3.3.1 on page 38) and the homogenisation method (2.3.3.2 on page 38 – *A* and *B* speeds of 2,000 and 2,000 rmp) using PLGA 50:50 (Table 2.1 on page 39) and sized using method 2.3.4.2 on page 41.

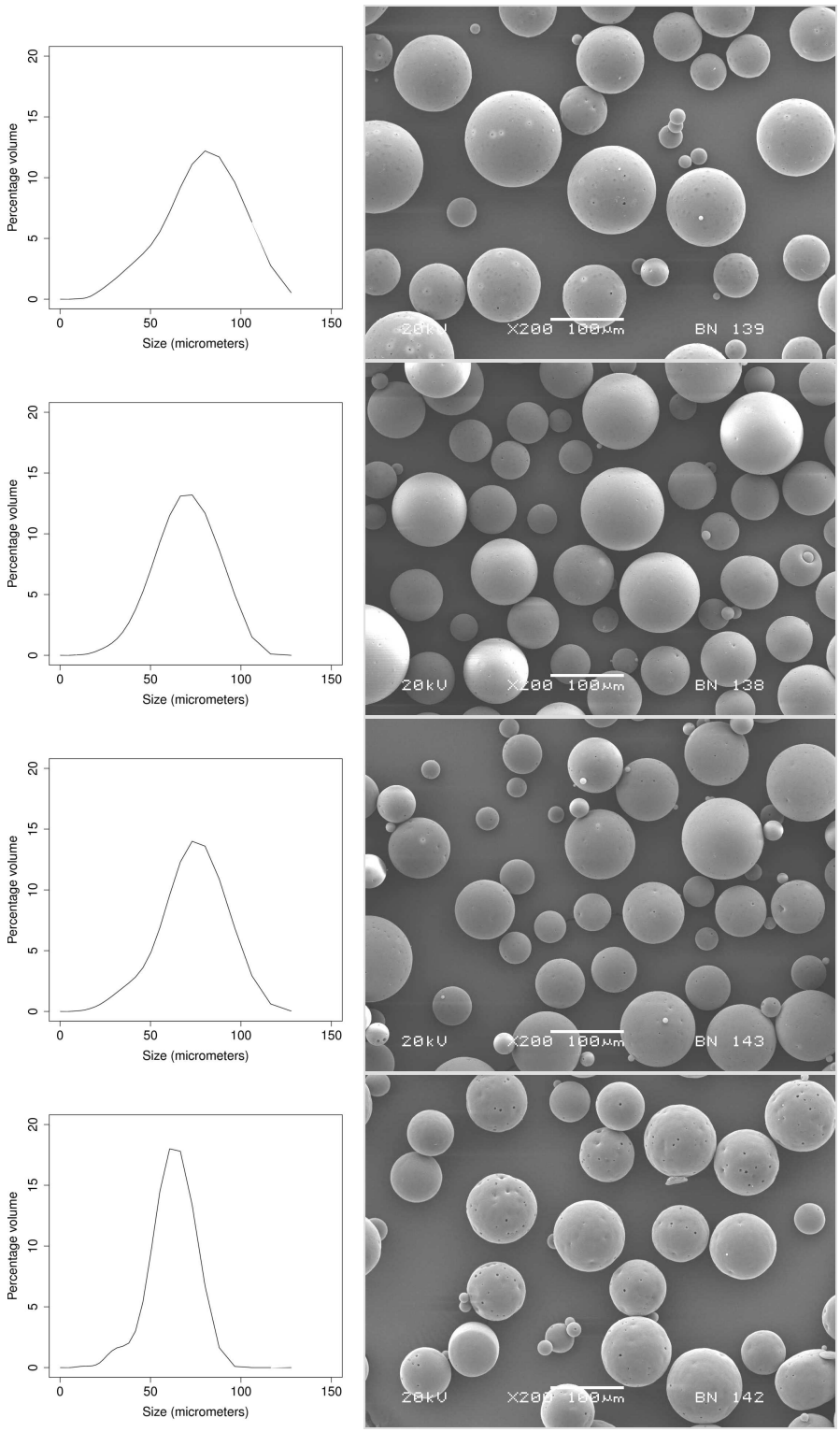

Figure 2.4: Images of microparticles obtained using SEM alongside their corresponding size distributions obtained using laser diffraction. Microparticles were fabricated using the homogenisation method (2.3.3.2 on page 38 – *A* and *B* speeds of 2,000 and 2,000 rmp) using PLGA 50:50 (Table 2.1 on page 39), sized using a laser diffraction method 2.3.4.2 on page 41 and imaged using electron microscopy (2.3.4.1 on page 41). Microparticles contained different amounts of PLGA-PEG-PLGA, in descending order; 0 %, 10%, 20 % and 30% (w/w)).

Changing the homogenisation speed of the primary and secondary emulsions enabled control of the resulting microparticle size (Figure 2.5). Additional factors such as organic solvent volume and surfactant bath volume also affect the resulting size but these and other variables were kept constant for this study. Two homogenisation conditions were decided upon for further study. These yielded microparticles with modal sizes of 21.7–26.2 µm and 73.0–88.0 µm.

Larger microparticles in the 73–88 µm size range were taken forward for assessment for use in the segmental defect. The smaller microparticles in the 22–26 µm size range were briefly explored for their potential application in small mammal studies (Section **??**, Page **??**). This smaller particle size is more conducive with injectable delivery into a small site of interest.

2.4.1.4 Assessment of Protein Entrapment

Microparticles were fabricated in the 73.0 - 88.0 µm size range and HSA encapsulated within them (1 % *w/w*). Polymer formulations consisted of both PLGA 50:50 and 85:15 with levels of PLGA-PEG-PLGA incorporation at 0 %, 10 % and 30 %. No significant differences in encapsulation were observed between formulations (p=0.05). The mean entrapment efficiency was 94 % with a standard deviation of 8.9 %.

Measurement of entrapment efficiency was a highly laborious process and *pH* variations could lead to errors. Since entrapment efficiency appeared to be independent of polymer formulation, percentage protein release would be plotted based on loaded protein rather than a measured value. This also facilitated the additional scale showing the levels of actual protein release. This was considered more relevant when determining a therapeutic effect of growth factor released from a fixed mass of microparticles.

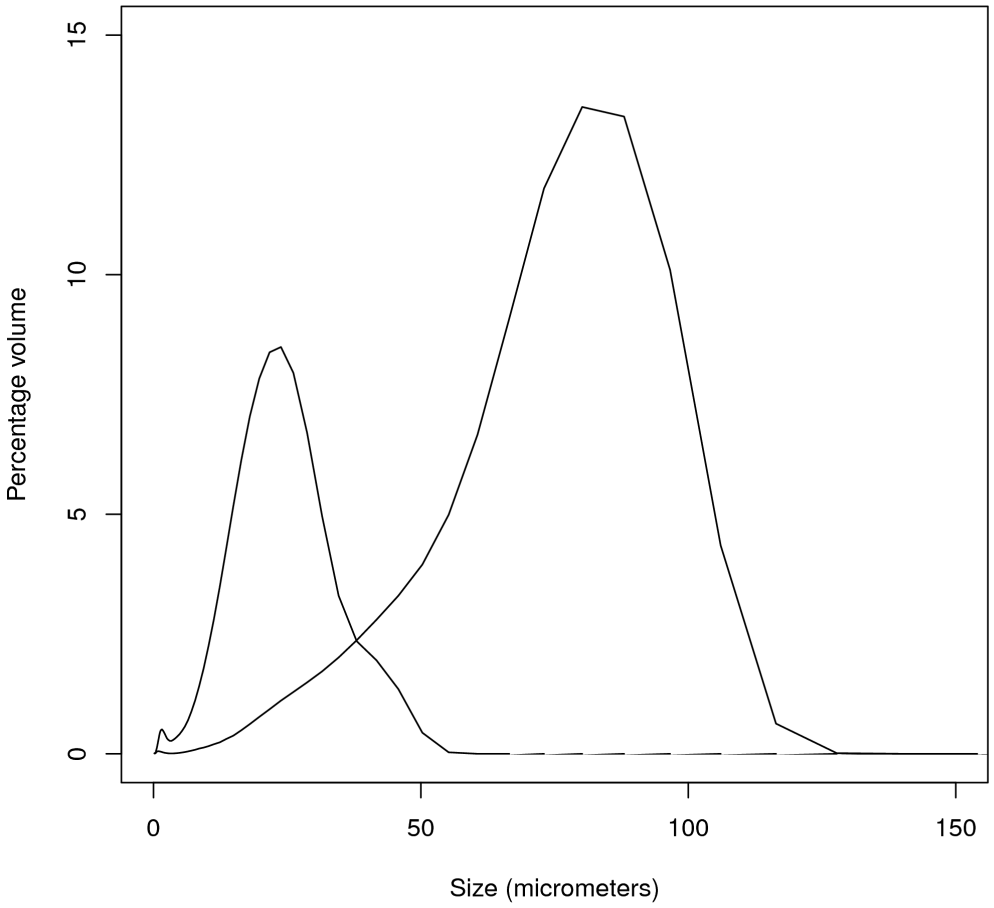

Figure 2.5: Size distributions of two different representative batches of PLGA 50:50 (Table 2.1, page 39) microparticles formed using different homogenisation protocols (method 2.3.3.2 on page 38 – *A* and *B* speeds of 2,000 & 2,000 and 4,000 & 9,000). Microparticles were sized using laser diffraction (method 2.3.4.2 on page 41). Batches of microparticles with modal sizes of 21.7 - 26.2 µm and 73.0 - 88.0 µm are shown. This shows how variations to the protocol are able to vary the resulting size of microparticle batches.

2.4.2 Quantification of protein release

2.4.2.1 Formulation assessment

Initial release studies were carried out with a model protein; lysozyme. A model protein was used because of the high cost of growth factors. Lysozyme was chosen because it has similar physicochemical properties to BMP-2 (Table 2.3). It was hoped that it would therefore be a good substitute for BMP-2 from a release standpoint. The three growth factors of interest have basic isoelectric points ($_pI$) so will all be positively charged at physiological pH. Their molecular weights are relatively similar; although VEGF may require an additional model protein with a higher molecular weight to accurately mimic its release characteristics.

The activity of lysozyme can be assessed with a kinetic assay, this enabled us to assess whether encapsulation and release was significantly detrimental the the conformational activity of lysozyme. It also allowed us to differentiate lysozyme release from HSA release. An overall protein loading of 1 % *w/w* was selected. It exhibited high encapsulation efficiencies during previous assessment (Figure **??**) and would allow us to load growth factor at very high concentrations if necessary. Loaded protein was a combination of active factor and HSA. Complementary levels of HSA were used to achieve a 1 % *w/w* loading. In this case a 1:9 *w/w* ratio of lysozyme and HSA were used as initial calculations suggested that this loading of growth factors would be required in the segmental defect model to achieve therapeutic levels of delivery.

Protein	Molecular weight (kDa)	Isoelectric point ($_pI$)
HSA	66.5	5.3
Lysozyme	14.3	11.35
BMP-2	26	8.5
VEGF	38.2	8.5
PDGF	24.3	9.8

Table 2.3: Physicochemical characteristics of all proteins to be assessed within microparticles in this thesis. The data was obtained from literature [172–177].

In order to quickly identify achievable release profiles, a selection of formulations were chosen. A PLGA-PEG-PLGA ratio of 30 % was the highest whereby the microparticles still flowed at room temperature. Above this the microparticles tended to aggregate. Ratios of 0 %, 10 % and 30 % (*w/w*) PLGA-PEG-PLGA were selected for each PLGA

formulation. Cumulative protein release from these formulations can be seen in figures 2.6 and 2.7.By day 72 the microparticles had visibly degraded and protein was no longer detected.

In order to correctly interpret this data it is important to have an understanding of the underlying mechanisms that take place during degradation. A high initial release in the first 12 to 24 hours (often termed 'burst' release) is due the detachment of surface-bound protein and diffusion of protein near to the surface. A burst-type release is only observed in PLGA 50:50 (30 % *w/w* PLGA-PEG-PLGA). As no other formulations exhibit this burst, we hypothesised that the thorough washing protocol during fabrication removed this surface-bound protein. The burst in this particular formulation was attributed to physical polymer characteristics favouring water ingress and facilitating a higher level of surface diffusion. PLGA 50:50 had a lower glass transition (T_g) temperature than the corresponding 85:15 formulation [178]. Combining this formulation with a high amount of PLGA-PEG-PLGA plasticiser will serve to further modify its physical characteristics while increasing the hydrophilic component. For this reason we deduced that the observed burst release could be attributed to protein diffusion facilitated by water ingress.

A lag phase prior to protein release can be seen from PLGA 50:50 (0 % *w/w* PLGA-PEG-PLGA) and PLGA 85:15 (10 % *w/w* PLGA-PEG-PLGA). A lag phase is generally thought to be undesirable as release is often below therepeutically active levels. However in certain situations this could be advantageous. For example if we want to mimic the temporal expression of a particular growth factor (expressed after another) without additional invasive procedures.

Formulations of particular interest are PLGA 50:50 (10 % *w/w* PLGA-PEG-PLGA) and PLGA 85:15 (30 % *w/w* PLGA-PEG-PLGA) as these exhibit no burst release. They instead immediately begin to steadily release protein at a consistent rate for a duration of 7 and 25 days respectively. PLGA 85:15 (30 % *w/w* PLGA-PEG-PLGA) exhibited almost perfect zero-order release over the first 7 days before tailing off (Figure 2.8). This release occurred before the polymer had degraded since polymer was still present at day 7. It was theorised that the release was instead due to swelling and diffusion induced by the high level of PLGA-PEG-PLGA. Steady release over the initial 25 days was exhibited by PLGA 50:50 (10 % *w/w* PLGA-PEG-PLGA) (Figure 2.9). This 25 day release does not demonstrate perfect zero-order kinetics as the release appears to be a combination of a mitigated burst release combined with degradation mediated release. Addition of 10 % PLGA-PEG-PLGA allowed us to tune the release kinetics of PLGA 50:50 to provide a consistent protein release that could not be achieved with PLGA

alone.

By day 30 all of the PLGA 50:50 microparticles had completely degraded and stopped releasing protein but some of the 85:15 formulations continued releasing up to day 70.

Incomplete protein release was apparent in formulations releasing beyond two weeks. It was speculated that this was partly due to a drop in *pH* induced by solubilised lactic acid and glycolic acid. More regular buffer replenishment may have mitigated this issue but the sampling/buffer-replenishment schedule was dictated by the levels of protein release. As protein release reduced, the rate of sampling was reduced so that the protein concentration was high enough to be within the linear working range of the protein assay. The BCA assay relies on the reduction of Cu^{2+} to Cu^{+} which proceeds under alkaline conditions [136]. The drop in *pH* may have adversely affected this. In addition this drop in *pH* most likely affected protein aggregation and adsorption. A *pH* drop could lead to aggregation and reduced release of some proteins such as albumin [111] or reduced adsorption of other proteins such as lysozyme [101]. It is hypothesised that these factors are the main cause of incomplete release. Switching to a more acid compliant protein assay such as the Bradford assay and using a higher concentration of buffer salts are means by which we could have tackled this issue. There appears to be no ideal release situation. Sometimes greater complete release can be demonstrated *in vitro* under artificial conditions [101, 179] but these may not be representative of *in vivo* performance. If great effort is made to try to maintain a physiological *pH*, the requirements may have a detrimental affect on the proteins. For example higher buffer salt concentrations would change the ionic strength and could reduce polymer degradation or induce protein aggregation [180]. It was decided that in order to keep release data comparable and applicable *in vivo*, future release studies would be carried out under the same conditions.

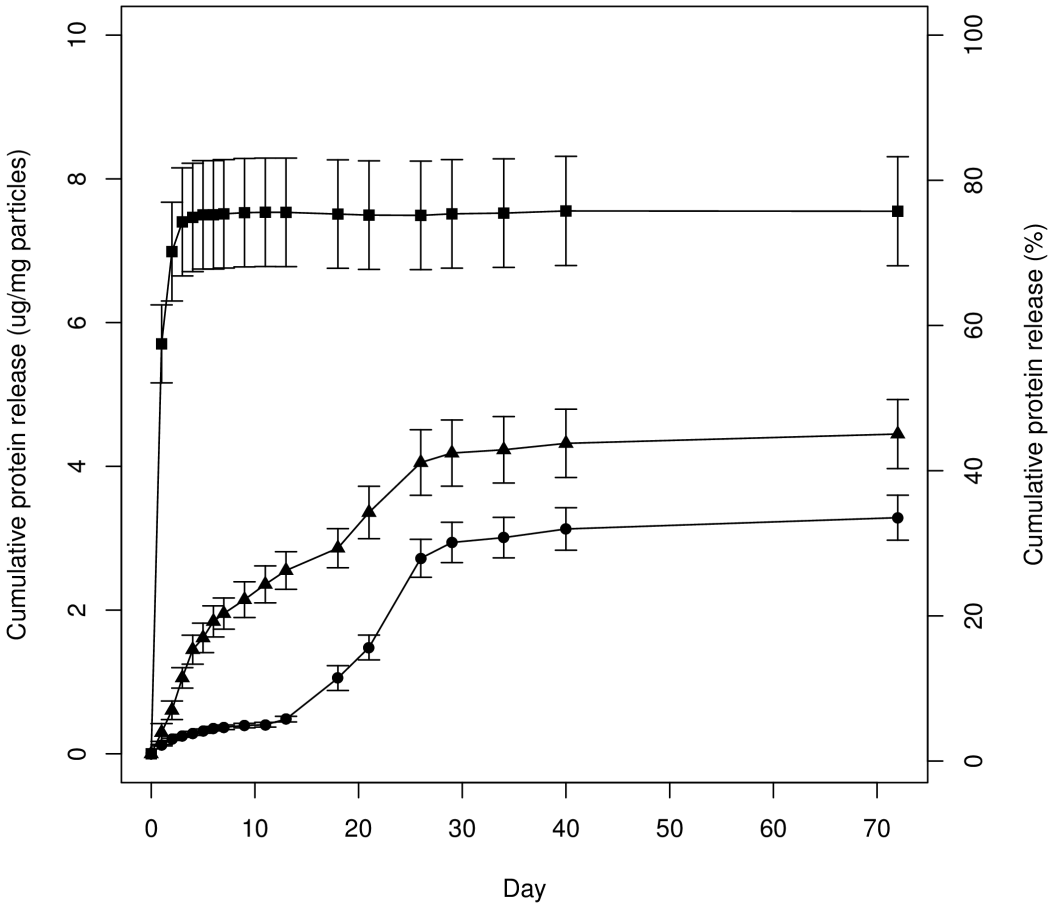

Figure 2.6: Cumulative release of HSA/Lysozyme from microparticles formulated from 50:50 PLGA (Table 2.1 on page 39) with 30 % (■), 10 % (▲) and 0 % (●) *w/w* of PLGA-PEG-PLGA copolymer (Section 2.3.1). Protein release was quantified using a BCA assay (Section 2.3.5.3). Error bars show ± standard deviation of the mean; n=3.

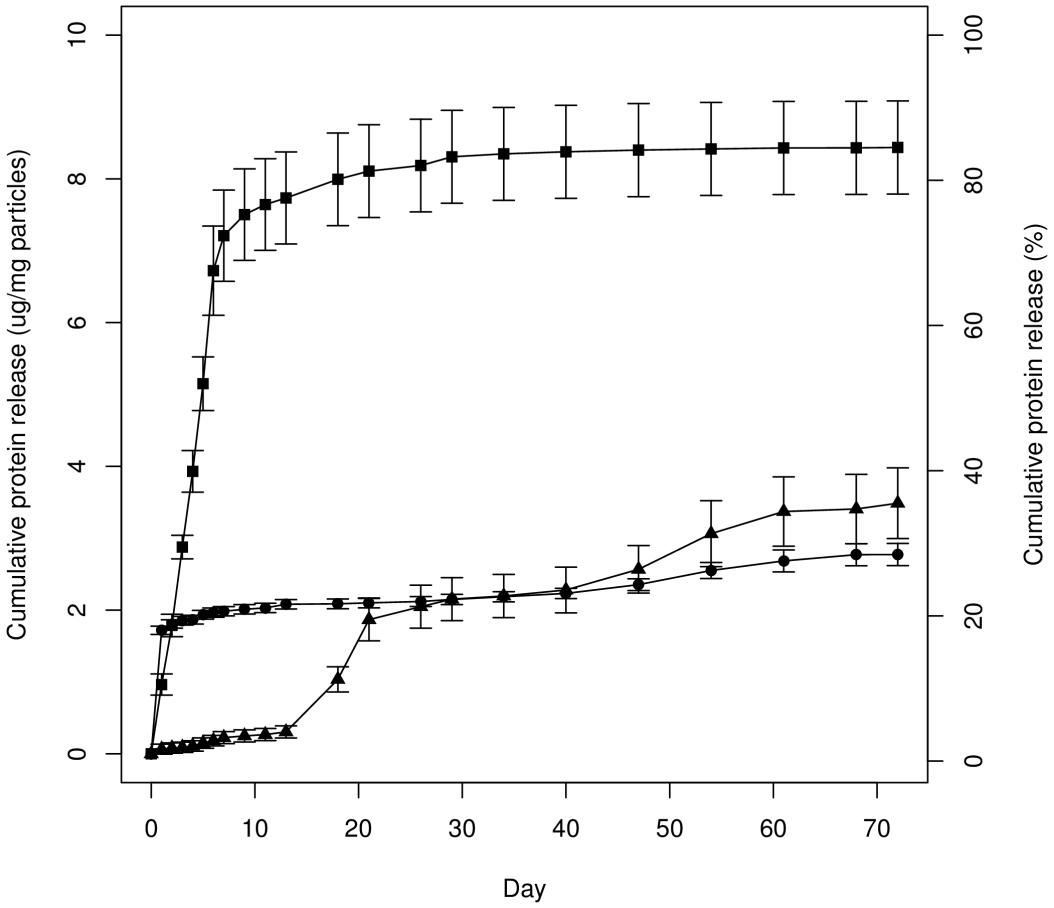

Figure 2.7: Cumulative release of HSA/Lysozyme from microparticles formulated from 85:15 PLGA (Table 2.1 on page 39) with 30 % (■), 10 % (▲) and 0 % (●) *w/w* of PLGA-PEG-PLGA copolymer (Section 2.3.1). Protein release was quantified using a BCA assay (Section 2.3.5.3). Error bars show ± standard deviation of the mean; n=3.

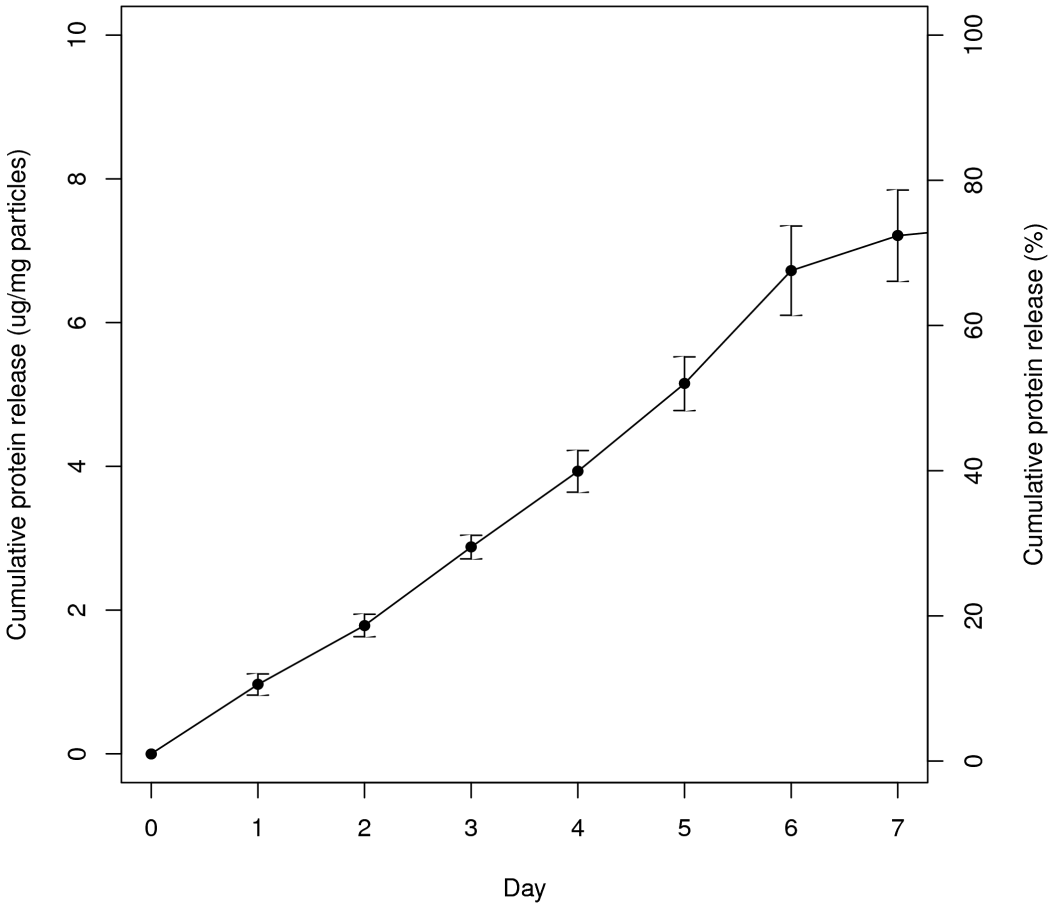

Figure 2.8: Cumulative release of HSA/Lysozyme from microparticles formulated from 85:15 PLGA (Table 2.1 on page 39) with 30 % *w/w* of PLGA-PEG-PLGA copolymer (Section 2.3.1). Protein release was quantified using a BCA assay (Section 2.3.5.3). Error bars show ± standard deviation of the mean; n=3.

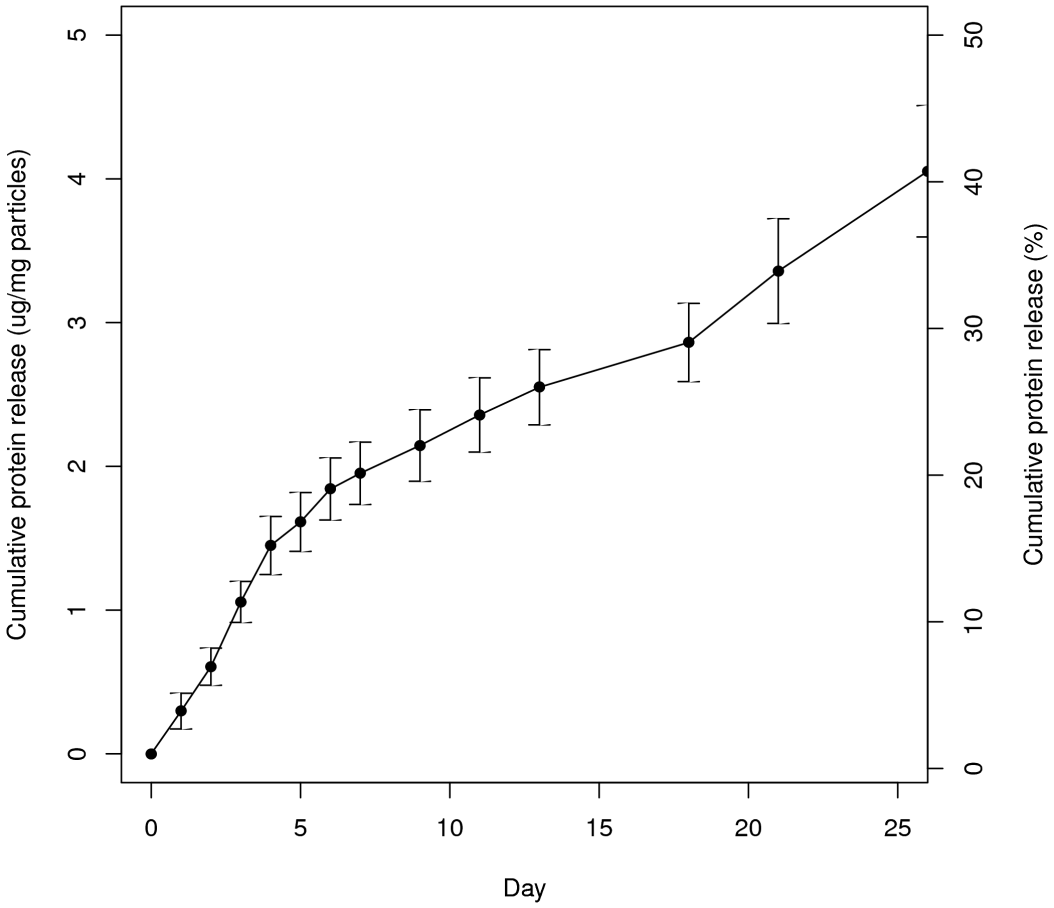

Figure 2.9: Cumulative release of HSA/Lysozyme from microparticles formulated from 50:50 PLGA (Table 2.1 on page 39) with 10 % *w/w* of PLGA-PEG-PLGA copolymer (Section 2.3.1). Protein release was quantified using a BCA assay (Section 2.3.5.3). Error bars show ± standard deviation of the mean; n=3.

2.4.2.2 Biological activity of model protein

The significance of detecting only lysozyme is two-fold: Most importantly we can verify that protein released at early and late time points is active and that the process of fabrication and release from microparticles has not been detrimental. Secondly we can differentiate the release of the model protein from the carrier protein (HSA). This helped us to understand more complex issues regarding polymer degradation mechanisms and how this can selectively discriminate the release of different proteins. This is potentially an important factor when dealing with proteins with very different physiochemical characteristics to the carrier protein.

The formulation that released protein over the shortest period (PLGA 50:50 (30 % *w/w* PLGA–PEG–PLGA)) demonstrated a very close match between the expected release of lysozyme and the measured activity of lysozyme. The expected release of lysozyme was calculated based on the assumptions that 10 % of the total protein was lysozyme and the proteins behave homogeneously. Table 2.4 shows how closely these values correlate. This data indicates that for this fast releasing formulation, there are no limiting factors that differentiate the proteins; they behave homogeneously. This shows that the mechanism of release is independent of physiochemical characteristics that differ between HSA and lysozyme.

Day	Expected lysozyme (µg)	Active lysozyme (µg)
1	57.0 ± 5.4	56.6 ± 14.1
2	12.8 ± 4.2	19.1 ± 4.7
3	4.1 ± 3.1	6.8 ± 3.9
4	0.6 ± 0.5	1.0 ± 0.6
5	0.4 ± 0.2	0.0 ± 0.9

Table 2.4: Active lysozyme release from PLGA 50:50 (Table 2.1) (30 % PLGA–PEG–PLGA (Section 2.3.1)) measured using a kinetic activity assay (Section 2.3.5.4) compared with expected levels.

If, however we look at the release of lysozyme from formulations that offered a more sustained release we don't see this same correlation. The levels of released lysozyme are higher at early points in the release window and trail off as the levels of lysozyme are depleted (Table 2.5, Page 62). This suggests that the mechanism of release is different and this mechanism exploits differences between Lysozyme and HSA to differentiate them.

If the mechanism of release relied on diffusion through the micro–porous structure of the polymer then we might expect to see this effect since the molecular weight

of Lysozyme is a quarter that of HSA. Lysozyme could diffuse through this porous network at a higher rate than HSA. This will likely be less of a pronounced issue for the growth factors of interest because their molecular weights are all higher than that of lysozyme.

Lysozyme is most active in the region of pH 6.2–9 [181] so as the PLGA degraded and the pH dropped activity measurements became less sensitive. For the faster degrading formulation PLGA 50:50, there were no successful Lysozyme detections beyond day 12. The actual pH levels of the release supernatants were determined (Figure 2.10). It can be seen that day 12 is when PLGA 50:50 hydrolytic by-products cause a pH drop. A similar correlation is seen with PLGA 85:15. The last successful lysozyme activity determination was at day 26. As a result no comparisons between active lysozyme and expected lysosyme were made beyond this point.

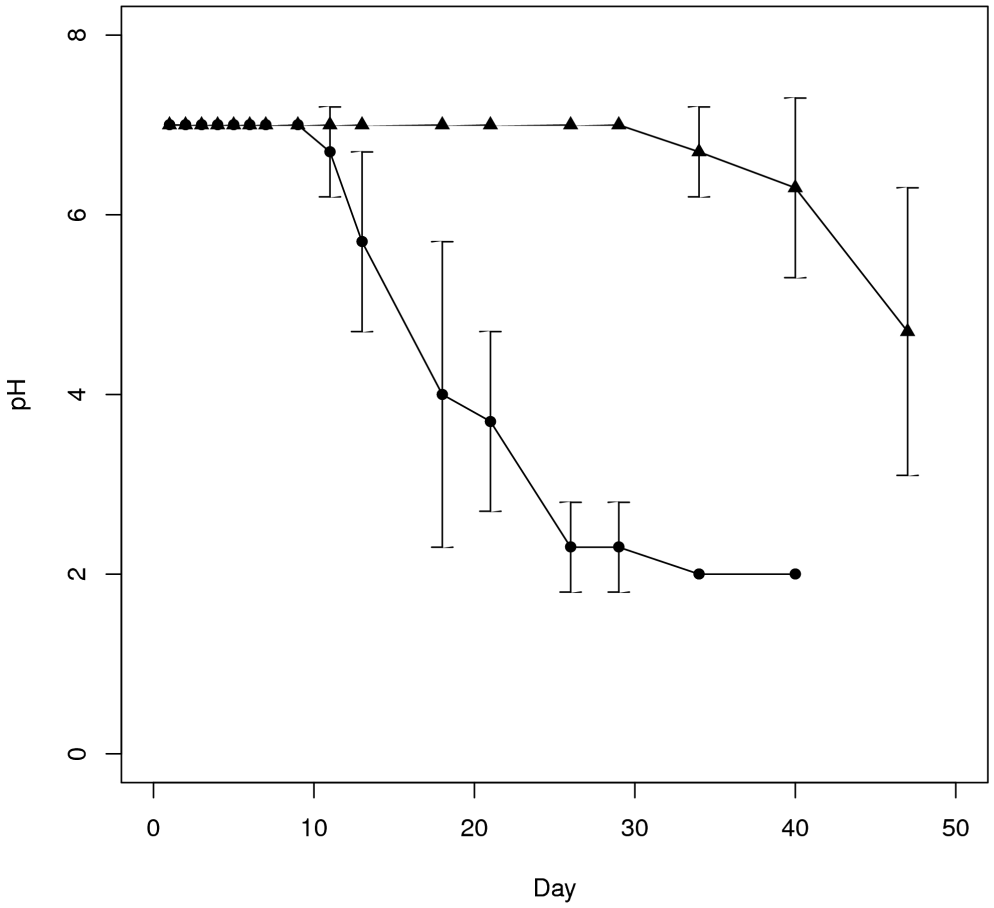

Figure 2.10: Drop in *pH* induced by polymer microparticle degradation from PLGA 50:50 • and PLGA 85:15 ▲. This is not likely to be representative of the situation *in vivo* because fluids will be continually replenished and metabolic pathways will process the acidic monomers. Error bars indicate ± standard deviation; n=6.

Microparticle polymer formulation: PLGA 50:50 (10 % (w/w) PLGA–PEG–PLGA)		
Day	Expected lysozyme (µg)	Active lysozyme (µg)
1	3.0 ± 1.2	24.0 ± 4.3
2	3.1 ± 0.4	5.6 ± 1.0
3	4.5 ± 0.6	11.4 ± 1.8
4	3.9 ± 1.4	9.4 ± 1.7
5	1.6 ± 0.3	7.9 ± 0.7
6	2.3 ± 0.7	6.8 ± 1.8
7	1.1 ± 0.2	3.0 ± 0.9
Microparticle polymer formulation: PLGA 8515 (30 % (w/w) PLGA–PEG–PLGA)		
Day	Expected lysozyme (µg)	Active lysozyme (µg)
1	9.6 ± 1.5	26.6 ± 0.8
2	8.2 ± 0.5	18.0 ± 0.1
3	10.9 ± 0.5	17.3 ± 1.1
4	10.5 ± 2.4	15.7 ± 0.9
5	12.2 ± 2.4	15.7 ± 2.1
6	15.7 ± 5.0	2.7 ± 2.7
7	4.9 ± 1.3	1.7 ± 0.4
Microparticle polymer formulation: PLGA 8515 (10 % (w/w) PLGA–PEG–PLGA)		
Day	Expected lysozyme (µg)	Active lysozyme (µg)
13	0.4 ± 0.1	1.6 ± 0.9
18	7.3 ± 1.5	19.2 ± 3.0
21	8.3 ± 2.4	23.9 ± 3.5
26	1.8 ± 0.5	7.9 ± 2.0
29	1.0 ± 0.3	0.0 ± 0.0

Table 2.5: Lysozyme release precedes that of the albumin carrier. Active lysozyme was measured using a kinetic activity assay (Method 2.3.5.4) and compared with expected levels as arithmetically determined from total protein release (Method 2.3.5.3).

2.4.2.3 Robustness

For this microparticle system to be a robust platform technology it was essential that the results were repeatable. A small repeatability study was carried out with formulations of interest. Three independent operators each fabricated a batch of microparticles of the same formulation following a standard operating procedure. The protein release from each sample was assessed (Figures 2.11 and 2.12). Although some variability can be seen, the shape of the release profiles remained distinct between different formulations. All samples from PLGA 50:50 (10 % (w/w) PLGA-PEG-PLGA) released until day 30 (Figure 2.11) and all samples from PLGA 85:15 (30 % (w/w) PLGA-PEG-PLGA) released up to day 10 (Figure 2.12).

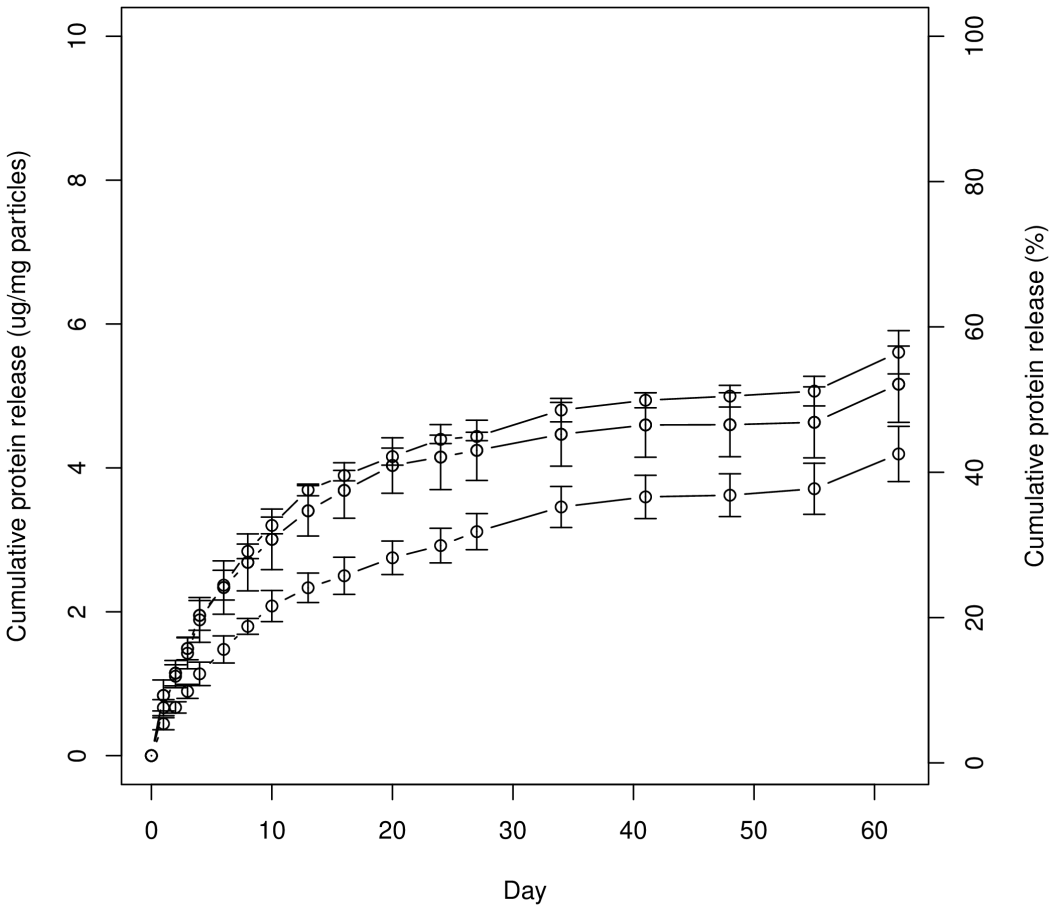

Figure 2.11: Cumulative release of HSA/Lysozyme from microparticles formulated from 50:50 PLGA (Table 2.1) with 10 % *w/w* of PLGA-PEG-PLGA copolymer (Section 2.3.1). Protein release was quantified using a BCA assay (Section 2.3.5.3). Plots show protein release from three batches each released in triplicate. Error bars show $\pm$ standard deviation of the mean; n=3.

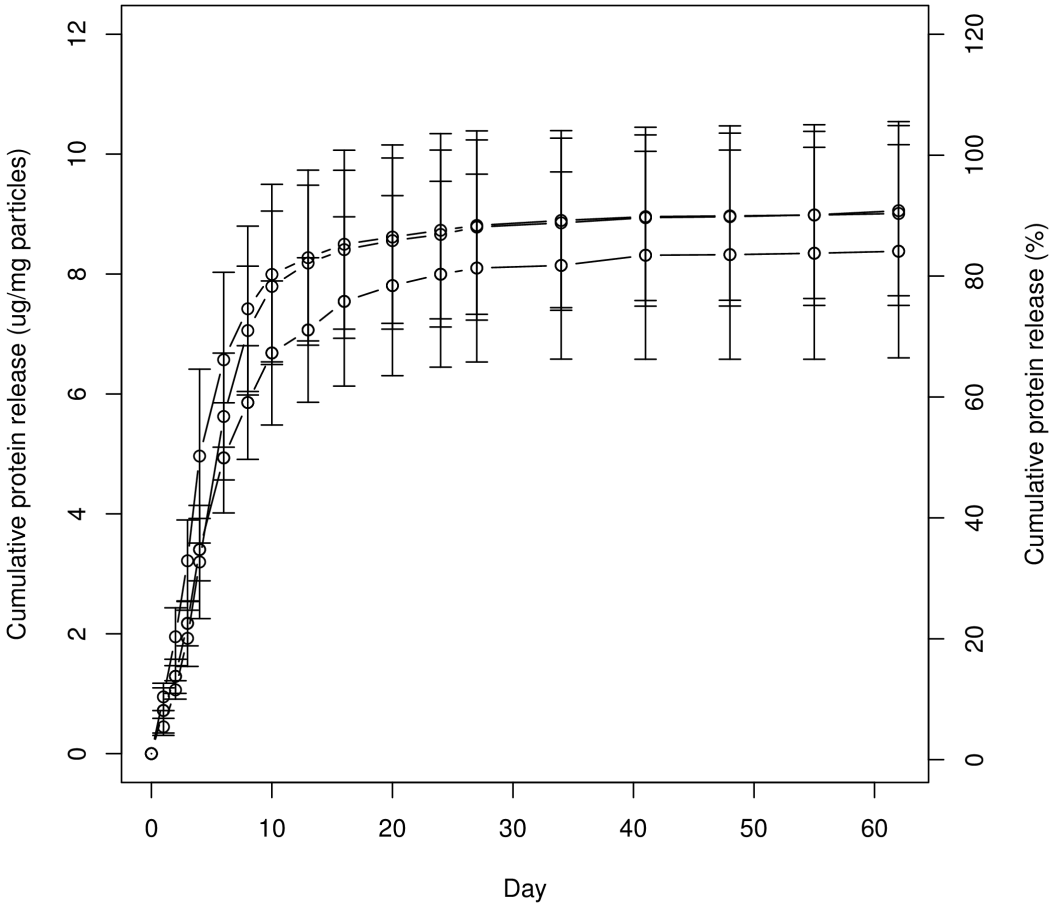

Figure 2.12: Cumulative release of HSA/Lysozyme from microparticles formulated from 85:15 PLGA (Table 2.1) with 10 % *w/w* of PLGA-PEG-PLGA copolymer (Section 2.3.1). Plots show protein release from three batches each released in triplicate. Protein release was quantified using a BCA assay (Section 2.3.5.3). Error bars show $\pm$ standard deviation of the mean; n=3.

2.4.2.4 Blending formulations

Another method to tailor release profiles (besides changing the individual formulations) would be to blend mixtures of microparticles from two differently formulated populations. A small study was carried out to assess The effect of blending. The formulations PLGA 50:50 10 % and 30 % *w/w* PLGA-PEG-PLGA exhibited very different protein release profiles (Figure 2.6, Page 55). One released over 3 days, the other released over 30 days. It was hypothesised that a 1:1 *w/w* blend of these formulations would produce an intermediate level of release resulting in a high initial burst release followed by a sustained release. A formulation of PLGA 50:50 (20 % (*w/w*) PLGA-PEG-PLGA) was also assessed to see how this would compare to the blend.

The release profiles confirmed the hypothesis that an intermediate release profile can be attained by blending different formulations of microparticles (Figure 2.13). The blend exhibits the high initial release over the first two days as seen in the 30 % PLGA-PEG-PLGA formulation but also sustains protein release up to day 20. This kind of release profile may be useful for a therapeutic entity that has to quickly attain therapeutic levels then sustain these levels.

It should be noted that although some formulations appear to release more that 100 % of encapsulated protein this is simply an artefact of the way that total protein is calculated. This method makes the assumption that the protein encapsulation within the polymer microparticles is homogeneous. Release studies are carried out on a sample of microparticles and some samples appear to have higher levels of protein than the numerically calculated average.

A comparison of protein release from the blended formulation with the equivalent single formulation was carried out (Figure 2.14). These release profiles appear similar. They both exhibit high initial release followed by a more sustained release. This indicates that blending of formulations is not necessary to achieve this kind of release profile but a blending method can be used to simulate formulations that have not been fabricated.

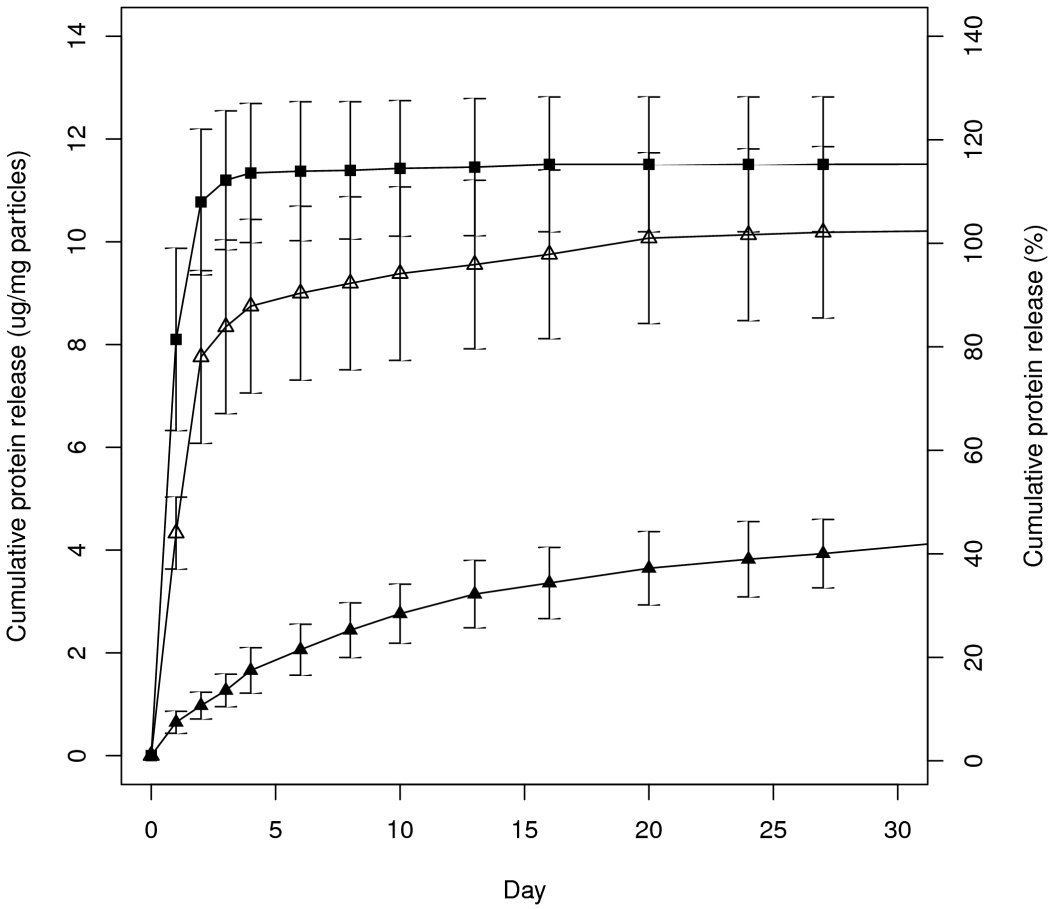

Figure 2.13: Cumulative release of HSA/lysozyme from microparticles formulated from PLGA 50:50 (Table 2.1) with 10 % (▲) and 30 % (■) *w/w* PLGA-PEG-PLGA (Section 2.3.1) compared with HSA/lysozyme release from an equal mixture of the two formulations (△). Protein release was quantified using a BCA assay (Section 2.3.5.3). Error bars show ± standard deviation of the mean; n=6.

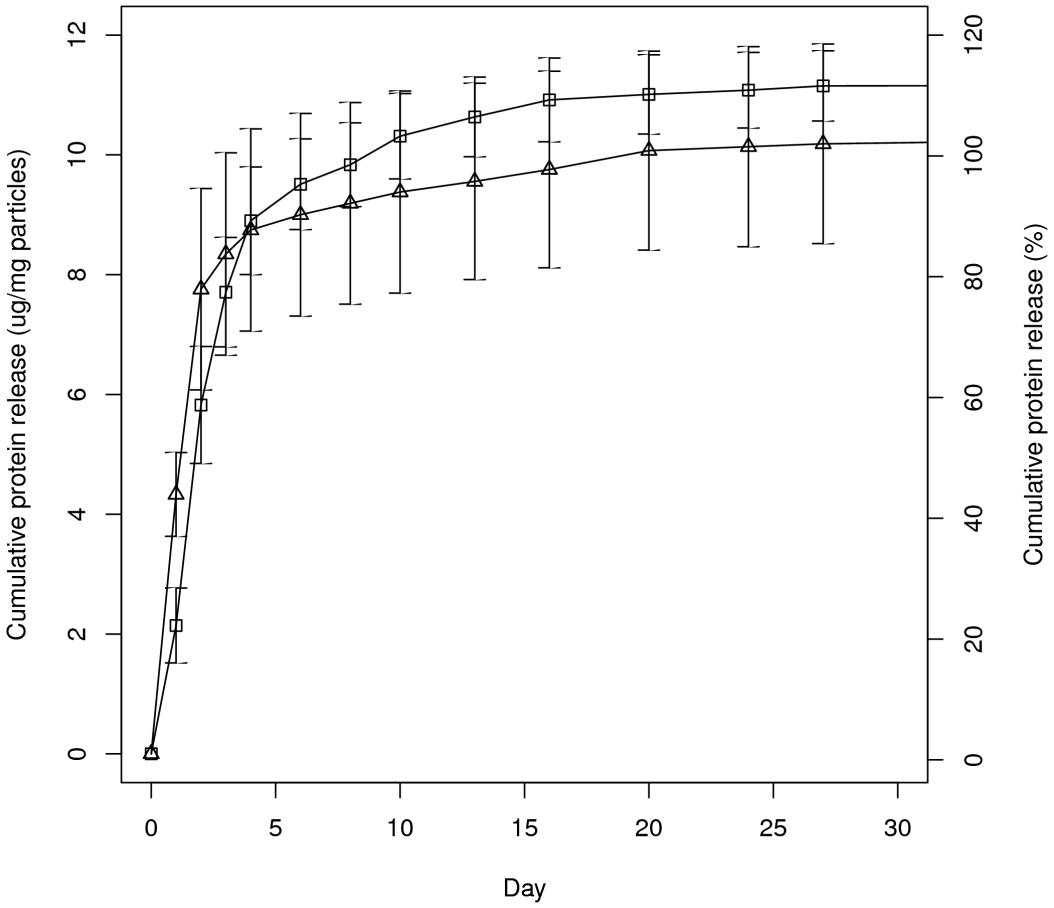

Figure 2.14: Cumulative release of HSA/Lysozyme from microparticles formulated from PLGA 50:50 (Table 2.1) with 20 % (□) *w/w* PLGA-PEG-PLGA (Section 2.3.1) compared with the blended formulation (△) detailed in figure 2.13. Protein release was quantified using a BCA assay (Section 2.3.5.3). Error bars show ± standard deviation of the mean; n=6.

2.4.2.5 Applicability of the model protein

Formulations of interest were identified with lysozyme as a model protein. Sustained release formulations were identified and repeatability determined. A comparison between lysozyme and BMP-2 was required to ensure that similar release profiles could be generated.

A formulation of PLGA 50:50 (10 % (*w/w*) PLGA-PEG-PLGA) had been of particular interest (Figures 2.6, 2.11 and 2.13) due to the low level burst release and sustained duration of release. This was hypothesised as being a desirable characteristic for the release of BMP-2 in a segmental defect.

Two batches of microparticles were fabricated using this formulation. One contained the typical HSA/lysozyme protein loading and the other substituted lysozyme with BMP–2. Total protein release was assessed using BCA substrate.

These two batches showed similar release profiles (Figure 2.15). They both exhibit a small step at day 20 which is most likely a result of switching between different mechanisms of release: The point at which diffusion mediated release begins to tail off and bulk erosion of the polymer begins to mediate the majority of protein release. The release from both batches ended during the period of day 30-40.

This study indicates that the release profiles obtained using model proteins are applicable to other factors with similar physiochemical properties. Specifically the profiles obtained using lysozyme appear to be applicable to BMP–2.

It would have been advantageous to assess the release of BMP–2 using a protein specific method and compare this to the release of lysozyme only. Since these actives make up only 10 % of the total protein, subtle differences may have been masked by HSA release. Unfortunately Assessment of released BMP–2 using an enzyme-linked immunosorbent assay (ELISA) was inconclusive and indicated BMP–2 levels lower than anticipated. This was further explored in Chapter 3.

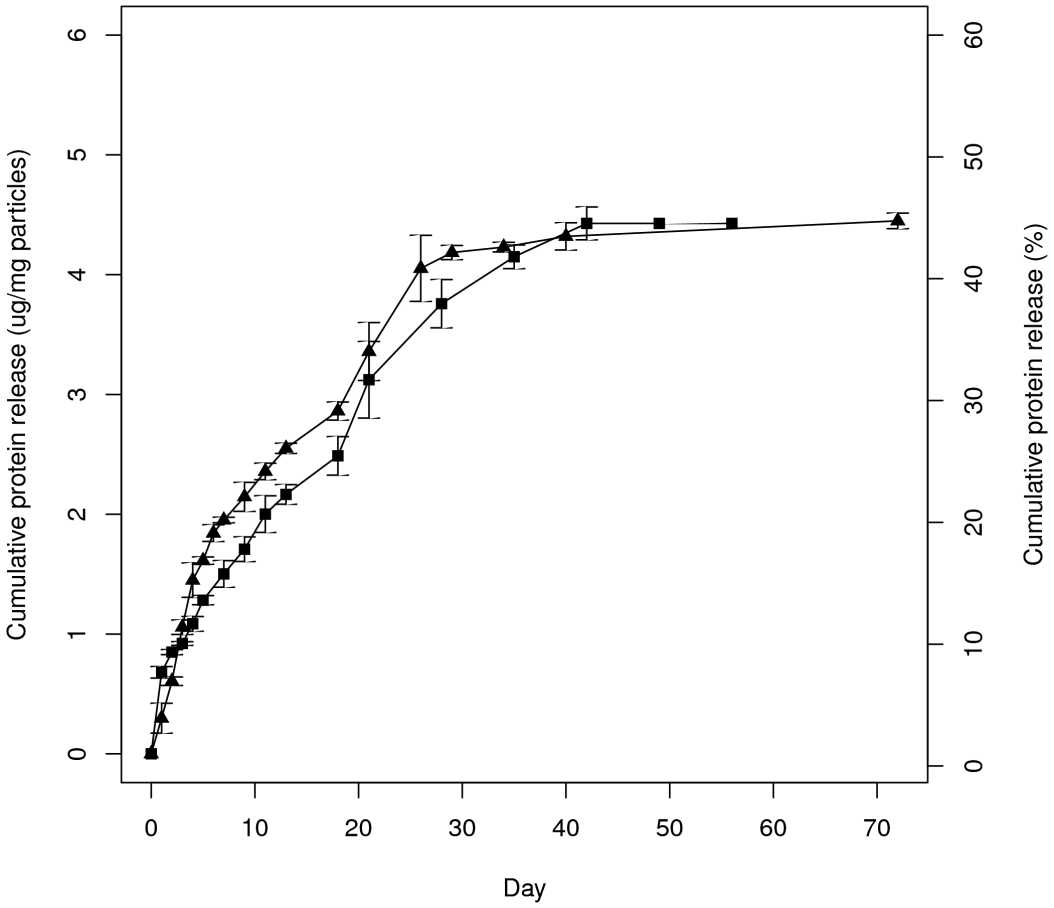

Figure 2.15: The release profile of model protein/HSA matches the release of BMP–2/HSA. This indicates that Lysozyme was a good model. Cumulative protein release from two batches of microparticles of an identical formulation; one containing lysozyme/HSA (▲) and the other containing BMP–2/HSA (■). The polymer formulation was PLGA 50:50 (Table 2.1) (10 % (*w/w*) PLGA-PEG-PLGA (Section 2.3.1)). For clarity, error bars indicate ± standard deviation of the mean; n=3.

2.4.3 Micro-positioning of Microparticles

This is a brief introduction to a process with the potential to generate growth factor gradients. The aim was to accurately position microparticles within a hydrogel with a positioning accuracy in the order of hundreds of microns.

In order to produce accurate and complex growth factor gradients on a small scale, for research purposes, it was desirable to position microparticles accurately with a high degree of precision. The paradigm that was selected was the use of a micro-manipulator in conjunction with a micro-injector. This facilitated the accurate placement of a needle followed by accurate deployment of a microparticle suspension. In practice this was a little more complex. Due to forces such as hydrophobic interactions and surface tension on these small scales, microparticles required 'nudging' from a smaller needle to achieve precise placement.

Using the methods selected A degree of precision in the order of hundreds of microns was achieved (Figure 2.16). This would facilitate the potential generation of gradients able to influence individual mammalian cells on a monolayer. Using time-lapse imaging or immunohistochemistry techniques the effects of individual growth factors or even complex mixtures could be assessed.

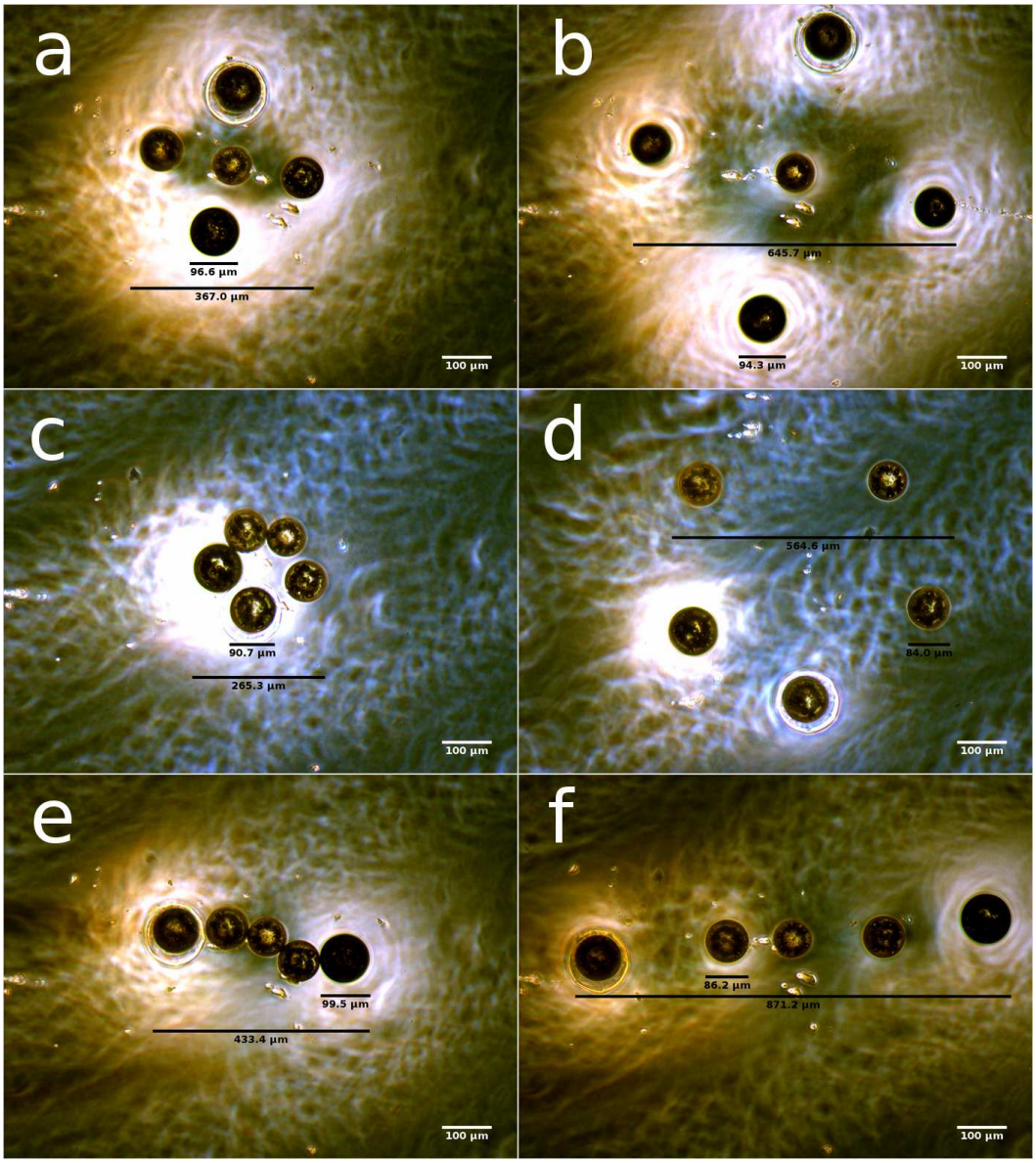

Figure 2.16: Microparticles positioned in 1 % agarose-gelatin hydrogel (Method 2.3.6 on Page 43) using a micro-manipulator and micro-injector (Method 2.3.7 on Page 43). These images demonstrate the greatest degree of positional accuracy that can be achieved with these therapeutic microparticles.

2.5 Conclusions

A comparison between emulsification methods between vortex agitation and the use of a homogeniser led to a method of fabrication with consistent microparticle size distributions. The microparticles exhibited regular spherical morphologies with minimal pores or defects. Comparisons between operators indicated a high degree of robustness of the fabrication protocol. Increasing levels of PEG within the polymer formulation led to a smaller average distribution of microparticles although all assessed formulations were within acceptable tolerances. It was hypothesised that the triblock copolymer increased the emulsion stability leading to the smaller size distribution.

A high entrapment efficiency was exhibited for all formulations. Entrapment efficiency was independent of microparticle formulation. The inclusion of a high level of HSA and short emulsion steps appear to have acted as expected in producing high entrapment efficiencies but comparisons would have to be carried out to be sure.

Lysozyme was identified as a model protein and release studies assessing the release of total protein identified that different microparticle formulations exhibited different protein release profiles. The release profiles released protein over as little as 2 days to as long as 30 days (with consistent release). It appears that the inclusion of the triblock copolymer enabled stable protein release before the PLGA began to degrade.

Issues of incomplete protein release were identified for longer-releasing formulations. It was speculated that this incomplete release was due to protein aggregations/adsorption. This was potentially caused by acidic degradation products. Acidic environments were identified in release samples. Degradation *in vivo* would, of course, be different and these acidic products would be metabolised. It was speculated that although incomplete issues were identified, the actual release profiles were representative of the likely *in vivo* release.

The biological activity of released lysozyme was confirmed up to day 26. Beyond this, acidity within the samples prevented accurate analysis.

The protein release from BMP-2/HSA loaded microparticles was found to be highly comparable to the release of lysozyme/HSA. This indicates that the methods developed here could lead to similar release from other growth factors with similar physicochemical characteristics.

A method to utilise the fabricated microparticles was briefly assessed involving positioning the microparticles within a hydrogel with a high degree of positional accuracy. Positional accuracy of hundreds of microns could be achieved using this

method. This makes it suitable for the study of individual cell interactions in a monolayer environment. To achieve a greater degree of accuracy, different techniques such as optical tweezers would be required.

The aim of this chapter was to verify the release of protein from PLGA-based microparticles in preparation for a segmental defect model. The ability to control the release rate of protein was verified as well as the release of an active model protein. Methods to validate batches of microparticles have been explored and will prove useful for the assessment of potential experimental batches.

2.6 Future Work

The issues of incomplete release should be further addressed. Incomplete protein release from PLGA microparticles is a well known issue [137] and a number of important reviews have been published on the subject. If the particular issues here can be elucidated and mitigated in an *in vivo* environment then this could lower the growth factor requirements of potential therapeutics.

The activity of released lysozyme was verified. The next important steps are to verify the activity of released growth factors. Once the activity of a growth factor can be verified, this system can be prepared for for its main application *in vivo*.

CHAPTER 3

Results II: Bioactivity Assessment of Encapsulated BMP-2

3.1 Introduction

In Chapter 2 some of the potential causes of protein denaturation resulting from entrapment and release from a polymeric system were introduced. One of the main causes is the water/oil interface present during emulsification. Procedures were implemented to specifically address this. These included an albumin carrier to competitively block the interface and a processing method that minimised interface exposure time. The release of active lysozyme was verified showing that active protein release was possible.

Encapsulated proteins would still be exposed to physiological temperature and, once the polymer hydrates, water and a physiological ionic strength. A *pH* drop within the polymer is still thought to occur. The interior of the polymer structures would initially be at physiological *pH* but as the polymer degrades this would become more acidic. This *pH* drop may cause aggregation and adsorption of growth factors. As the *pH* continues to drop the risk of acid-catalysed hydrolysis increases.

A *pH* drop will be more of an issue in long-term formulations such as the one required for BMP-2 release. It was seen as a priority to assess the activity of this potentially challenging formulation.

Assessment of BMP-2 *in vitro* was carried out to test whether the BMP-2 was active in sufficient quantity to elicit a biological response. This was a crucial step that dictated whether the proposed *in vivo* models could go ahead based on current encapsulation protocols. Problems would require the process to be re-assessed and modified.

Assessment involved measuring the effect of released BMP-2 on a cell monolayer. There are two ways to approach this. One method involves carrying out a release study, sampling the media at various time points and then culturing cells with this media. This method had practical limitations. If denaturation is observed it may have occurred after release but before culture on cells. This would give a false negative result. The selection of a buffered solution to release into would also have been difficult. Previous studies used PBS but cells require culture media. If PBS was mixed with culture media after release, concentrations of BMP-2 may have been too low to detect. Lyophilisation then re-suspension of the protein solution would have left phosphate salts, potentially denaturing the growth factor. Release into cell culture media was an option but this renders protein assays useless because of all of the native protein in culture media. Without a protein assay there was no way to assess whether cell culture media affects the protein release rate. The issues of post-release denaturation are still also present and risks of bacterial/fungal infection during sampling are increased.

The other method to assess released BMP-2 activity is to assess the effect of cells cultured directly with microparticles. The inherent limitation here is that there is no way to know if a biological effect is from initially released BMP-2 and whether later-released BMP-2 is still active and inducing a continued biological effect. Additional controls are required in this kind of set-up to ensure that biological changes are a result of released BMP-2 and not just the presence of the microparticles. This method was selected because it more accurately mimics the intended *in vivo* application.

Bone Morphogenetic Protein-2 (BMP-2) induces bone formation and plays an important role in osteoblast formation through the differentiation of pre-osteoblasts [182] and mesenchimal stem cells [183]. Differentiation can be measured in a number of ways, generally early up-regulation of alkaline phosphatase (ALP) is assessed. Up-regulation of ALP is usually associated with differentiation but can also be non-specifically expressed so this is usually measured in conjunction with other indications. Bone-like mineralised matrix is a strong indication of osteoblasts. This is generally stained for and assessed qualitatively. A later marker, osteocalcin can also be measured as higher levels are linked with osteoblast production [182].

A murine calvarial osteoblast cell line (MC3T3-E1) was selected for this differentiation study. Cell lines are generally easier to culture than primary cells and high numbers of cells can be easily generated. This cell line responds to BMP-2 by expressing higher levels of ALP and producing mineralised matrix [184, 185]. Mineral deposition is usually homogeneous and obvious which is useful for a qualitative subjective assessment.

Quantification of BMP-2 was carried out using a different cell line. A murine myoblast cell line (C2C12) was selected. This is because C2C12 cells respond to BMP-2 in a proportional way [186, 187]. Expression of ALP correlates to BMP-2 concentrations in culture media. This means that by measuring ALP concentrations, active BMP-2 concentrations can be determined. This cell line was not used for co-culture and differentiation because there is very little literature regarding terminal differntiation of C2C12 cells into osteoblast-like cells, specifically matrix mineralisation. It has been suggested that mineral deposition from C2C12 cells can be inhomogeneous and difficult to assess.

3.2 Aims

The purpose of this set of experiments was to test whether the released BMP-2 was active and able to induce a biological effect. The nature of this longer-releasing formulation means that a proportion of protein release is mediated by bulk degradation of the polymer. This exposes the encapsulated protein to less favourable micro-environments.

This chapter aims to show that a polymer formulation providing a gradual and prolonged release of BMP-2 is able to induce a biological effect *in vitro*. This formulation exhibits a very small burst release so any biological response will most likely have been induced by BMP-2 released after the first day or two.

The activity of BMP-2 batches were assessed in preparation for *in vivo* work. The non-commercial source of rhBMP-2 and previous issues of detection using an ELISA necessitated this verification.

3.3 Methods

3.3.1 Microparticle Fabrication

Microparticles were fabricated from PLGA 85:15 (10 % (*w/w*) PLGA-PEG-PLGA) in the larger size range (Section 2.3.3.2, Page 38). Protein loading was analogous to initial lysozyme studies (0.1 % (*w/w*) BMP-2 and 0.9 % (*w/w*) HSA). Control microparticles were loaded with HSA alone.

3.3.2 Microparticle Sterilisation

Microparticles were sterilised for cell culture using ultravoilet irradiation. Briefly, microparticles were placed in a Class 2 biological safety cabinet (*Contamination control laboratories, 5001-1-LH*) and exposed to an ultraviolet sterilisation cycle for 20 minutes. The particles were then agitated and exposed for a second cycle. This is a common method of sterilising polymeric biomaterials for cell culture [188].

3.3.3 Growth Factor Batches

Recombinant human BMP-2 was obtained from *Walter Sebald* (*University of Wurzburg, Germany*). All BMP-2 documented in this thesis was obtained from this source. The BMP-2 was obtained in three batches:

1. June, 2010.
2. September, 2010.
3. Febuary, 2011.

Batches of BMP-2 will from here on be referred to as 1, 2 and 3. Batch 1 was used for microparticle encapsulation and release within this chapter and batch three was used for biological quantification method development. Batch 2 was supplied in greater quantity and was set aside for use in the segmental defect *in vivo* study.

3.3.4 Cell Culture

3.3.4.1 Subculturing of murine preosteoblast derived cells (MC3T3-E1)

Initial MC3T3-E1 work was carried out using a cell line provided by B. Hoflack (*Dresden, Germany*) and subcultured at the Institute of Health and Biomedical Innovation (IHBI) (*Queensland University of Technology, Brisbane, Australia*). Later work, carried out in the UK, utilised a cell line obtained from LGC Standards. Subculturing and expansion was carried out using α Minimum Essential Medium (αMEM) supplemented with 10% *v/v* Foetal Bovine Serum and Penicillin/Streptomycin at a concentration of 50 U/ml and 50 µg/ml respectively. Cells were maintained at 37 °C with 5% CO_2 in a humidified atmosphere.

Osteogenic cell differentiation was induced with the addition of 10 mM β-glycerophosphate, 0.1 mM ascorbate-2-phosphate and 100 nM dexamethasone to the aforementioned expansion media. Cells were cultured in this media for the duration of differentiation.

3.3.4.2 Subculturing of murine myoblast derived cells (C2C12)

This cell line was obtained from LGC Standards. Subculturing and expansion was carried out using Dulbecco's Modified Eagle Medium (DMEM) supplemented with 10% *v/v* Foetal Bovine Serum, Penicillin/Streptomycin at a concentration of 50 U/ml and 50 µg/ml respectively and L-glutamine at a concentration of 2 mM. Cells were maintained at 37 °C with 5% CO_2 in a humidified atmosphere.

3.3.4.3 Cell passaging

Cells were washed using PBS and incubated with a small volume of trypsin (0.25 %)/EDTA (0.02 %) for approximately 4 minutes, until cells visibly detached. Trypsin was deactivated by adding an equal volume of complete media. The cell suspension was centrifuged at 180 g for 5 minutes. The supernatant was aspirated, the cells re-suspended and added to fresh flasks. Cells were never cultured beyond 80 % confluency and a split ratio of 1 in 6 to 1 in 12 was used depending on the cells and rate of growth.

3.3.4.4 Cell counting

Cells were counted using a heamocytometer. Cell counting ensured that consistent seeding densities were achieved during passaging and assays. A suspension of cells was introduced into a haemocytometer, cells within a specific volume were counted using phase contrast microscopy and multiplied by the volume to obtain a number of cells per millilitre.

3.3.4.5 Staining for mineral deposition

Alizarin red S was prepared at a concentration of 20 mg/ml in deionised water. The pH was adjusted using ammonium hydroxide (0.5 M) solution until the alizarin red solution was in the pH range 4.1 – 4.3. The cell monolayer was washed with PBS and fixed with ice cold methanol. Alizarin red solution was added to the cell monolayer which was incubated at 37 °C for 5 minutes. Deionised water was used to wash away excess stain and the cell layer was immediately imaged.

3.3.4.6 Alkaline phosphatase detection and quantification

To determine alkaline phosphatase levels a p-nitrophenyl phosphate (pNPP) solution is used. Alkaline phosphatase dephosphorylates pNPP to produce p-nitrophenyl (pNP). This is a yellow molecule with strong absorbance at 405 nm that can be quantified colorimetrically. The levels of pNP correlate with the levels of alkaline phosphatase.

A cell lysis buffer was prepared by adding 0.1% Triton™ X-100 to 0.2 M tris buffer. The cell monolayer was washed with PBS then incubated with this cell lysis buffer at $-20\,^{\circ}$C. The resulting cell lysate was centrifuged at 10,000 rpm for 10 minutes at a temperature of $4\,^{\circ}$C. The resulting supernatant was mixed in equal parts with buffered p-nitrophenyl phosphate solution, incubated in darkness at room temperature for 30 minutes. The absorbency at 405 nm was measured. Negative controls (lysis buffer – no cells) were subtracted from data and results were compared to a calibration plot to determine specific alkaline phosphatase levels.

3.3.4.7 Experimental groups

Two different amounts of microparticles (control and BMP-2-loaded) were cultured in 48-well tissue culture treated plates along with MC3T3-E1 cells. Indications of differentiation were assessed at three time points (10, 17 and 24 days). Experimental groups are defined in table 3.1. Appropriate control groups were included to avoid potential false positive results induced by the microparticle system.

Group	Description
1.mp.low	BMP-2 loaded microparticles (0.5 mg/well)
2.mp.high	BMP-2 loaded microparticles (5 mg/well)
3.ostegenic	Osteogenically supplemented media (Section 3.3.4.1, Page 78)
4.control	Control cells; no additional treatment
5.mp.low.control	HSA loaded microparticles (0.5 mg/well)
6.mp.high.control	HSA loaded microparticles (5 mg/well)

Table 3.1: Experimental groups for co-culture of microparticles with a murine calvarial osteoblast cell line (MC3T3-E1)

3.3.5 Statistical comparisons and data analysis

Statistical analyses were carried out using the software environment 'R' [168, 169] (version 2.10.1). Sample data was assessed for normality and variance using quantile-

quantile plots and F-tests, respectively. Statistical methods were chosen accordingly. Statistical significance was defined with a confidence interval of 95%. Comparisons with a p-value of less than 0.05 were considered significant. For certain graphical comparisons box plots were favoured over bar graphs as they are better for representing averages. Outliers (in normally distributed data) were defined as values that were $\geq$ 2.5 quantiles from the mode.

All data analysis was carried out on an i486-pc-linux-gnu platform running Ubuntu 10.04 LTS. OpenOffice.org (version 3.2.0) and Python^{TM} (version 2.6) were utilised to manage and process data.

Pairwise statistical comparisons were carried out using a Welch t-test. This was selected because unequal variance was observed between groups. Full results of statistical comparisons can be found in Appendix F.

3.4 Results and Discussion

3.4.1 Protein release from a sustained release microparticle formulation

This study was carried out in parallel with initial release studies before all the release data was available. It was initially speculated (based on the results of a previous PhD student; *Andrew Olaye* [189]) that a polymer formulation of PLGA 85:15 (10 % (*w/w*) PLGA-PEG-PLGA) would be suitable for a sustained duration of release. This formulation was later dropped in favour of a faster-releasing more sustained formulation.

The microparticle sizes were verified to have a mean size of 97.9 µm and lower and upper quartiles of 79.1 and 118.9 µm respectively. Electron microscopy images indicated a regular spherical morphology.

A short protein release study was carried out to verify the microparticles were releasing protein. Sustained protein release for the full duration of the 2 week study was demonstrated (Figure 3.1).

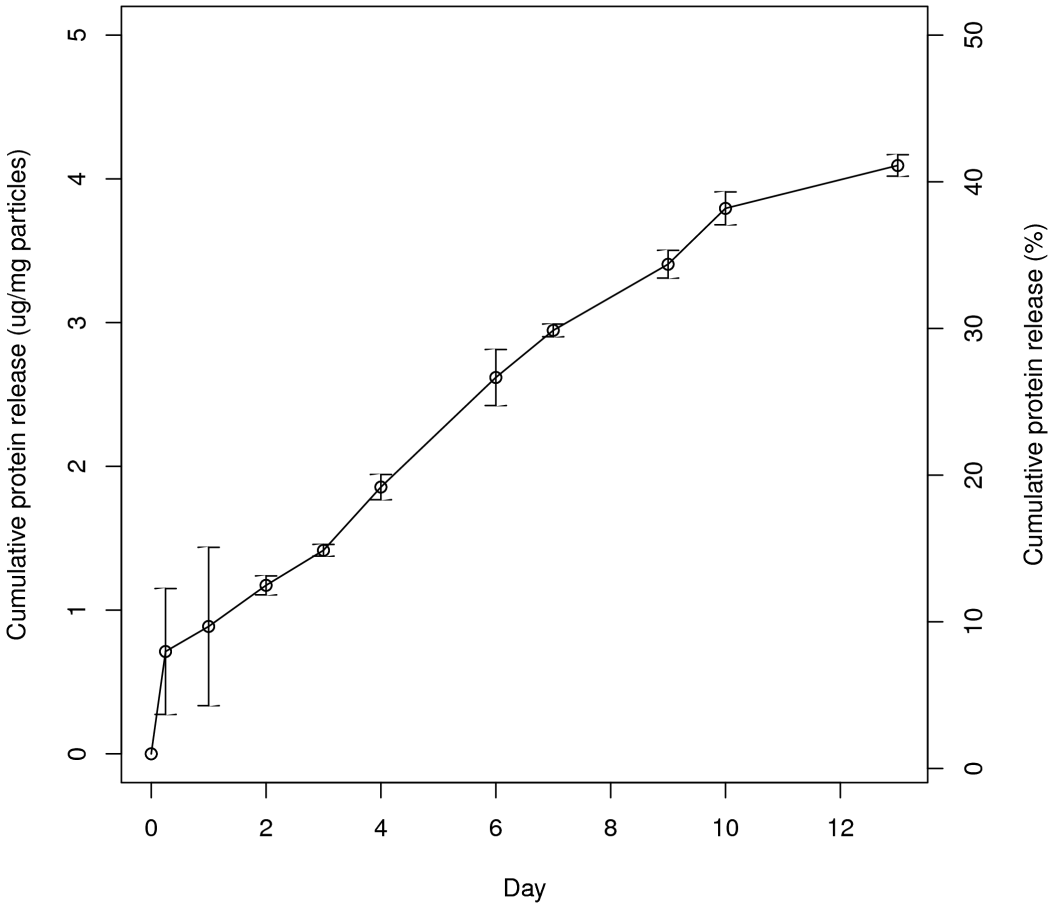

Figure 3.1: Cumulative release of HSA/BMP-2 from microparticles formulated from 85:15 PLGA (Table 2.1) with 10 % *w/w* of PLGA-PEG-PLGA copolymer (Section 2.3.1). A steady release rate of protein is seen over the two week duration. Protein was quantified using a BCA assay (Section 2.3.5.3). Error bars show standard deviation of the mean; n=9.

3.4.2 Effect of released BMP-2 on cells – ALP response

Alkaline phosphatase (ALP) is a hydrolase enzyme, the cellular expression of which is enhanced at the early stages of osteogenic differentiation. It can be used (in conjunction with other methods) to determine whether osteogenic differentiation is occurring. ALP expression was quantified at three experimental time points. The period of ALP expression as well as the levels varies between cell types and culture conditions. Since no data was available for the sustained release of BMP-2 in this way and its effect on MC3T3-E1 cells, the time points chosen were estimations.

Expression of ALP from groups cultured with microparticles exhibited a higher standard deviation in some cases. This could have been due to differences in the amounts of microparticles or non-homogeneous protein encapsulation within the microparticles causing varying effects. This is something that would require further investigation. If non-homogeneous protein encapsulation occurs, this would have a more significant effect when looking at smaller populations or even individual microparticles.

At day 10 (Figure 3.2), no significant difference was observed between osteogenically supplemented media and a low amount of microparticles. Comparisons between all other groups indicated significant differences. The control group expressed the lowest level of ALP. The higher amount of BMP-2 loaded microparticles resulted in the highest expression of ALP ($p<0.001$). This indicated that active BMP-2 is inducing differentiation. Furthermore, it indicated a dose dependant response. The lower amount of microparticles did not induce the same level of ALP expression (on day 10) as the higher amount, they instead have an effect analogous to osteogenically supplemented media.

A similar trend was seen on days 17 and 24 (Figure 3.3). On both days there was no significant difference in ALP expression between a high level of BMP-2 loaded microparticles and osteogenically supplemented media. On day 17 all groups expressed significantly higher levels of ALP than the control group.

Further analysis at different time points would have been illuminating as ALP expression could have been more gradual from the osteogenically supplemented media group in comparison to BMP-2-releasing microparticles.

The important result from this study is that the BMP-2 loaded microparticles induce a greater than (or equal to) level of ALP expression to osteogenic supplements at all time points and a greater level of ALP than control groups at all time points.

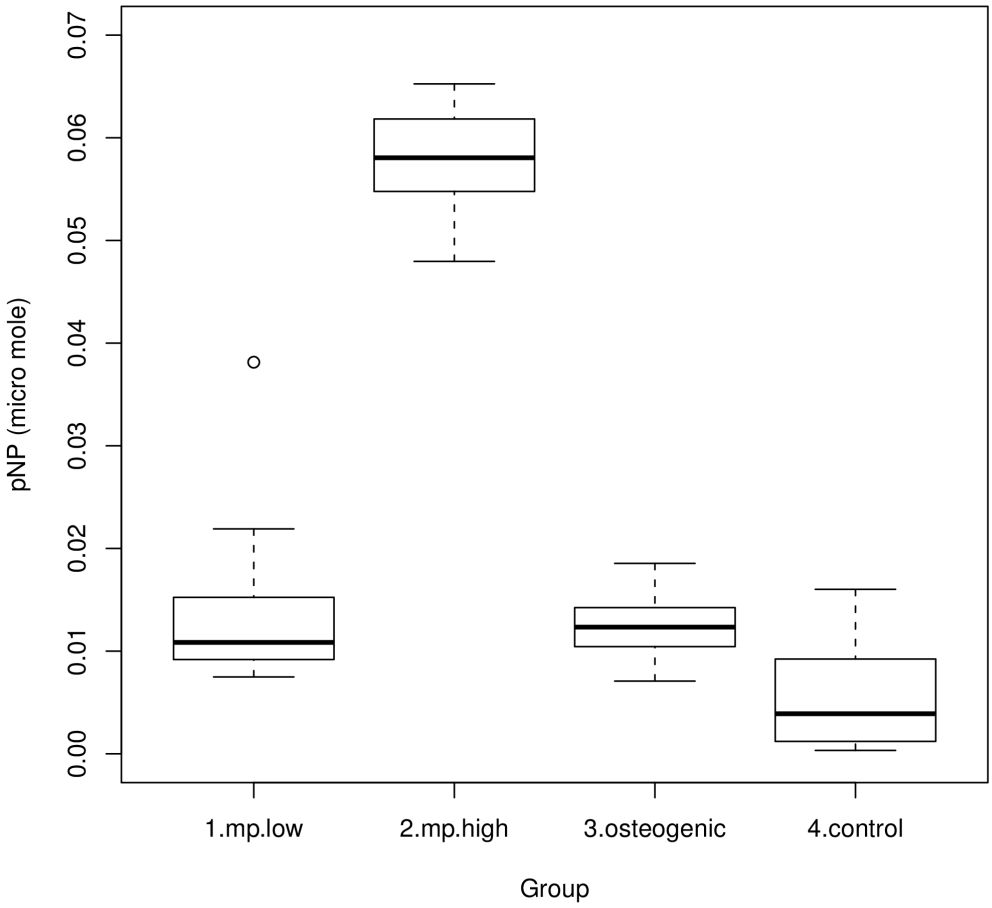

Figure 3.2: Boxplot showing the level of alkaline phosphatase (ALP) expressed at day 10 of culture with MC3T3 cells. ALP was quantified through dephosphorylation of pNPP to form pNP (Section 3.3.4.6). All groups express significantly more ALP than the control. A large amount of BMP-2 releasing microparticles (2.mp.high) had the highest effect ($p<0.001$).

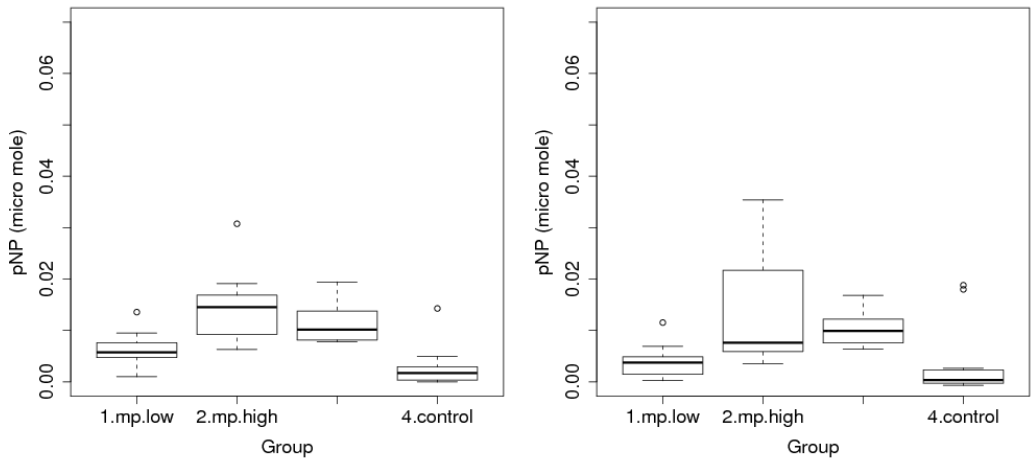

Figure 3.3: Boxplots showing the level of alkaline phosphatase (ALP) expression at day 17 (left) and 24 (right) of culture with MC3T3 cells. A higher amount of BMP-2 releasing microparticles (2.mp.high) causes the expression of significantly more ALP than control groups at both time points. Effects at these timepoints are less significant than at day 10 because ALP is known to be expressed at early stages during osteogenic differentiation.

3.4.3 Effect of released BMP-2 on cells – Mineral deposition

Alizarin red is used to qualitatively assess mineral deposition histologically as it strongly binds to the calcium in mineralised matrix. Mineral deposition was assessed because it a more difinitive indication of osteogenic differentiation than ALP. Mineral deposition is analogous to early bone formation.

Both amounts of BMP-2 releasing microparticles showed mineral deposition at all measured time points in contrast to control microparticles which show no mineral deposition (Figure 3.4). By day 24, osteogenically supplemented media samples formed mineralised nodules typically seen with MC3T3-E1 cells. The mineralised nodules formed in the presence of BMP-2 releasing microparticles had a different appearance. They were smaller and more homogeneous across the well. Optical microscopy images of the nodules indicated that they formed a uniform distance from the microparticles and followed the contours of the microparticles (Figure 3.5). This indicates a potential concentration or gradient effect. Mineral deposition stained in the presence of microparticles turned from red to yellow over time. This is why the mineral deposition in Figure 3.5 appears slightly yellow. ALizarin red stain turns yellow under acidic conditions. It was hypothesised that residual acidic monomers present from hydrolytic breakdown on the polymer induced this change.

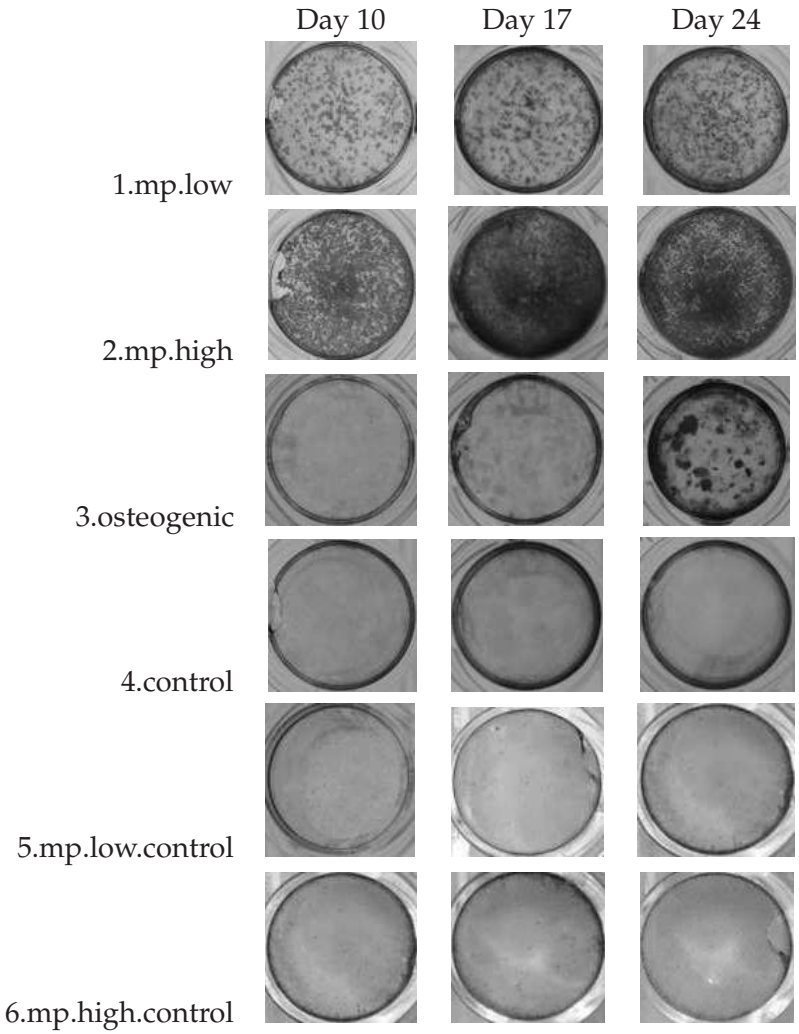

Figure 3.4: Representative images showing mineral deposition from a murine calvarial osteoblast cell line visalised using alizarin red. Labels indicate experimental groups and time points. See Table 3.1 on Page 80 for full details of experimental groups. The important observation to note here is that the BMP-2 microparticle group and the osteogenic positive control group both show indications of bone-like mineral deposition.

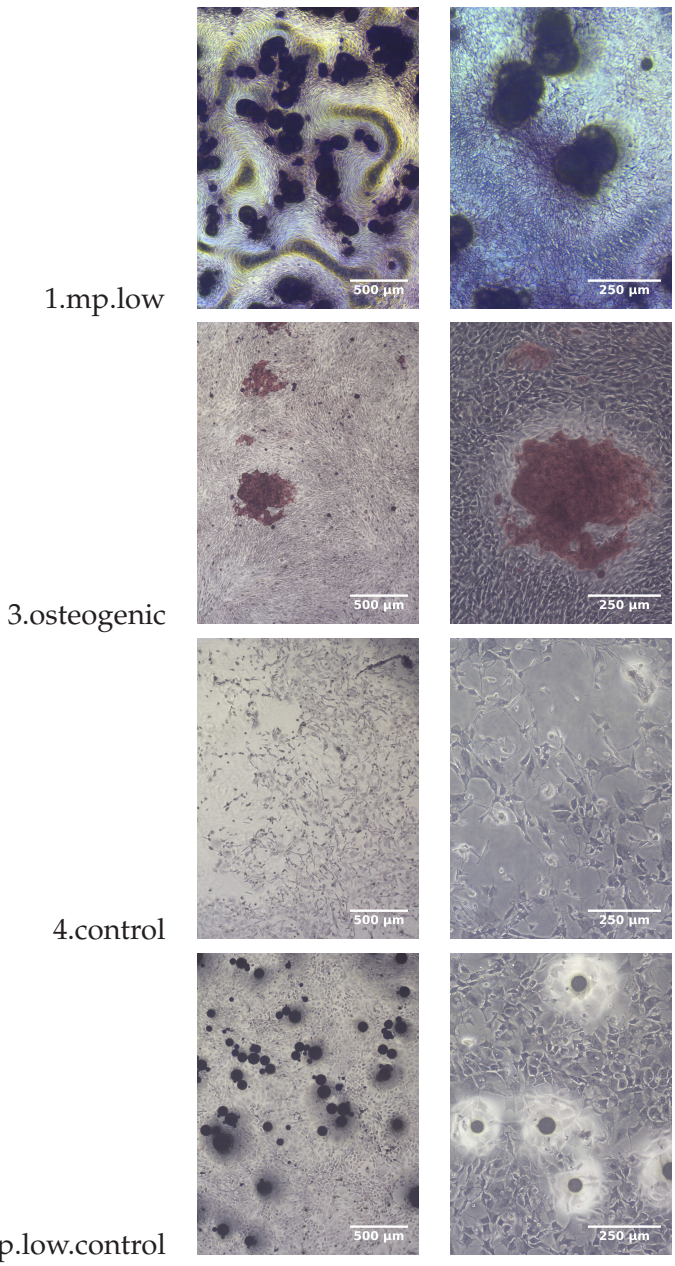

Figure 3.5: Mineral deposition from a murine calvarial osteoblast cell line (MC3T3-E1). Images of MC3T3 cells with microparticles were taken after 10 days of culture and control images were taken on day 24. This is because only at this time point did the osteogenically supplemented control group exhibit mineral deposition. Mineral deposition was stained with alizarin red and images were obtained using phase contrast optical microscopy.

3.4.4 Quantification of released BMP-2 using an ELISA

Activity of released BMP-2 was established. A quantitative analysis was the next step. This would determine the level of BMP-2 (if any) that was becoming denatured and enable us to better estimate the amount of microparticles that would be required to elicit an appropriate biological response *in vivo*.

Samples from the verification release study (Figure 3.1, Page 83) were assessed using an enzyme-linked immunosorbent assay (ELISA). This method detects molecules based on a specific binding site. The assumption is generally made that any small molecules able to bind to this site are structurally undamaged, so active.

The ELISA was supplied with a small quantity of BMP-2 reference standard for calibration plots. Due to the convenient small aliquot of the reference standard this was used for a calibration plot rather than the batch of BMP-2 used in the microparticles. This decision was mainly based on practicality. Reconstituting a larger BMP-2 aliquot from the original batch was seen as unnecessary as different sources of BMP-2 *should* have similar activity levels

The ELISA produced a good calibration plot but samples of release supernatant exhibited a lower activity than expected (although still within the linear working range of the assay). A comparison between expected BMP-2 values (based on total protein quantification) and measured values (measured using ELISA) highlights this discrepancy (Table 3.2).

Day	Predicted (µg)	Measured (µg)
0.25	7.12	1.32
1	8.86	1.67
2	11.72	1.84
3	14.16	1.99
4	18.56	2.11
6	26.18	2.20
7	29.46	2.25
9	34.06	2.50
10	37.95	2.63
13	40.93	2.84

Table 3.2: Predicted cumulative amount of BMP-2 release based on total protein release from microparticles compared with measured levels of BMP-2 release (as quantified using an ELISA). Levels of BMP-2 were lower than expected.

The values determined using the ELISA were up to 20 times lower than expected. This effect could have been caused by three circumstances:

1. The BMP-2 was becoming denatured as a result of encapsulation / release.
2. The experimental batch of BMP-2 was of a lower activity than the reference standard.
3. The ELISA was not detecting the experimental batch of BMP-2 correctly.

Due to limited samples it was not possible to fully explore these circumstances. It was decided that a biological method for quantification was more desirable. A quantifiable biological response was explored to determine the cause of these low activity readings.

3.4.5 Quantification of BMP-2 batches using a cell line

A proportional expression of ALP (in response to BMP-2) was verified (Figure 3.6). This response indicates a limit of detection between 0 and 100 ng/ml and a saturation point beyond 1000 ng/ml. This linear expression is not novel but it was important that protocols be developed and verified for this method so that it could be used as an analytical tool.

The BMP-2 was supplied from a non-commercial source, as a result there was no certificate of analysis. The lack of any reference standard meant that only relative comparisons between batches were possible. Batch 3 exhibited a biological response within anticipated concentrations (Figure 3.6) [187]. This indicated that this batch is active within an expected range. Batch 1 was encapsulated within the microparticles and assessed with the ELISA, it demonstrated lower activity (Table 3.2).

The three batches of BMP-2 were assessed. Assuming they had identical activity, the biological effect exhibited by C2C12 cells would have been the same.

Comparison of the biological activity between the three BMP-2 batches showed that batch 1 had significantly lower activity than the other two batches (Figure 3.7). Batches 2 and 3 have more similar (though statistically different) levels of activity. The lower than expected activity of batch 1 shows that this was a contributing factor to the lower than expected detection in the ELISA. Subsequent work used the more active batches 2 and 3.

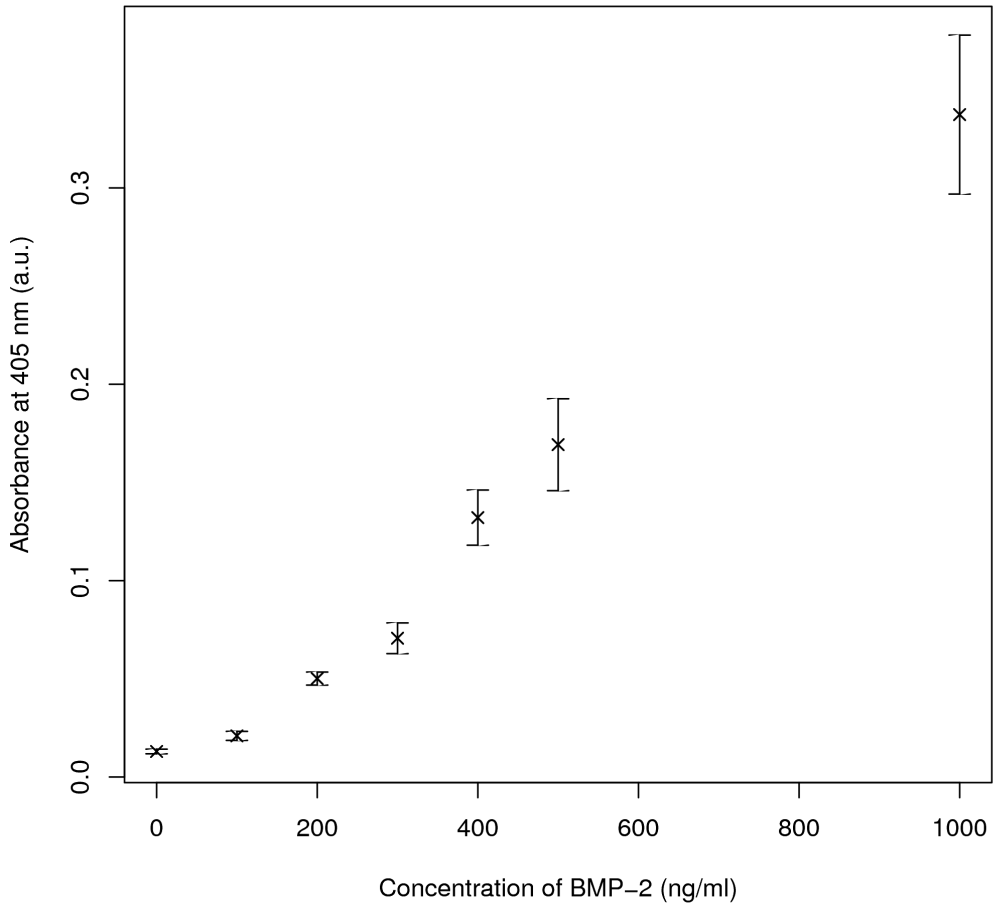

Figure 3.6: Expression of alkaline phosphatase (ALP) from C2C12 cells in response to different concentrations of BMP-2. ALP was quantified through its enzymatic dephosphorylation of para-nitrophenylphosphate to para-nitrophenol (Section 3.3.4.6). Para-nitrophenol was quantified colorimetrically. Error bars indicate $\pm$ standard deviation; n=6.

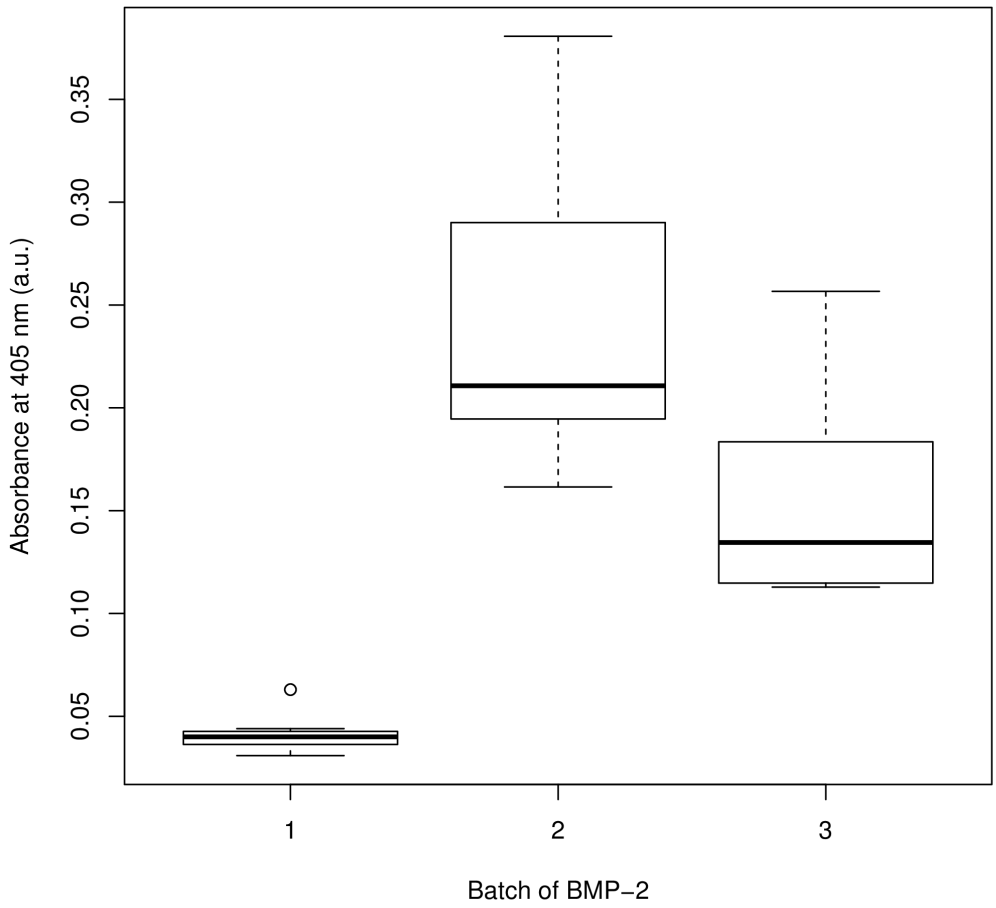

Figure 3.7: Expression of alkaline phosphatase (ALP) from C2C12 cells in response to an identical concentration of BMP-2 from three different batches. ALP was quantified through its enzymatic dephosphorylation of para-nitrophenylphosphate to para-nitrophenol (Section 3.3.4.6). Para-nitrophenol was quantified colorimetrically.The relative activities of the different batches were significantly different ($p<0.05$).

3.5 Conclusions

Co-culture of BMP-2 loaded microparticles induced osteogenic differentiation within a murine osteoblast cell line. This showed that the released BMP-2 was biologically active and able to induce a biological effect. The publication of these results assisted our collaborators in gaining ethical approval for an *in vivo* study.

Relative comparison of three BMP-2 batches identified a less active batch. This batch was isolated from further study. This defective batch of BMP-2 was still able to induce differentiation when released from microparticles showing that the controlled release system was effective even under sub-optimum conditions. The largest batch of BMP-2 (batch 2) exhibited the highest level of biological activity. This batch was set aside for the large mammal *in vivo* study.

The variation in these batches was almost certainly due to the lack of quality control from our supplier. This was a non commercial source of BMP-2 as part of a collaboration so we had no options for obtaining a commercial batch with full quality control certification.

3.6 Future Work

The strange pattern of mineral deposition indicated (Figure 3.5) is worthy of further analysis. It needs to be determined whether this is a result of a BMP-2 concentration gradient or if the microparticles have some kind of influence over the pattern of mineral deposition.

In order to accurately formulate a clinical growth factor release therapy it will be essential to determine the concentration of BMP-2 release. A cell line such as C2C12 murine myoblasts that respond proportionally to BMP-2 concentrations could be used.

This chapter confirms that an osteogenic growth factor (BMP-2) can be released and is biologically active, in addition an active batch of BMP-2 had been selected for the segmental defect study. Verification of the release of an angiogenic growth factor will benefit the study. The next chapter addresses this and the application of this microparticle system *in vivo*.

CHAPTER 4

Results III: Preparation for an *in vivo* study

4.1 Introduction

The previous two chapters have shown the development of a microparticle system for the controlled release of growth factors. The release of growth factors over sustained periods and the biological activity of these released proteins has been shown. The next step for this technique to become of benefit to humans is preclinical trials. These trials are carried out in non-human animals. They are required to demonstrate both safety and efficacy. This chapter details the process of taking experimental material from a lab and preparing and characterising it in such a way that it can be implanted *in vivo*.

A large mammal, critically sized, segmental defect model was selected to assess the effect of multiple growth factor release. Of the large mammal models canine, ovine and porcine are the most well published. Social pressures have reduced the favorability of canine models in recent years and although porcine models are very physiologically comparable to humans, the short length of their tibial long-bones precludes the use of some implants designed for use in humans.

It has been suggested that a model species should have similar physiological and pathophysiological conditions to humans in order for the model to be representative. Humans and sheep have no major difference in bone mineral composition [190] and sheep metabolic and remodelling rates are similar to that of human bones [191]. Ovine studies are thought to be good models for human bone turnover and remodelling [192]. Mature sheep have a similar body weight to adult humans and their long bone dimensions allow the use of human implants [193]. Despite these clear advantaves of an ovine model there are also disadvantages. Trabecular bone in immature sheep has

a high collagen content. This means that it has a lower density and stiffness leading to a higher flexibility that human bone [194]. Secondary osteonal remodelling does not take place until an average of 7–9 years [193] and mature sheep exhibit a higher trabecular density and greater bone strength compared to humans [194]. In order to mitigate these factors, ovine candidates were selected in the age range of 6–7 years. It is thought that at this age, bone density will be similar to humans and these relatively old sheep possess the secondary osteon remodelling which is characteristic of human bone.

Segmental defects are often used to assess bone repair strategies as they show a quantitative level of new bone generation. This is useful to assess the osteoinductive and osteoconductive effects of repair strategies. A critically sized osseous defect should be of dimensions to preclude spontaneous healing [195], this makes it possible to determine whether a therapeutic approach is significantly effective. The specific definition of a critically sized defect varies. It has been defined as:

> "the smallest size intraosseous wound in a particular bone and species of animal that will not heal spontaneously during the lifetime of the animal" [196, 197].

But also as as a defect which shows less than 10 % bony regeneration during the lifetime of the animal [197]. It is also clear from the literature that the minimum size that renders a defect 'critical' is not well understood. It is unlikely that there will ever be a blanket definition for a single species since other factors such as defect location, soft tissue or biomechanical conditions, age, metabolism, systemic conditions, related morbidities, gender and body weight all play a role in the rate and degree of repair [196, 198].

As a general rule in large mammals, a defect greater than 2–2.5 times the diameter of the bone has been described as 'critical' [198, 199] or in the case of sheep, up to three times the diameter of the corresponding diaphysis [199].

Our proposed repair strategy combines the microparticle growth factor delivery system with a highly porous, structurally supportive scaffold composed of poly ε-caprolactone and tricalcium phosphate. Poly ε-caprolactone has a very low rate of degradation. A novel combination of Poly ε-caprolactone and tricalcium phosphate (PCL-TCP) was first proposed in 2005 [200]. The TCP component has been shown to spontaneously bond to and integrate with bone as well as provide pH buffering against polymer degradation [201, 202]. This particular PCL-TCP composite has demonstrated a homogeneous distribution of TCP and favourable mechanical properties [203]. It has been suggested that the mechanical properties of porous polymer constructs can be

improved through the addition of TCP [204].

A fused deposition modelling (FDM) method of scaffold fabrication can provide reproducible three-dimensional constructs with fully interconnected channel networks [81]. Scaffolds produced in this way from PCL-TCP (80 %-20 % *w/w*) have demonstrated cell attachment *in vitro* [205], osteoprogenitor proliferation and differentiation [205, 206] and been shown to support bone formation *in vivo* [200].

The scaffold was designed to fit the proposed defect site. A cylindrical scaffold with a central void was designed to mimic the tubular structure of a long bone diaphysis. The scaffold had 70 % porosity and 100 % pore interconnectivity. The pore sizes were 350–500 µm and the polymer strands had a 0/90° lay down pattern (Figure 4.1). This open structure should be favourable for nutrient supply and host tissue ingress.

It is hypothesised that angiogenic factors released from within this scaffold should help early vascularisation of the defect site. It is hoped that this early angiogenesis will facilitate the recruitment of progenitor cells and support localised tissue regeneration.

There are concerns that clinical use of BMP-2 can result in bone overgrowth [53]. It is hoped that a sustained delivery of growth factors will lead to a more physiological morphology.

4.2 Aims

The aim of this chapter was to develop a formulation and manufacturing method to fabricate growth factor loaded microparticles. A method was then developed to combine printed PCL scaffolds with with this growth factor delivery system. This would enable successful surgical implantation.

This involved fabricating microparticles that would release VEGF and PDGF over a short time and would release BMP-2 for a longer period. Additionally these growth factors had to be released at concentrations theorised to elicit a therapeutic response.

A method was devised to combine the microparticles with the poly ε-caprolactone/tricalcium phosphate scaffold. This method had to be suitable for use immediately prior to surgery so that the microparticles could be stored dry and only begin to hydrate after implantation.

A successful outcome to this chapter will be successful preparation and implantation of this novel biomaterial.

4.3 Methods

4.3.1 Determination of a Therapeutic Dose

Before fabricating growth factor loaded microparticles for this study it was important to estimate the amount of growth factor required to achieve a therapeutic dose. This was not an easy task as a number of factors can affect the outcome independent of BMP-2 dose. These include location of administration, condition within the location and measured outcome. Furthermore, the effect can be species dependent [208]. The majority of published literature regarding the use of BMP-2 and critically sized osseous defects is for small mammal models and often uses a bolus delivery. Stability limitations mean that studies using non-sustained, bolus delivery generally use supra-physiological amounts of BMP-2 just to see an effect.

The lowest dose of BMP-2 that appears to have an effect was utilised in a Rat cranial defect model [209]. This system delivered 1–2 ng/mm^3/day of BMP-2. A VEGF dose greater that that of a BMP-4 dose can be detrimental to bone development [210]. A VEGF dose slightly lower than that of BMP-2 has been shown to increase bone formation in a rat cranial model [211]. It was decided, based on this evidence, to aim for a VEGF dose of 1 ng/mm^3/day. Recent studies have shown that equal expression of PDGF to VEGF has been a suitable level to stabilise the VEGF-induced vasculature and significantly improve function in a murine ischemic limb muscle model [40].

4.3.2 Fabrication of Growth Factor Loaded Microparticles

Growth factors rhVEGF$_{165}$ and rhPDGF-BB were sourced from PEPROTECH (PeproTech House, London, UK). These particular isomers were selected because of their documented and effective use in angiogenic and osteogenic regenerative situations [40, 212–216]. As well as an important role in angiogenesis, PDGF-BB has shown the ability to induce osteoblast chemotaxis [217]. Batch 2 of BMP-2 was used (Section 3.3.3, Page 78). Microparticles were fabricated in the larger size range (Section 2.3.3 – homogenisation protocol) from three different formulations to achieve desired release profiles for each growth factor. For BMP-2 delivery a slow-releasing formulation of PLGA 50:50 with 10 % *w/w* PLGA-PEG-PLGA selected. This would provide a sustained release for approximately 30 days. Polymer formulations selected for VEGF and PDGF microparticles were PLGA 85:15 with 30% *w/w* PLGA-PEG-PLGA and PLGA 50:50 with 20 % *w/w* PLGA-PEG-PLGA respectively.

Blank microparticles were fabricated to ensure that each defect site would have exactly

the same mass and combination of polymers. This would ensure that any difference seen would be due to the effect of growth factors and not scaffold variations.

As before, microparticles contained 1 % *w/w* protein loading. Protein consisted of a 1:9 ratio of growth factor to HSA. This level of carrier protein exhibited active protein release is previous studies carried out in Chapter 3. Released BMP-2 with this level of HSA was able to stimulate the expression of alkaline phosphatase (Section 3.2 on Page 85).

4.3.3 Fabrication of Coloured Microparticles

Coloured microparticles were fabricated to enhance visibility when they were attached to the poly ε-caprolactone/tricalcium phosphate scaffold. During microparticle fabrication, 5 mg of the lipophilic dye Oil Red O was added to the organic phase. This was adequate to colour the microparticles bright red. Microparticles were fabricated as per the method is Section 2.3.3; homogenisation protocol.

4.3.4 Microparticle Sterilisation

Microparticles were fabricated under clean (but not aseptic) conditions. They were sterilised using an ultraviolet method (Section 3.3.2). This was deemed the least detrimental method. Other sterilisation methods such as gamma irradiation are thought to damage polymers to a greater extent [130]. Previous activity measurements were carried out on microparticles that had been UV sterilised so this method was thought to not be significantly detrimental to growth factor activity.

4.3.5 Attaching Microparticles to a Scaffold – DMSO method

An aqueous solution of dimethyl sulphoxide (DMSO) (10 % *v/v*) was used to soften a suspension of microparticles. This solution was applied to the scaffold pores and was drawn in through surface tension. Excess solvent was wicked away and the composite was gently washed.

4.3.6 Attaching Microparticles to a Scaffold – Fibrin

A procedure was developed whereby a fibrinogen suspension of microparticles could be injected into the porous scaffold (Figure 4.7). Each end was then clotted using thrombin. This produced a fibrin plug keeping the microparticles in the scaffold during

implantation.

A small polytetrafluoroethylene (PTFE) disk was placed in the bottom of a well in a 24-well plate. This prevented the fibrin solution sticking. 50 µl of thrombin solution was added to the well. The microparticles for one tibial defect (2000 mg) were mixed with 1100 µl of fibrinogen solution. This microparticle suspension was added to a modified 5 ml syringe (Figure 4.3). Air bubbles were allowed to escape and the scaffold was placed on the end of the syringe. This was then inverted and placed into the prepared well. The microparticle suspension was smoothly injected into the scaffold. Thrombin solution (30 µl) was added to the top of the scaffold to clot the fibrin. This scaffold was now ready for implantation.

Fibrinogen Solution Fibrinogen solution (20 mg/ml) was prepared by dissolving fibrinogen in deionised water at 37 °C.

Thrombin Solution Thrombin solution (8 NIH units/ml) was prepared by dissolving thrombin in deionised water at 37 °C.

Modified Syringe The microparticle suspension behaves like a non-Newtonian fluid. When shear is applied it resists flow. The suspension could not be extruded form a standard syringe because as soon as pressure was applied it clogged. This problem was overcome by truncating a 5 ml syringe at the zero mark. This eliminated bore narrowing so the microparticle suspension could be ejected from the syringe.

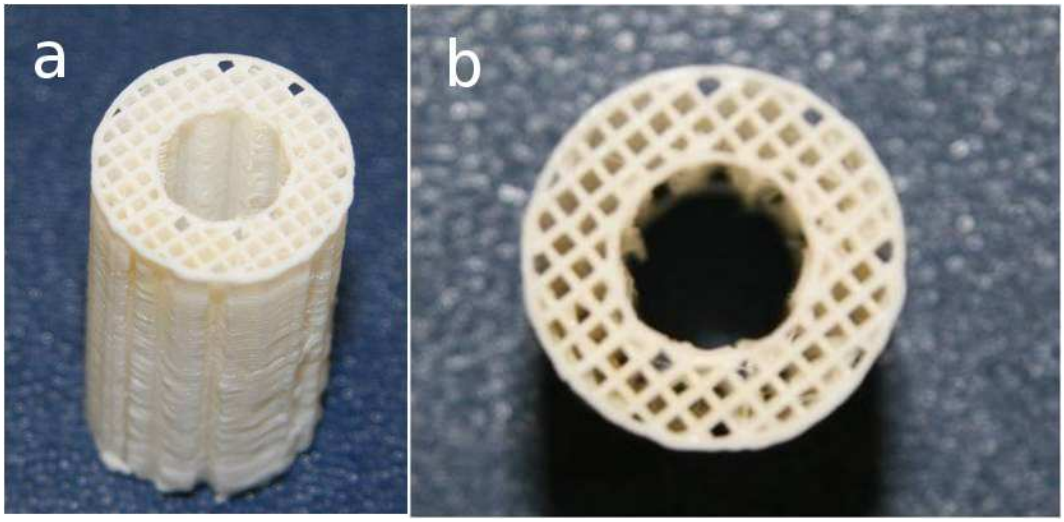

Figure 4.1: Bioresorbable cylindrical scaffolds made from medical grade poly ε-caprolactone/tricalcium phosphate 20 % *w/w* and produced by fused deposition modelling [207]. Side view (**a**), top view (**b**). Outer diameter: 20 mm, height: 300 mm, inner diameter: 8 mm, 70 % porosity, 100 % pore interconnectivity, 350–500 µm pore size, 0/90° lay down pattern. This scaffold was provided by our collaborators Dietmar Hutmacher and Maria Woodruff (Queensland University of Technology, Brisbane, Australia).

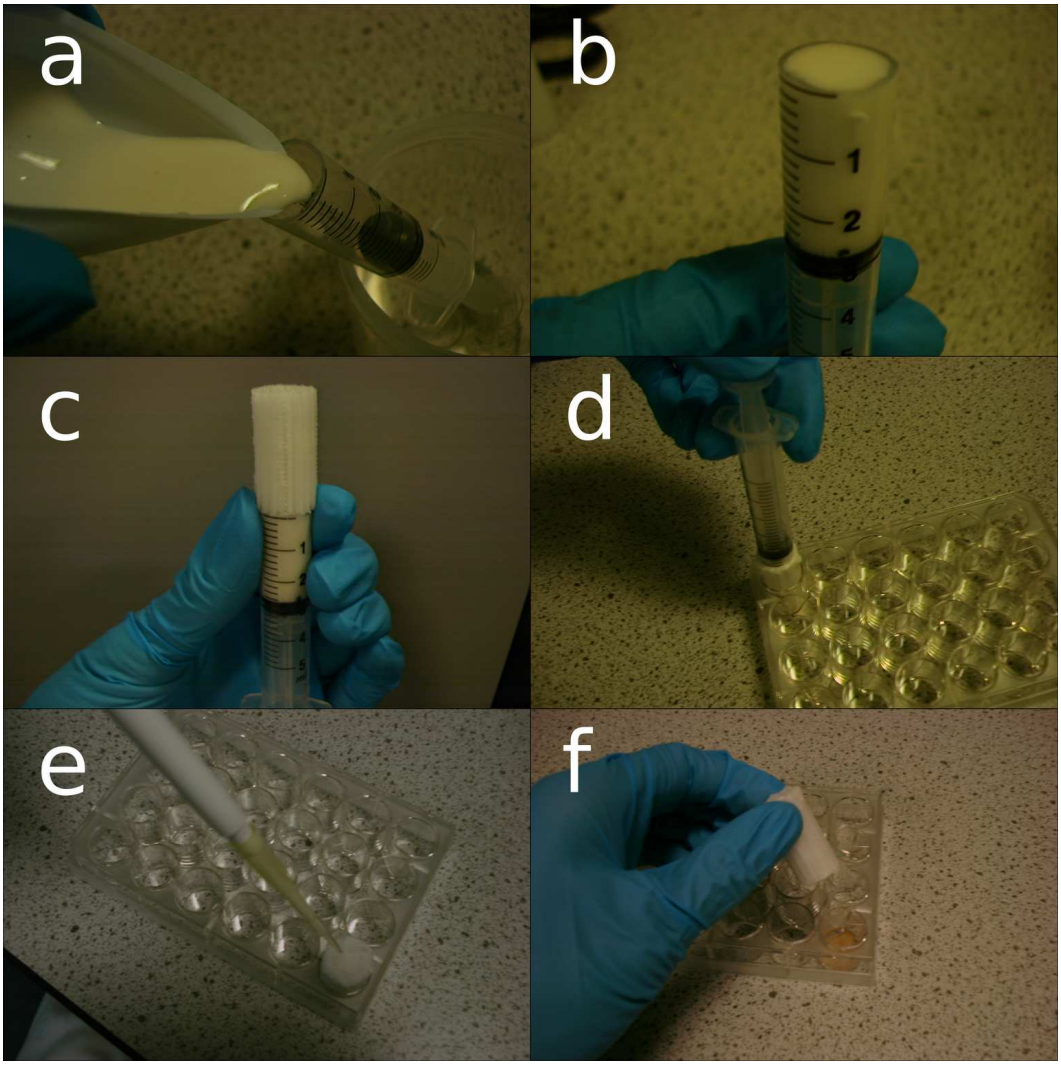

Figure 4.2: Preparation procedure for incorporating microparticles into the poly ε-caprolactone/tricalcium phosphate scaffold. Microparticles were suspended in a fibrinogen solution (a) and transferred to a modified syringe (b).The modified syringe is married to the scaffold (c) and the microparticle suspension extruded into the scaffold (d). The ends of the scaffold are clotted with thrombin solution (e) and the scaffold composite is now ready to handle/implant (f). This methods is described in Section 4.3.6.

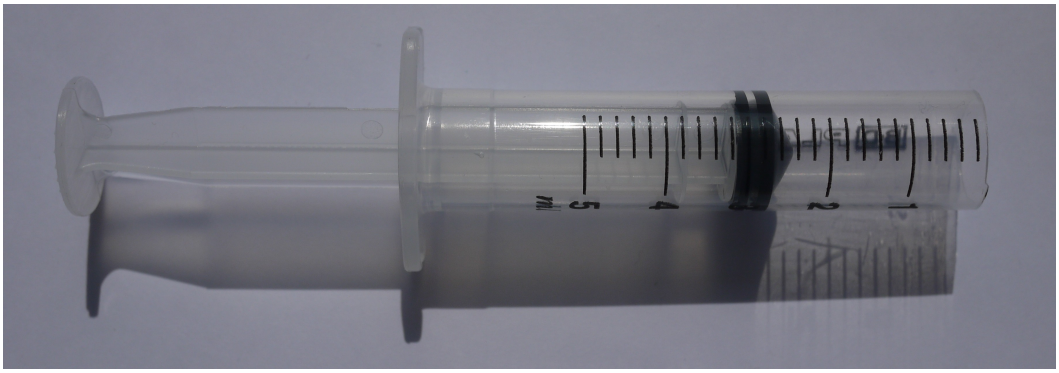

Figure 4.3: Modified syringe. The end was cut off a 5 ml syringe to eliminate bore narrowing. This syringe was used to deliver a microparticle suspension into the porous scaffold. This method was described in Section 4.3.6.

4.3.7 Imaging microparticles and scaffolds optically

Pilot scaffolds and microparticles were visualised using optical techniques. For low magnification overviews a digital camera (*Sony DSC F717*) was used with a macro setting. For higher magnification images a phase contrast optical microscope was used (*Nikon A1*). In order to obtain images with an adequate depth of field, the aperture was closed down and the light level pushed up.

4.3.8 Micro Computerised Tomography Imaging

Scaffolds were characterised by micro x-ray computed tomography (μCT). Scaffolds were mounted on a stage at a height of 10 mm within the imaging system and scanned. Measurements were obtained at a voltage of 40 kV, current of 800 μA and voxel resolution of 20.6 μm. The transmission images were reconstructed using Skyscan supplied software (*NRecon*) and quantitative analysis of porosity and pore architecture was obtained using direct morphometry calculations in the Skyscan CTAn software package.

Care was taken to define an accurate scaffold boundary to ensure that porosity analysis did not induce a positive bias by assessing regions outside the scaffold.

4.4 Results and Discussion

4.4.1 Microparticle Fabrication

Microparticles were fabricated over a two week period. Effort was made to ensure consistency between batches. Protein release studies were carried out on every batch that was to be used *in vivo* and representative batches were sized. Batches containing BMP-2 were paired up during fabrication and filtered together because each defect would require two batches, this effectively halved the number of batches requiring protein release analysis. All others were kept separate.

Release was carried out in triplicate and assessed from 12 batches containing BMP-2, 3 containing VEGF and 3 containing PDGF. No batches appeared anomalous (Figure 4.4).

Microparticles loaded with VEGF and PDGF exhibited less separation than was anticipated (Figure 4.5, a). The majority of protein release from these formulations takes place by day 3-4. It can be hypothesised that the release rate *in vivo* will be slower than this. Sink conditions were maintained for the *in vitro* release studies, this will most likely not be the case *in vivo*. In addition, growth factors will be released into the fibrin clot initially so there will be few proteolytic enzymes present to denature the growth factors. It can be reasonably estimated that these angiogenic factors will be active within the defect site for up to a week.

When these formulations were being chosen it was thought that thought that temporal separation between VEGF and PDGF was desirable since PDGF facilitates pericyte recruitment to stabilise the vascular network induced by VEGF. It was even demonstrated that VEGF followed by PDGF-BB release was more effective than the growth factors individually at inducing mature vessel formation and improving function in a myocardial infarction model [24]. This makes logical sense since one mechanism follows the other. A more recent publication investigating a murine skeletal muscle ischemic model showed that early expression of PDGF-BB did not limit VEGF driven capillary growth and that increased pericyte recruitment in the first four days did not have a net negative effect on VEGF angiogenesis [40]. This indicates that our delivery system for VEGF and PDGF should still be highly effective even though we didn't achieve the desired VEGF and PDGF temporal separation.

Formulations releasing BMP-2 demonstrated a long duration of release (Figure4.5, b). The release is less regular than had been seen from this formulation previously (Figure 2.15, Page 70). This was attributed to PLGA-PEG-PLGA intra-batch variability.

Most of the protein was released at one of two stages. A burst release in the first day

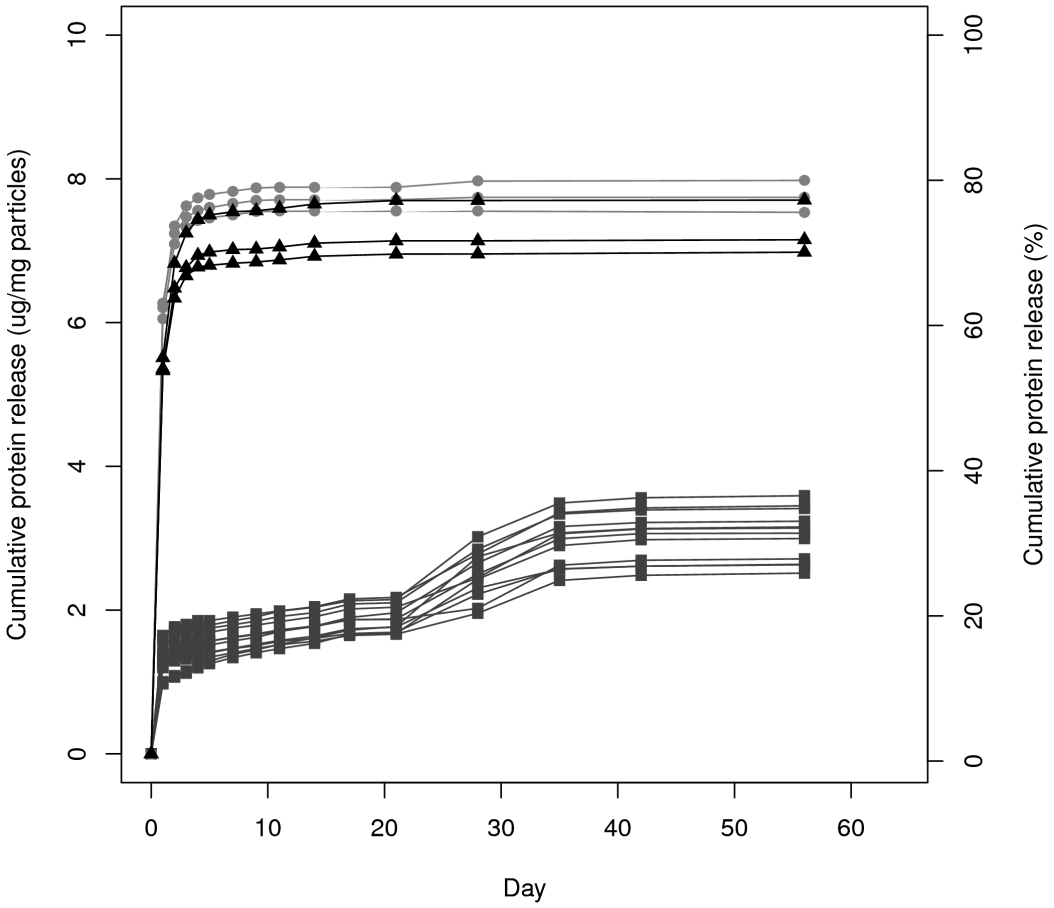

Figure 4.4: Cumulative protein release from each batch of microparticles to be used *in vivo*. Cumulative release of HSA/VEGF (●), HSA/PDGF (▲) and HSA/BMP-2 (■) from PLGA microparticles. No batches exhibited anomalous release behaviour. No error bars are shown because this plot shows individual data points, not averages. All microparticles shown were fabricated using the homogenisation method (Section 2.3.3). The PLGA formulations are described in Section 4.3.2.

a

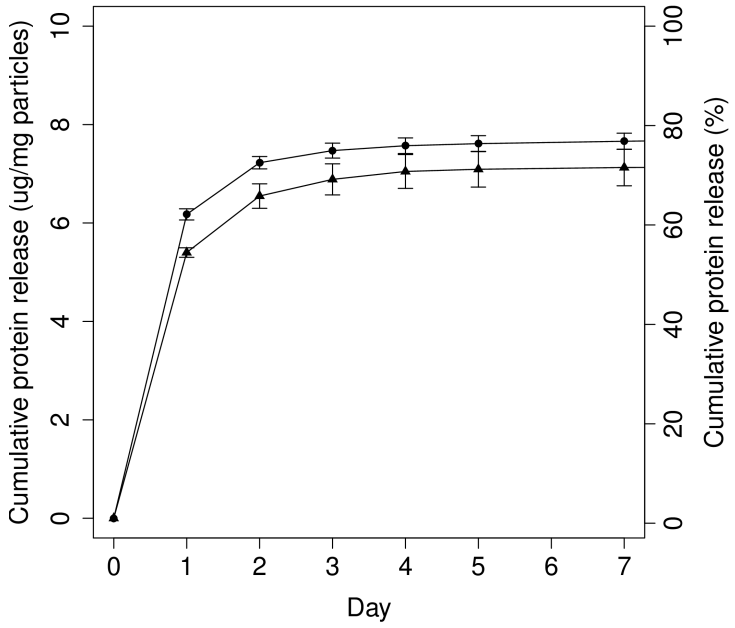

b

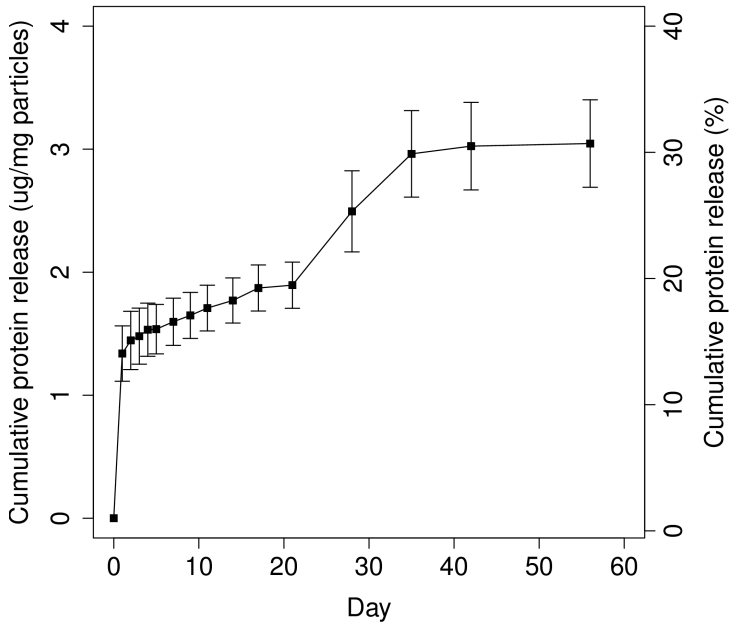

Figure 4.5: (a) Cumulative release of HSA/VEGF (•) and HSA/PDGF (▲) from PLGA microparticles. These angiogenic factors are delivered over the first few days. No further release is detected. **(b)** Cumulative release of HSA/BMP-2 (■) from PLGA microparticles. An initial burst release is followed by sustained release that accelerates at day 21 until day 35.Error bars show ± cumulative standard deviation of the mean; n=9. All microparticles shown were fabricated using the homogenisation method (Section 2.3.3). The PLGA formulations are described in Section 4.3.2.

and a steady release from day 21–35. As with the angiogenic factors, this is unlikely to be an accurate representation of *in vivo* release. What is clear is that angiogenic factors will be released at an early stage and the osteogenic factor will be present at a later stage. Representative batches of these microparticles were sized using laser diffraction (Section 2.3.4.2 on Page 41). The size is important because it can affect the release rate of protein as well as the flow characteristics. It was important that the microparticles didn't separate resulting in a non-homogeneous distribution of growth factors *in vivo*. The sizes fell within anticipated ranges (Figure 4.6). The formulation delivering BMP-2 (PLGA 50:50 with 10 % PLGA-PEG-PLGA) were larger than the other two formulations. This is consistent with previous data indicating that an increasing PEG concentration leads to smaller microparticles (Figure 2.4, Page 49).

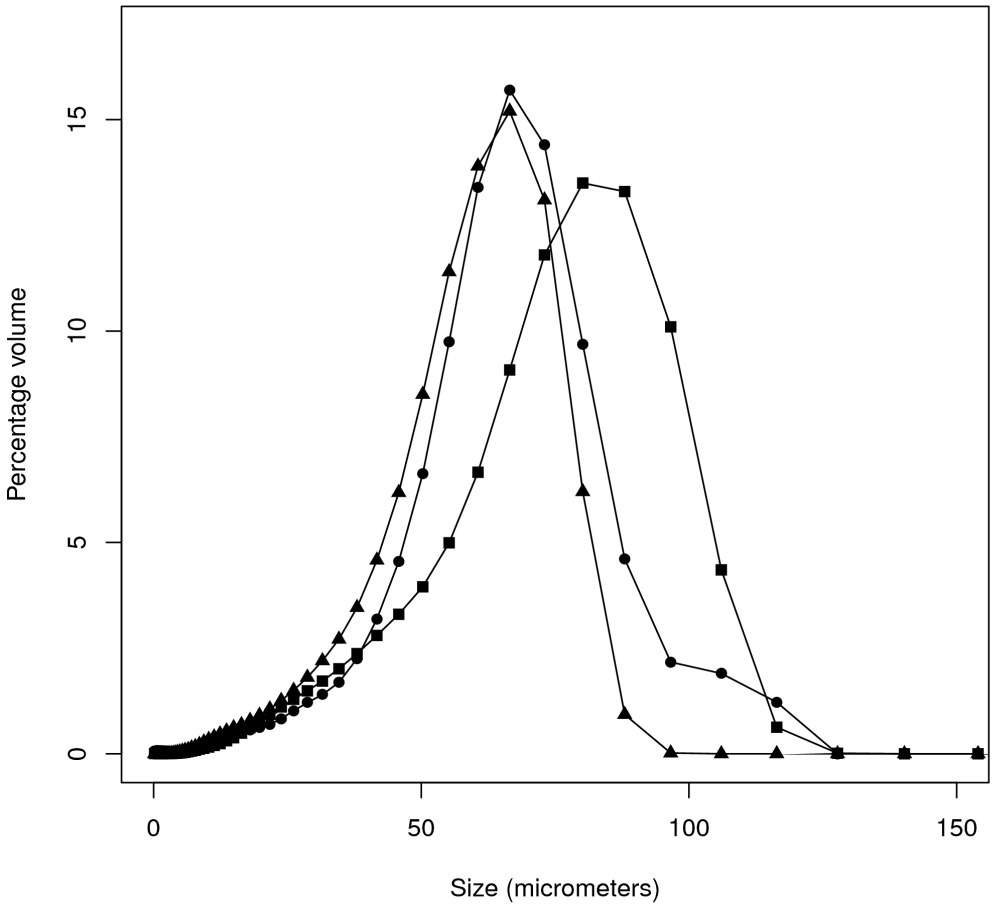

Figure 4.6: Size distributions of representative batches of microparticles from each formulation. PLGA 85:15 with 30% PLGA-PEG-PLGA (HSA/VEGF) (●), PLGA 50:50 with 20% PLGA-PEG-PLGA (HSA/PDGF) (▲) and PLGA 50:50 with 10% PLGA-PEG-PLGA) (HSA/BMP-2) (■) (Section 4.3.2) using the homogenisation method (Section 2.3.3.2). Microparticles were sized using laser diffraction (Method 2.3.4.2). The size distributions fell within the anticipated ranges shown in Chapter 2.

4.4.2 Preparation of the Scaffold/Microparticle Composite

It was important to combine the microparticles with the scaffold in such a way that they would remain in place after implantation and during protein release. There were two ways to approach this:

1. Utilising intrinsic properties of the PLGA to adhere the microparticles to the scaffold structure. Microparticles become 'sticky' when exposed to heat or solvent. They could then be affixed to the scaffold and solidified by either cooling or allowing the solvent to evaporate.

2. The use of extrinsic components to affix the microparticles to the scaffold. Hydrogels were a likely candidate. Glues and chemical cross-linkers were considered as well.

Method 1 was explored by affixing coloured microparticles (Section 4.3.3, Page 100) to small PCL-TCP scaffolds using DMSO as a solvent (Section 4.3.5, Page 100).

This method (after some optimisation) gave good distribution of microparticles throughout the small test scaffolds (Figure 4.7 a & b). At higher magnifications is was apparent that the microparticles were deformed by the process and aggregated together (Figure 4.7 c & d). There were concerns that this would affect protein release. This method was also only suitable for the smaller test scaffolds. For larger scaffolds it was difficult to get the microparticles into deep pores.

Method 2 was selected for use in the large mammal study as it was thought to pose the least risk of particle damage. A fibrin clot was selected at the suggestion of our collaborators who were carrying out the *in vivo* work. They had used it for other osteochondral applications successfully. The fibrinogen would clot and immobilise the microparticles during implantation then become enzymatically degraded *in vivo*. This fibrin clot mimics conditions that would result normally. The defect site would bleed, this would penetrate into the scaffold and form a natural clot.

A full-scale PCL-TCP scaffold was obtained from our collaborators for microparticle attachment studies. Microparticles were immobilised within the scaffold and held in place with a fibrin clot (Section 4.3.6, Page 100). Different combinations of fibrinogen concentration and volume were assessed because the final microparticle suspension had to adhere to two key requirements.

1. The total volume of the microparticles in suspension had to be less than or equal to the available space within the scaffold.

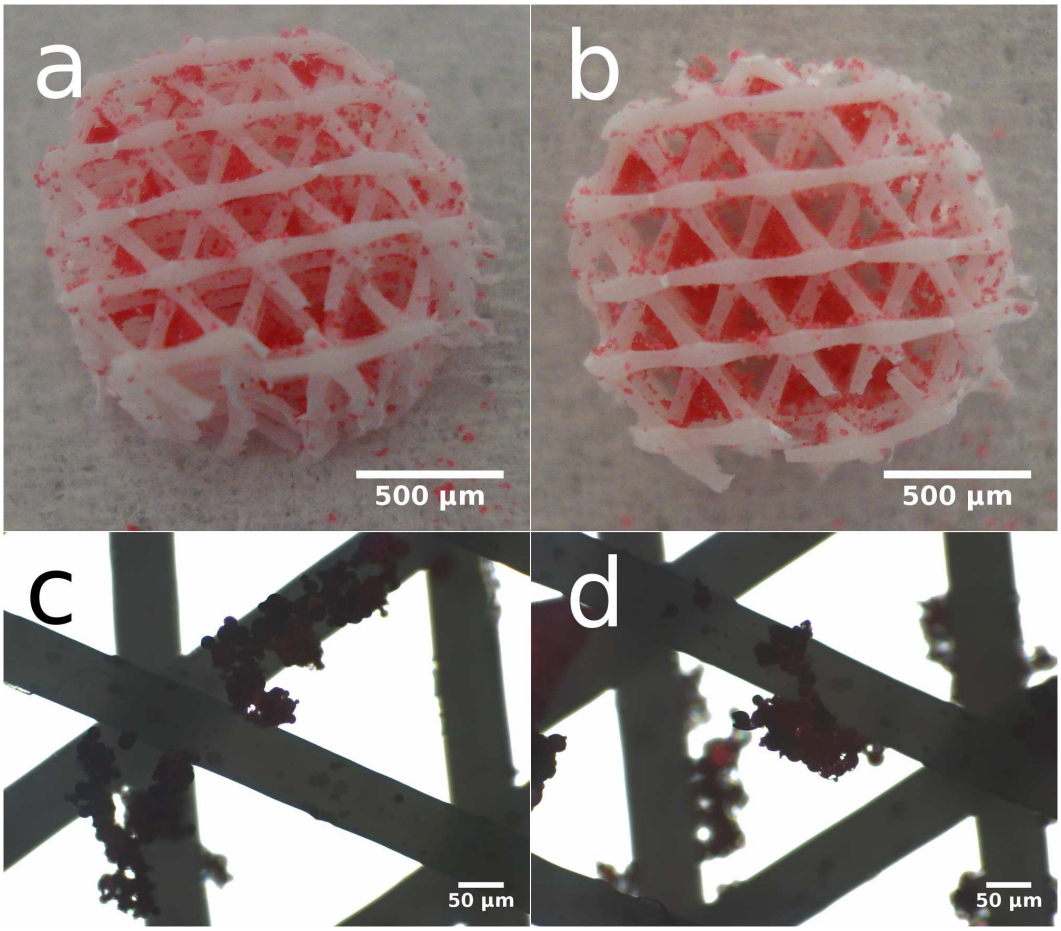

Figure 4.7: Images of microparticles attached to small poly ε-caprolactone/tricalcium phosphate test scaffolds. Microparticles were dyed red to enhance contrast to the scaffold (Section 4.3.3). Microparticles were attached to the scaffold using a DMSO solvent softening method (Section 4.3.5). Homogeneous attachment can be seen at low magnification (a,b) but at higher magnification microparticles have aggregated and deformed as a result of the solvent treatment (c,d). Scaffolds were imaged using a commercial digital camera and optical microscopy techniques (Section 4.3.7).

2. The viscosity of the microparticle suspension had to allow it to flow into the scaffold and keep it within the scaffold after each end was clotted with thrombin.

The final protocol facilitated these needs. The scaffold with the particles within it (Figure 4.8) could be immediately handled after clotting with thrombin.

The prepared scaffold was assessed using micro computerised x-ray tomography (μ-CT) to investigate the distribution of microparticles within the scaffold. An even distribution was preferable to allow an even diffusion of growth factors after implantation. It can be seen from a longitudinal x-ray image (Figure 4.9, a) and a computer generated transverse 'slice' (Figure 4.9, b) that the microparticles are mainly confined to the central section of the scaffold. This leaves a porous outer structure available for tissue ingress and remodelling. This porous structure can be easily seen in the three-dimensional computer-generated tomographic images (Figure 4.10).

Once the microparticles degrade, the central section would once again become empty. This would more accurately mimic physiological bone structure.

The porosity of the whole scaffold, once filled with microparticles, was 53 % and the microporosity within the central microparticle filled section was 11 %. The voxel resolution was 20.6 μm so porosity below this size could not be resolved. There would most likely be a degree of microporosity. This would facilitate the diffusion of released bioactive molecules.

A high degree of porosity is required for effective tissue ingress [73]. The open outer structure of this scaffold meets these requirements.

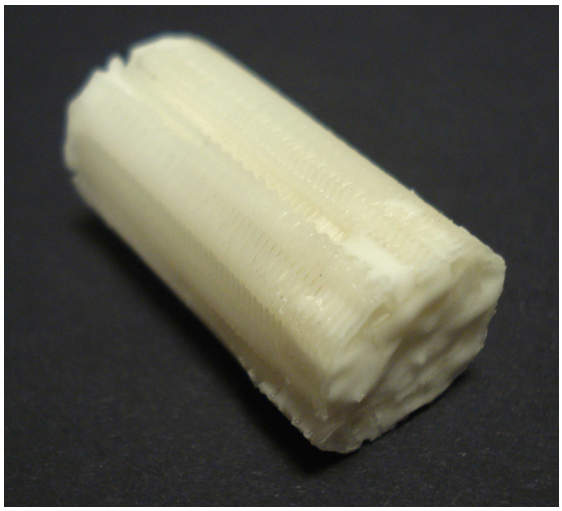

Figure 4.8: Image of poly ε-caprolactone/tricalcium phosphate scaffold after microparticles had been added. The central void contains the majority of the microparticles. The pores appear to also contain microparticles. Micro-CT analysis later revealed that the microparticles are only in the periphery of the pores. The open porous structure remains within. This scaffold was imaged using a commercial digital camera described in Section 4.3.7.

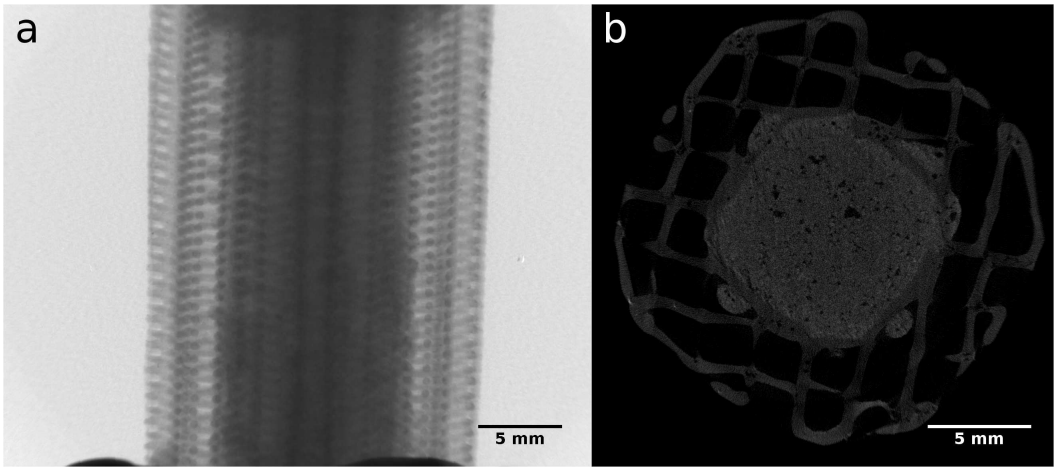

Figure 4.9: Images of the poly ε-caprolactone/tricalcium phosphate scaffold and microparticle composite obtained using X-rays and computer reconstruction (Section 4.3.8). Microparticles can be seen in the periphery of the pores at top top of the scaffold (a). Microparticles mainly inhabit the central section of the scaffold. A medial slice (reconstructed from multiple lateral X-rays) confirms that the microparticles contained within the central section of the scaffold. The outer pores are available for tissue ingress.

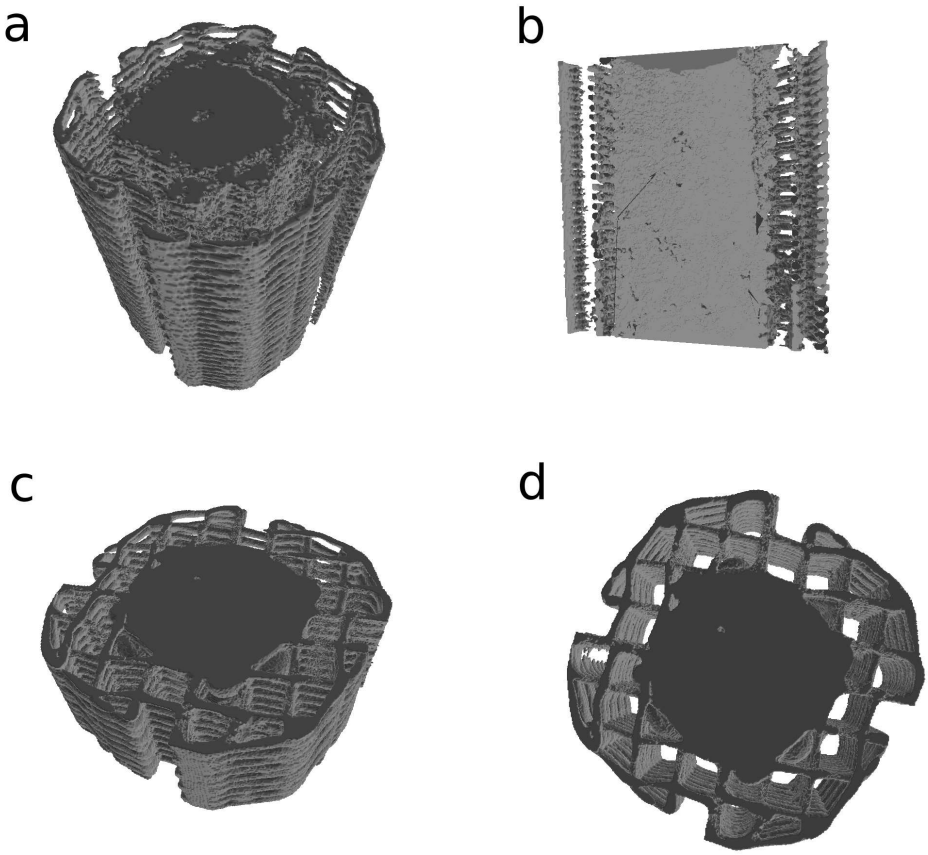

Figure 4.10: Three dimensional reconstructed images of the poly ε-caprolactone/tricalcium phosphate scaffold and microparticle composites (Section 4.3.8). These images compliment initial X-ray images. The outer structure is available for tissue ingress and physiologically matches the shape of a bone collar.

4.5 Conclusions

The goals of this work were achieved. Populations of microparticles were fabricated with the growth factors VEGF, PDGF and BMP-2 encapsulated within them. Protein release rate was assessed from each batch of microparticles. Each batch was found to meet the hypothesised requirements. Angiogenic factors (VEGF and PDGF) were delivered initially with the aim of defect vascularisation. Over a more sustained duration and at a later time point, BMP-2 was delivered.

Actual protein release data was used to prepare therapeutic doses of the microparticle combinations for use *in vivo*. A method was devised to combine these microparticle populations with the structurally supportive scaffold in theatre immediately prior to implantation. This combination of microparticles and scaffold was assessed to ensure the porous structure of the scaffold still remained.

Implantation of the biomaterial was successfully carried out in a critically sized defect model.

The mass of microparticles implanted *in vivo* was calculated from available data as a best guess in order to achieve therapeutic loadings within the defect site (Section 4.3.1). Most of the quantitative data regarding the delivery of growth factors utilises a non-controlled release method of delivery making it very difficult to extrapolate meaningful data for a controlled release formulation. For this study assumptions were made and the levels of growth factor were administered at the top end of estimated therapeutic levels. The high volume of microparticles compromised the hollow nature of the scaffold but still left the channels within the wall clear. Ideally a lower overall volume of microparticles would have been delivered in order to maximise porosity. To achieve this in future either a more concentrated formulation of growth factor within the miroparticles would be used or a lower dose of growth factor will be used.

4.6 Future Work

The synergistic nature of VEGF, PDGF and BMP-2 has been previously shown in various combinations but rarely under controlled delivery or at specific temporal intervals. We hope to highlight the importance of temporal delivery of these growth factors. If we can express these growth factors *in vivo* at times conducive with the physiological healing process and at physiological concentrations we hope to achieve a better clinical outcome. Not just a faster healing time but a better final tissue structure.

With the aid of additional funding, further *in vivo* assessment could take place to

identify optimum combinations and concentrations of these growth factors.

CHAPTER 5

Final Conclusions and Future Work

5.1 Discoveries made

The scope of this research was to carry out the groundwork necessary so that the controlled release of growth factors (GFs) could be assessed *in vivo* in future studies. This research was approached in a very stepwise and pragmatic way. The discoveries made here are an essential step towards future clinical therapies.

The objective of this study was to develop a controlled delivery system for growth factors with tunable release kinetics. The strategy was to include a hydrophilic polymer within the PLGA microparticles in order to modulate water ingress, affecting protein diffusion and polymer degradation. This thesis demonstrates for the first time that protein release kinetics can be altered from PLGA using the triblock copolymer PLGA-PEG-PLGA. This novel delivery system was able to deliver different growth factors with independent release kinetics. These kinetics could be tailored to the physiological expression of these growth factors in order to assess the next generation of GF therapies.

This microparticle delivery system was able to provide GF release kinetics decoupled from polymer degradation. A quasi zero order release profile was achieved using 10 % *w/w* PLGA-PEG-PLGA with 50:50 PLGA. Other formulations were able to deliver shorter release durations. Three of these formulations were selected as promising candidates from clinical growth factor delivery.

The structure of proteins released from polyesters will always be difficult to maintain and this loss of structure leads to protein denaturation. Using a surfactant copolymer, a chaperone protein (HSA) and carefully refined fabrication and processing protocol, issues of denaturation were mitigated. I demonstrated the release of active lysozyme and verified the release of active BMP-2 using a pre-osteoblast cellular assay.

Furthermore, a method was demonstrated whereby this microparticle controlled delivery system could be combined with a scaffold offering structural support. This would theoretically help to localise any physiological effect to a desired location as well as offering structural support. The growth factors explored were selected with bone regeneration as a focus so mechanical stability is an essential aspect.

5.2 Lessons learned

The current state of growth factor controlled delivery research is disjointed. even similar delivery systems vary between research groups as the fabrication protocols inevitably vary. A number of studies have assessed different growth factors from different formulations using *in vitro* and *in vivo* models. This makes if very difficult to draw sweeping conclusions regarding optimum systems or dosages or combinations of growth factors. The main limiting factor prohibiting larger growth factor studies is the high cost. Both he high cost of recombinant growth factors, but also the man-hours required to carry out lengthy studies and assess the results effectively.

One essential method to mitigate costs is the use of model proteins for initial exploratory studies. This thesis effectively verifies lysozyme as an effective model for BMP-2. Selection of suitable model proteins can be difficult. the physicochemical characteristics of the molecule must be similar to the growth factor of interest but the model protein must also be low-cost and have simple and effective methods to determine structural changes such as an enzymatic assay.

5.3 Future work

The expression of different growth factors at different stages of fracture repair can be measured and it is often assumed that these are the correct levels and combinations required for effective healing. This needs further exploration and validation. Until this takes place, the administration of growth factors for therapeutic purposes is guess work. This microparticle system provides a tool for the exploration of growth factors and will imminently lead to a large mammal preclinical model. I feel that there is scope to justify a number of smaller animal models simply assessing a variety of release rates of different growth factors. Something simple such as a Murine subcutaneous implantation would provide information very useful for furthering the development of growth factor therapies. Factors such as an effective therapeutic dose of growth factors still needs to be determined.

The difficulties in achieving effective and validated controlled release *in vitro* are extreme. I strongly believe that money and time would be far more productively spent if *in vivo* models are used at a far earlier stage to assess biological effects. The pathway through *in vitro* studies should be laid out prior to studies commencing and required outcomes determined so that this stage is not all consuming. It is far too easy to try and analyse too many variables when their impact on clinical outcomes may be minimal.

The triblock copolymer, PLGA-PEG-PLGA, has proven effective in modulating the release of protein from polyesters. Further exploration of different molecular weights of PLGA-PEG-PLGA was beyond the scope of this thesis but may provide a plethora of additional protein release profiles. Even simple aspects such as the hydrolytic degradation of the polymers over time (in storage) should be addressed if this is ever to become a clinical therapy. This thesis looked at this superficially with GPC measurements at different time points but more sampling, to assess intra-batch variation, as well as accelerated degradation studies would reveal essential polymer stability information.

APPENDIX A

Chemicals & Reagents

Name	CAS / Product code	Address [company name; town; country]
α Minimum Essential Medium	VXA1049001	Life Technologies Ltd, Paisley, UK
β glycerophosphate	154804-51-0	Sigma-Aldrich Company Ltd., Gillingham, UK
0.1% TritonX-100	9002-93-1	Sigma-Aldrich Company Ltd., Gillingham, UK
Agarose	A2576-5G	Sigma-Aldrich Company Ltd., Gillingham, UK
Albumin from human serum	70024-90-7	Sigma-Aldrich Company Ltd., Gillingham, UK
Alizarin red S	130-22-3	Sigma-Aldrich Company Ltd., Gillingham, UK
Ammonium hydroxide 0.5 M	1310-73-2	Sigma-Aldrich Company Ltd., Gillingham, UK
Ascorbate-2-phosphate	50-81-7	Sigma-Aldrich Company Ltd., Gillingham, UK
Bicinchoninic acid	23335	Fisher Scientific, Loughborough, UK
BMP-2 ELISA	DBP200	Fisher Scientific, Loughborough, UK
CMC	C5013-500G	Sigma-Aldrich Company Ltd., Gillingham, UK
Dexamethasone	50-02-2	Sigma-Aldrich Company Ltd., Gillingham, UK
Dichloromethane	75-09-2	Fisher Scientific, Loughborough, UK
Dimethylsulphoxide	67-68-5	Sigma-Aldrich Company Ltd., Gillingham, UK
DL-lactide	95-96-5	Lancaster Synthesis, Ward Hill, MA, USA
Dulbecco`s Modified Eagle Medium	VX42430025	Invitrogen, Paisley, UK
Fibrinogen	F8630	Sigma-Aldrich Company Ltd., Gillingham, UK
Foetal Bovine Serum	F9665	Sigma-Aldrich Company Ltd., Gillingham, UK
Glycolide	PURASORB PDL-45	Purac, Gorinchem, Netherlands
Hydrochloric acid 0.1 N	2104	Sigma-Aldrich Company Ltd., Gillingham, UK
L-glutamine	56-85-9	Sigma-Aldrich Company Ltd., Gillingham, UK
Lysozyme	L6876	Sigma-Aldrich Company Ltd., Gillingham, UK
Micrococcus lysodeikticus	M3770	Sigma-Aldrich Company Ltd., Gillingham, UK
Oil Red O	1320-06-5	Sigma-Aldrich Company Ltd., Gillingham, UK
PDGF	100-14B	PeproTech House, London, UK
Penicillin/Streptomycin	VX15070063	Fisher Scientific, Loughborough, UK
pNPP	N2770	Sigma-Aldrich Company Ltd., Gillingham, UK
Poly(DL-lactic-co-glycolic acid 50:50	5050 DLG 4.5A	Surmodics, Birmingham, USA
Poly(DL-lactic-co-glycolic acid 85:15	8515 DLG 4A	Surmodics, Birmingham, USA
Polyethylene glycol 1500	25322-68-3	Sigma-Aldrich Company Ltd., Gillingham, UK
PVA	9002-89-5	Sigma-Aldrich Company Ltd., Gillingham, UK
Sodium hydroxide	1310-73-2	Sigma-Aldrich Company Ltd., Gillingham, UK
Sodium lauryl sulphate	151-21-3	Sigma-Aldrich Company Ltd., Gillingham, UK
Thrombin	T4648	Sigma-Aldrich Company Ltd., Gillingham, UK
Tin (II) 2-ethylhexanoate	301-10-0	Sigma-Aldrich Company Ltd., Gillingham, UK
Tris buffer	N2770	Sigma-Aldrich Company Ltd., Gillingham, UK
Trypsin (0.25 \%)/EDTA (0.02 \%)	T4174	Sigma-Aldrich Company Ltd., Gillingham, UK
VEGF	450-32	PeproTech House, London, UK

Table A.1: Chemicals and reagents..

APPENDIX B

Instruments and Apparatus

Name	Model	Address [company name; town; country]
GPC instrument	PL-GPC 120	Agilent technologies, Waterside, UK
GPC column	PolarGel-M	Agilent technologies, Waterside, UK
NMR instrument	DPX-300 (400MHz)	Bruke, Coventry, UK
Filter unit	595-4520	Fisher Scientific, Loughborough, UK
MicroCT instrument	1174	Bruker-microCT, Kartuizersweg, Belgum
Homogeniser instrument	L5M	Silverson Machines Ltd., Waterside, UK
Particle sizer	LS230	Beckman Coulter, High Wycombe, UK
Plate reader	Infinite M200	Tecan UK Ltd., Reading, UK
PTFE beaker	30ml 215-0165	VWR International, Leicestershire, UK
Scanning electron microscope	6060LV	Jeol, Hertfordshire, UK
SEM stubs	G301	Agar, Stanstead, UK
SEM adhesive carbon tabs	G3347N	Agar, Stanstead, UK
SEM sputter coater	SCD030	Balzers, Iramali, Liechtenstein
Vortex instrument	SA8	Stuart equipment, Stone, UK

Table B.1: Instruments and apparatus.

Appendix C

Protein Release Comparison

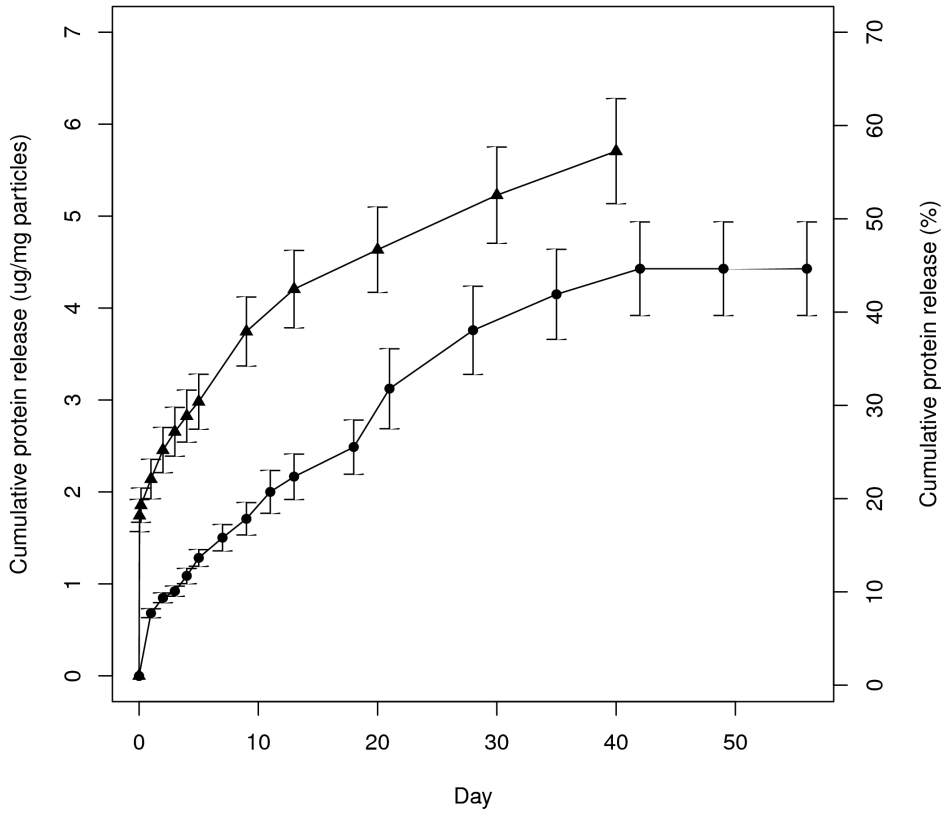

Figure C.1: Comparison of protein release from microparticles in the 22–26 µm (▲) and 70-100 µm (●) size ranges formulated form PLGA 50:50 (10 % *w/w* PLGA-PEG-PLGA). Both microparticle batches contain BMP-2 and HSA (1:9) loaded into the microparticles at 1 % *w/w*. Total protein release was assessed. The release of protein from 22–26 µm (▲) microparticles was carried out by Helen Cox. The different microparticles release protein for a similar length of time although a greater burst release if seen from the smaller microparticles. Error bars show ± cumulative standard deviation of the mean; n=3.

APPENDIX D

Agarose-gelatin Conjugate

D.1 Agarose-gelatin Conjugate Fabrication

A conjugate of agarose and gelatin was fabricated utilising a 1,1-carbonyldiimidazole (CDI) crosslinker (Figure E.1).A protocol was developed based on a published method [218].

Low melting point agarose (*A2576, Sigma Aldrich*) (0.2 g) was dissolved in DMSO (5 ml), this was combined with 2 ml of DMSO containing CDI crosslinker (*115533, Aldrich*) (1.3 or 32.7 mM). This caused the CDI to activate the agarose hydroxyl groups. Gelatin (*G1890, Sigma*) (0.2 g) in 3 ml DMSO was added and the reaction allowed to proceed for 12 hours at room temperature. The conjugate was then dialysed against deionised water to remove the DMSO. The resultant hydrogel was washed with bicarbonate buffer (0.1 M, *pH* 8.5). This removed remaining imidazolyl carbamate. The hydrogel was washed finally with more deionised water then lyophilised for storage.

The hydrogel was prepared for use by dissolving the agarose-gelatin in phosphate buffered saline to produce a 1 % *w/v* solution. This was carried out at 80 °C. This solution was pipetted into a 6-well plate (500 µl/well) or a 96-well plate (37 µl/well). There was a 10 minute window before gelation took place at room temperature, this is when microparticles could be added. The gel was sterilised under ultraviolet light for 20 minutes.

Protein assays were ineffective at assessing gelatin incorporation due to interference from the agarose. Gelatin incorporation was assessed based on yields. The assumption was made that 100 % agarose recovery occurred and any mass increase was due to gelatin.

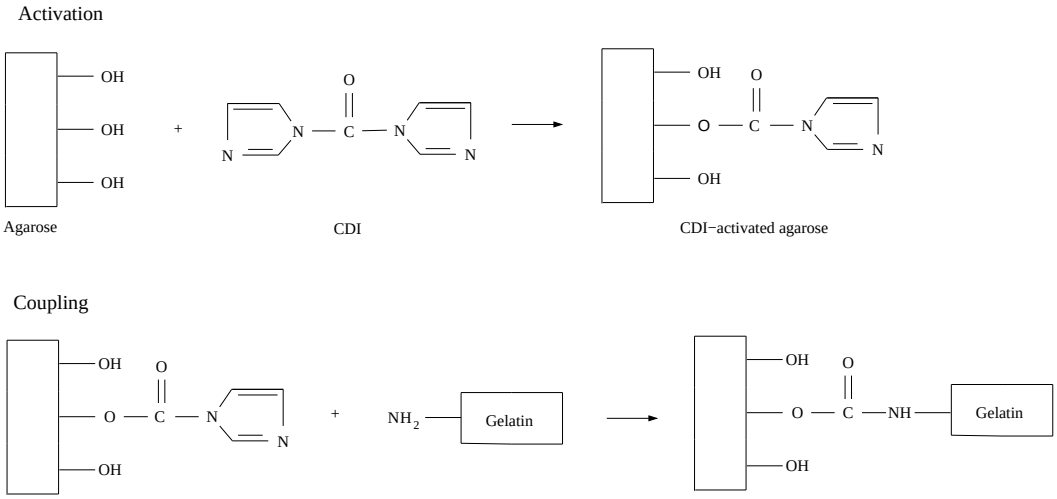

Figure D.1: Schematic showing the covalent coupling of gelatin to agarose through the activation of agarose hydroxyl groups with CDI.

D.2 Cell Quantification

The number of metabolically active cells was determined using the CellTiter 96® kit (*Promega*). This kit utilises a novel MTS[1] reagent that is reduced by dehydrogenase enzymes (found in metabolically active cells). This forms (in the presence of phenazine methosulfate, PMS) a soluble formazan product that can be photometrically quantified. The MTS kit was selected in preference to the more traditional MTT assay due to ease of use and also the flexibility. If necessary cell culture plates can be further incubated after photometric measurement and the cells remain metabolically active (unlike the MTT assay).

Reconstituted MTS working reagent (20 µl) was added to each well of a 96-well tissue culture plate containing cells and culture media (100 µl). This plate was then incubated in a cell culture incubator for the appropriate period of time and read photometrically at 490 nm.

Different cell types metabolise MTS at different rates so to ensure suitable resolution and accuracy of data is was essential to assess the response of MC3T3-E1 cells at known densities for different incubation periods. These results favoured a long incubation period of 260 minutes (Figure D.2).

[1] 3-(4,5-dimethylthiazol-2-yl)-5-(3-carboxymethoxyphenyl)-2-(4-sulfophenyl)-2H-tetrazolium

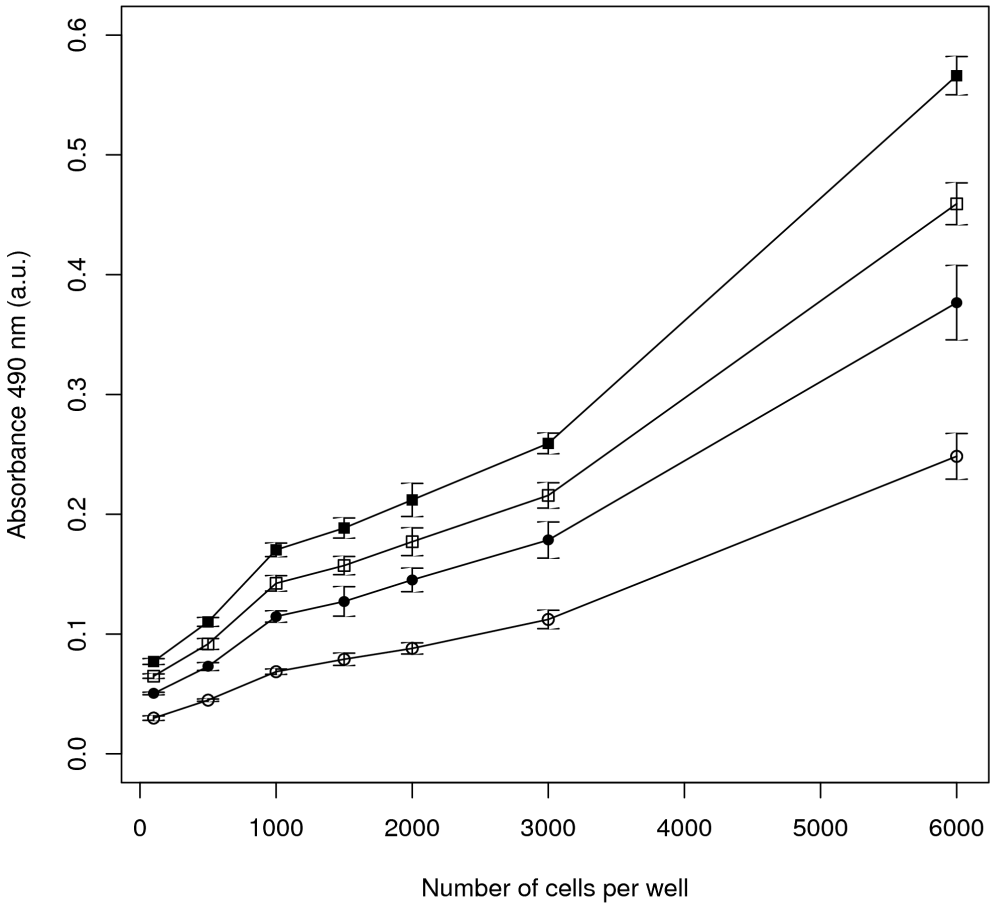

Figure D.2: Calibration plot to ascertain how long to incubate MC3T3-E1 cells with MTS working reagent. Working reagent as incubated for 80 minutes (○), 140 minutes (●), 200 minutes (□) and 260 minutes (■). The longest incubation (260 minutes ■) gave the greatest difference in absorbency in response to different cell densities with no indication of a saturation plateau. This time period was selected for further quantitative assessments.

D.3 Conjugate Biocompatibility

An agarose-gelatin conjugate was fabricated using two different cross-linker concentrations (1.3 and 32.7 mM) to produce a different amount of gelatin incorporation. Gelatin incorporation was found to be 12 % and 28 % respectively. This was close to the published values.

The gelation of these gels was assessed and the characteristics were found to be similar to those of non-functionalised agarose. The gels were suitable for micro-injection of microparticles.

Cell compatibility and proliferation was assessed on these agarose-gelatin hydrogels. Suitable control groups were selected. Experimental groups are detailed (Table D.1).

Numerical Identification	Description
1	Cell culture treated tissue culture plastic
2	Non treated tissue culture plastic
3	Agarose hydrogel
4	Physical mixture of agarose and gelatin (50:50)
5	Physical mixture of agarose and gelatin (80:20)
6	Agarose-gelatin conjugate (88:12)
7	Agarose-gelatin conjugate (72:28)

Table D.1: Experimental groups to assess the biocompatibility of various hydrogels with MC3T3-E1 cells.

The aim was to compare the biocompatibility of of the agarose-gelatin conjugate versus a physical mixture of agarose and gelatin. In addition this experiment would determine whether the different levels of gelatin incorporation affect cell proliferation/metabolic activity.

Cells were cultured on different substrates (Table D.1) and imaged after 48 hours in culture (Figure D.3). On tissue culture plastic (Figure D.3, Row 1) the cells are difficult to see because they become flat on the favourable surface. In contrast, non tissue culture treated plastic causes the cells to be more visible (Figure D.3, Row 2). Agarose hydrogel or physical mixtures of agarose and gelatin were highly unfavourable to cell attachment (Figure D.3, Rows 3–5). This highlights the initial problem. These gels have excellent gelation and physical characteristics meaning that they are good substrates for the positioning of microparticles *but* they are incompatible with mammalian cell culture.

Cell attachment and branching was exhibited by cells cultured on the agarose-gelatin

conjugate with the higher amount of gelatin incorporation (Figure D.3 Row 7). This indicates that this gel is both compatible with micro-injection and cell attachment.

Metabolic activity of these cultures was assessed at 72 hours using an MTS assay to determine the effect of the gels on proliferation and metabolic activity of MC3T3-E1 cells (Figure D.4). Cells cultured on tissue culture treated and non-tissue culture treated plastic (Groups 1 & 2) exhibited the greatest metabolic activity and optical microscopy confirmed a high number of cells. Cells cultured on agarose and agarose mixed with gelatin (Groups 3–5) showed very little difference to the expected metabolic activity upon seeding. The same was true for agarose cross-linked with only 12 % gelatin (Group 6). Agarose cross-linked with 28 % gelatin (Group 7) showed significantly higher ($p<0.005$) metabolic activity than all other gels assessed. This indicated that cells were proliferating and metabolically active. Optical microscopy images confirmed an increase in cell number.

This indicated that agarose cross-linked with 28 % gelatin is a potential candidate as a cyto-compatible substrate for microparticle patterning and diffusion studies.

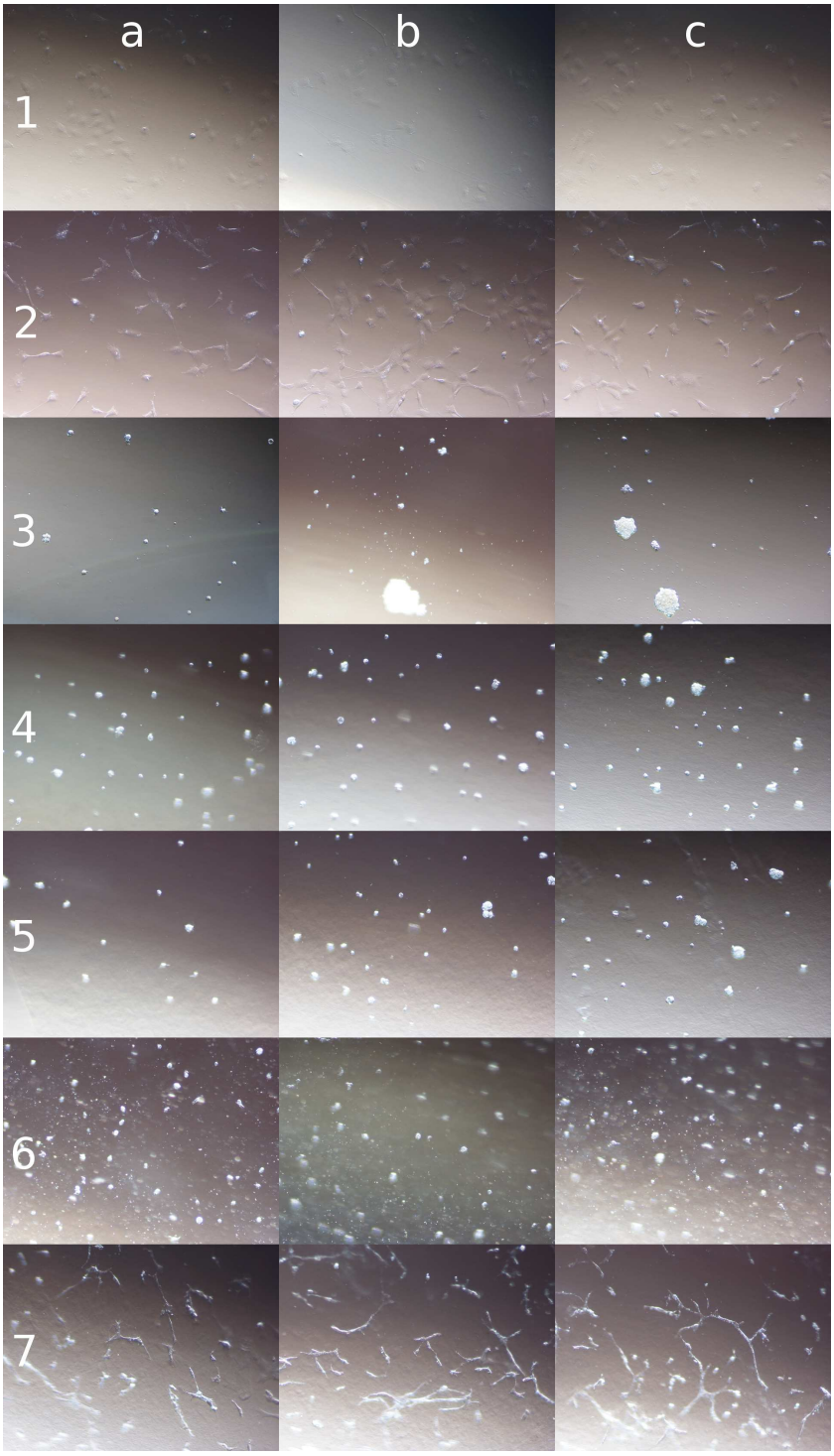

Figure D.3: Phase contrast optical microscopy images of MC3T3-E1 cells cultured on different substrates for 48 hours. Columns (a, b & c) show replicate images of representative sections, rows (1–7) correspond to experimental conditions (Table D.1, Page 129). The conjugate with a higher level of gelatin incorporation (Row 7) indicates cell anchorage and spreading. In contrast, agarose alone or physical mixtures of agarose and gelatin (Rows 3–5) show poor cell attachment and in the case of agarose (Row 3) the cells begin to aggregate.

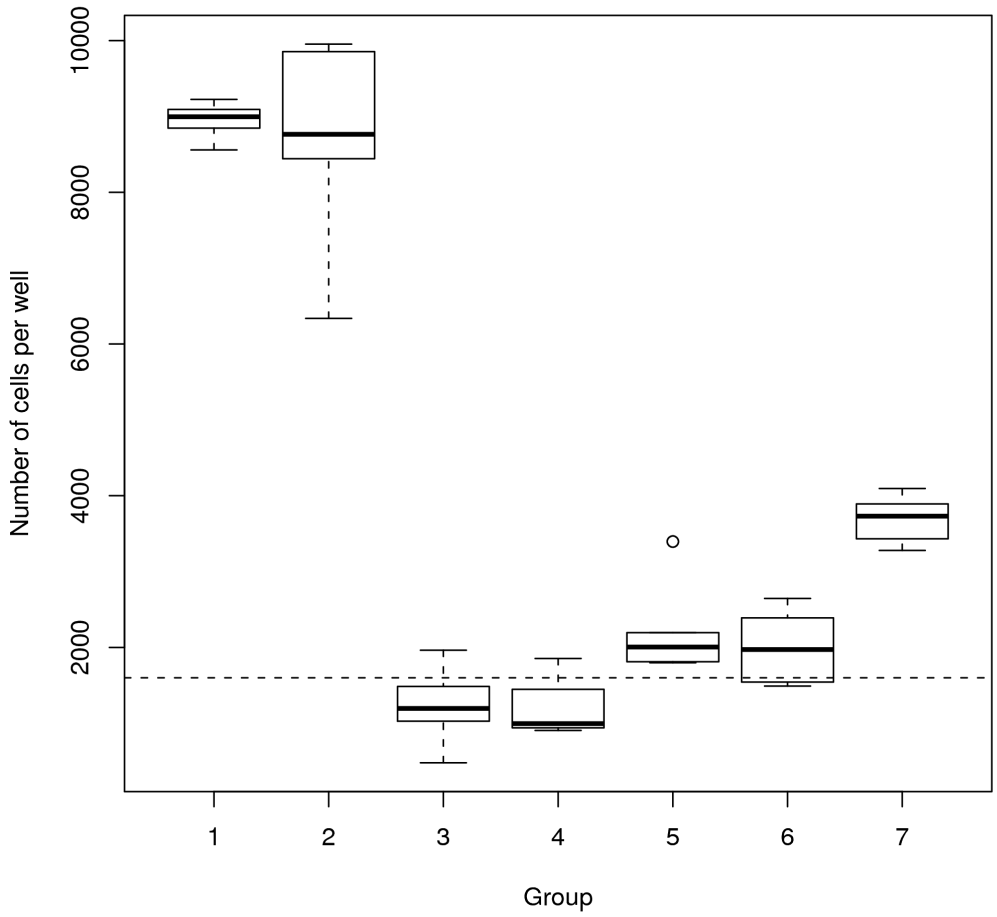

Figure D.4: Cell number assessed using a metabolic activity assay. MC3T3-E1 cells were cultured on different substrates (Table D.1) and assessed after 3 days in culture. The dashed line indicates the seeding density of cells. Activity was normalised to cell number based on initial calibration studies. Agarose crosslinked with 28 % gelatin (Group 7) appears significantly more favourable to cellular proliferation than physical mixtures of the gels although not at favourable as tissue culture plastics.

APPENDIX E

Para-nitrophenol Calibration

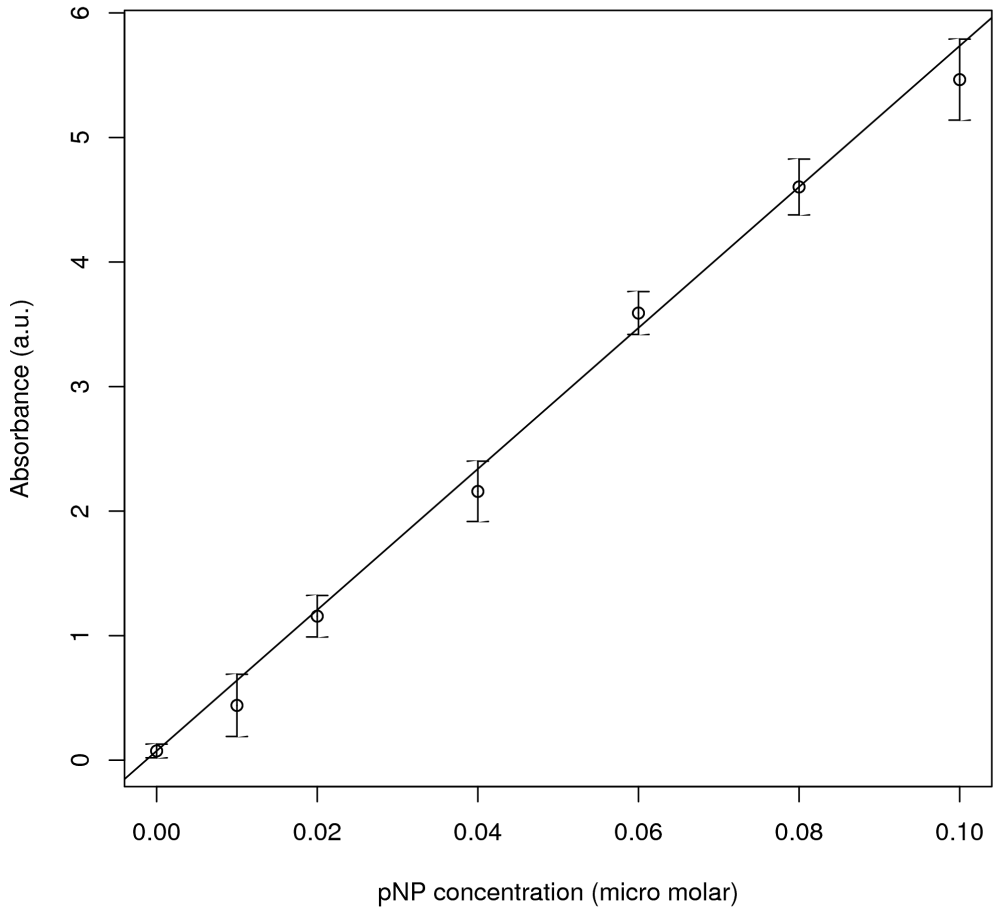

Figure E.1: Known concentrations of para-nitrophenol (*CAS: 100-02-7, Sigma*) were assessed photometrically to produce this calibration plot. The equation of this trend-line (least squares) was then used to convert absorbance values into concentrations of para-nitrophenol.

APPENDIX F

Statistical Results of ALP Expression for Section 3.4.2

Comparison	p-value
Day 10	
1.mp.low - 2.mp.high	0.00000000002142
1.mp.low - 3.mp.osteogenic	0.5787
1.mp.low - 4.control	0.01081
2.mp.high - 3.osteogenic	0.0000000000000002283
2.mp.high - 4.control	0.0000000000000002200
3.osteogenic - 4.control	0.0009948
Day 17	
1.mp.low - 2.mp.high	0.001205
1.mp.low - 3.mp.osteogenic	0.001684
1.mp.low - 4.control	0.01997
2.mp.high - 3.osteogenic	0.1499
2.mp.high - 4.control	0.00003789
3.osteogenic - 4.control	0.00001391
Day 24	
1.mp.low - 2.mp.high	0.01273
1.mp.low - 3.mp.osteogenic	0.00007766
1.mp.low - 4.control	0.8840
2.mp.high - 3.osteogenic	0.4417
2.mp.high - 4.control	0.01787
3.osteogenic - 4.control	0.007858

Table F.1: Statistical significance values from a Welch t-test comparing alkaline phosphatase expression from MC3T3 cells subjected to different environments at three time points. This data was discussed in section 3.4.2 on page 84.

References

[1] R Langer and JP Vacanti. Tissue engineering. *Science*, 260 (5110):920–926, 1993. doi: 10.1126/science.8493529. URL `http://www.sciencemag.org/content/260/5110/920.abstract`.

[2] H.H. Bayraktar, E.F. Morgan, G.L. Niebur, G.E. Morris, E.K. Wong, and T.M. Keaveny. Comparison of the elastic and yield properties of human femoral trabecular and cortical bone tissue. *Journal of biomechanics*, 37(1):27–35, 2004.

[3] A.E. Aubert, F. Beckers, B. Verheyden, et al. Cardiovascular function and basics of physiology in microgravity. *Acta cardiologica*, 60(2):129, 2005.

[4] R.K. Aaron, D.M.K. Ciombor, and B.J. Simon. Treatment of nonunions with electric and electromagnetic fields. *Clinical orthopaedics and related research*, 419: 21, 2004.

[5] X.L. Griffin, M.L. Costa, N. Parsons, and N. Smith. Electromagnetic field stimulation for treating delayed union or non-union of long bone fractures in adults. *status and date: New, published in*, (4), 2011.

[6] L.S. Phieffer and J.A. Goulet. Delayed unions of the tibia. *The Journal of Bone and Joint Surgery (American)*, 88(1):205–216, 2006.

[7] M. Shin, H. Abukawa, M.J. Troulis, and J.P. Vacanti. Development of a biodegradable scaffold with interconnected pores by heat fusion and its application to bone tissue engineering. *Journal of Biomedical Materials Research Part A*, 84(3):702–709, 2008.

[8] J.C. Banwart, M.A. Asher, R.S. Hassanein, et al. Iliac crest bone graft harvest donor site morbidity. a statistical evaluation. *Spine*, 20(9):1055, 1995.

[9] V.J. Sammarco, L. Chang, et al. Modern issues in bone graft substitutes and advances in bone tissue technology. *Foot and ankle clinics*, 7(1):19, 2002.

[10] G.J. Haidukewych and D.J. Berry. Nonunion of fractures of the subtrochanteric region of the femur. *Clinical orthopaedics and related research*, 419:185, 2004.

[11] S.R. Winn, H. Uludag, and J.O. Hollinger. Sustained release emphasizing recombinant human bone morphogenetic protein-2. *Advanced drug delivery reviews*, 31(3):303–318, 1998.

[12] A. Stavropoulos. Deproteinized bovine bone xenograft. *Musculoskeletal Tissue regeneration*, pages 119–151, 2008.

[13] J.R. Jones, L.M. Ehrenfried, and L.L. Hench. Optimising bioactive glass scaffolds for bone tissue engineering. *Biomaterials*, 27(7):964–973, 2006.

[14] E. Schepers, M. Clercq, P. Ducheyne, and R. Kempeneers. Bioactive glass particulate material as a filler for bone lesions. *Journal of Oral Rehabilitation*, 18 (5):439–452, 1991.

[15] J. Borrelli Jr, W.D. Prickett, and W.M. Ricci. Treatment of nonunions and osseous defects with bone graft and calcium sulfate. *Clinical orthopaedics and related research*, 411:245, 2003.

[16] G. Daculsi. Biphasic calcium phosphate concept applied to artificial bone, implant coating and injectable bone substitute. *Biomaterials*, 19(16):1473–1478, 1998.

[17] D.W. Howie, M.A. McGee, S.A. Callary, A. Carbone, R.B. Stamenkov, W.J. Bruce, and D.M. Findlay. A preclinical study of stem subsidence and graft incorporation after femoral impaction grafting using porous hydroxyapatite as a bone graft extender. *The Journal of arthroplasty*, 2011.

[18] A.S. Greenwald. Biological performance of materials. fundamentals of biocompatibility. *The Journal of Bone and Joint Surgery (American)*, 83(6):970–970, 2001.

[19] EJ Blom, J. Klein-Nulend, C. Klein, K. Kurashina, MAJ Van Waas, and EH Burger. Transforming growth factor-β1 incorporated during setting in calcium phosphate cement stimulates bone cell differentiation in vitro. *Journal of biomedical materials research*, 50(1):67–74, 2000.

[20] J. Zhao, G. Shen, C. Liu, S. Wang, W. Zhang, X. Zhang, D. Ye, J. Wei, Z. Zhang, X. Jiang, et al. Enhanced healing of rat calvarial defects with sulfated chitosan-coated calcium-deficient hydroxyapatite/bone morphogenetic protein 2 scaffolds. *Tissue engineering. Part A*, 18(1-2):185, 2012.

[21] R. Cancedda, P. Giannoni, and M. Mastrogiacomo. A tissue engineering approach to bone repair in large animal models and in clinical practice. *Biomaterials*, 28(29):4240–4250, 2007.

[22] R. Jay, D. Aaron, A. Thomas, et al. The role of growth factors in the repair of bone biology and clinical applications. *The Journal of Bone and Joint Surgery (American)*, 84(6):1032–1044, 2002.

[23] J.M. Wozney. Overview of bone morphogenetic proteins. *Spine*, 27(16S):S2, 2002.

[24] X. Hao, E.A. Silva, A. Månsson-Broberg, K.H. Grinnemo, A.J. Siddiqui, G. Dellgren, E. Wärdell, L.Å. Brodin, D.J. Mooney, and C. Sylvén. Angiogenic effects of sequential release of vegf-a165 and pdgf-bb with alginate hydrogels after myocardial infarction. *Cardiovascular research*, 75(1):178–185, 2007.

[25] K. Gaengel, G. Genové, A. Armulik, and C. Betsholtz. Endothelial-mural cell signaling in vascular development and angiogenesis. *Arteriosclerosis, thrombosis, and vascular biology*, 29(5):630–638, 2009.

[26] R.H. Li and J.M. Wozney. Delivering on the promise of bone morphogenetic proteins. *Trends in biotechnology*, 19(7):255–265, 2001.

[27] M.R. Urist. Bone: formation by autoinduction. *Science*, 150(3698):893–899, 1965.

[28] J.M. Wozney, V. Rosen, et al. Bone morphogenetic protein and bone morphogenetic protein gene family in bone formation and repair. *Clinical orthopaedics and related research*, (346):26, 1998.

[29] M. Geiger, RH Li, and W. Friess. Collagen sponges for bone regeneration with rhbmp-2. *Advanced drug delivery reviews*, 55(12):1613–1629, 2003.

[30] B.S. Yoon and K.M. Lyons. Multiple functions of bmps in chondrogenesis. *Journal of cellular biochemistry*, 93(1):93–103, 2004.

[31] T. Holland and A. Mikos. Review: Biodegradable polymeric scaffolds. improvements in bone tissue engineering through controlled drug delivery. *Tissue Engineering I*, pages 161–185, 2006.

[32] E.A. Wang, V. Rosen, J.S. D'Alessandro, M. Bauduy, P. Cordes, T. Harada, D.I. Israel, R.M. Hewick, K.M. Kerns, and P. LaPan. Recombinant human bone morphogenetic protein induces bone formation. *Proceedings of the National Academy of Sciences*, 87(6):2220, 1990.

[33] D.W. Leung, G. Cachianes, W.J. Kuang, D.V. Goeddel, and N. Ferrara. Vascular endothelial growth factor is a secreted angiogenic mitogen. *Science*, 246(4935): 1306, 1989.

[34] P.J. Keck, S.D. Hauser, G. Krivi, K. Sanzo, T. Warren, J. Feder, and D.T. Connolly. Vascular permeability factor, an endothelial cell mitogen related to pdgf. *Science*, 246(4935):1309, 1989.

[35] N. Ferrara et al. Vegf and the quest for tumour angiogenesis factors. *Nature Reviews Cancer*, 2:795–803, 2002.

[36] J. Andrae, R. Gallini, and C. Betsholtz. Role of platelet-derived growth factors in physiology and medicine. *Genes & development*, 22(10):1276, 2008.

[37] C.H. Heldin and B. Westermark. Mechanism of action and in vivo role of platelet-derived growth factor. *Physiological reviews*, 79(4):1283–1316, 1999.

[38] H. Seppä, G. Grotendorst, S. Seppä, E. Schiffmann, and G.R. Martin. Platelet-derived growth factor in chemotactic for fibroblasts. *The Journal of cell biology*, 92 (2):584–588, 1982.

[39] P. Shah, L. Keppler, and J. Rutkowski. A review of platelet derived growth factor playing pivotal role in bone regeneration. *Journal of Oral Implantology*, 2012.

[40] A. Banfi, G. von Degenfeld, R. Gianni-Barrera, S. Reginato, M.J. Merchant, D.M. McDonald, and H.M. Blau. Therapeutic angiogenesis due to balanced single-vector delivery of vegf and pdgf-bb. *The FASEB Journal*, 26(6):2486–2497, 2012.

[41] T.J. Wieman. Clinical efficacy of becaplermin (rhpdgf-bb) gel. *The American journal of surgery*, 176(2):74S–79S, 1998.

[42] O. Ghatnekar, U. Persson, M. Willis, and K. Odegaard. Cost effectiveness of becaplermin in the treatment of diabetic foot ulcers in four european countries. *Pharmacoeconomics*, 19(7):767–778, 2001.

[43] E.N. Mostow, G.D. Haraway, M. Dalsing, J.P. Hodde, and D. King. Effectiveness of an extracellular matrix graft (oasis wound matrix) in the treatment of chronic leg ulcers: a randomized clinical trial. *Journal of vascular surgery*, 41(5):837–843, 2005.

[44] J.A. Niezgoda, C.C. Van Gils, R.G. Frykberg, J.P. Hodde, et al. Randomized clinical trial comparing oasis wound matrix to regranex gel for diabetic ulcers. *Advances in skin & wound care*, 18(5):258, 2005.

[45] M.C. Gupta and S. Maitra. Bone grafts and bone morphogenetic proteins in spine fusion. *Cell and Tissue Banking*, 3(4):255–267, 2002.

[46] B. McKay and H.S. Sandhu. Use of recombinant human bone morphogenetic protein-2 in spinal fusion applications. *Spine*, 27(16S):S66, 2002.

[47] ME Bill McKay, S. Peckham, and J. Scifert. Biologics to promote spinal fusion. *Spine technology handbook*, page 241, 2006.

[48] J.K. Burkus, M.F. Gornet, C.A. Dickman, and T.A. Zdeblick. Anterior lumbar interbody fusion using rhbmp-2 with tapered interbody cages. *Journal of spinal disorders & techniques*, 15(5):337, 2002.

[49] E.J. Carragee, E.L. Hurwitz, and B.K. Weiner. A critical review of recombinant human bone morphogenetic protein-2 trials in spinal surgery: emerging safety concerns and lessons learned. *The Spine Journal*, 11(6):471–491, 2011.

[50] S.D. Boden, T.A. Zdeblick, H.S. Sandhu, and S.E. Heim. The use of rhbmp-2 in interbody fusion cages: definitive evidence of osteoinduction in humans: a preliminary report. *Spine*, 25(3):376, 2000.

[51] S.D. Boden, J. Kang, H. Sandhu, and J.G. Heller. Use of recombinant human bone morphogenetic protein-2 to achieve posterolateral lumbar spine fusion in humans: A prospective, randomized clinical pilot trial 2002 volvo award in clinical studies. *Spine*, 27(23):2662, 2002.

[52] G.J. Martin Jr, S.D. Boden, MA Marone, P.A. Moskovitz, et al. Posterolateral intertransverse process spinal arthrodesis with rhbmp-2 in a nonhuman primate: important lessons learned regarding dose, carrier, and safety. *Journal of spinal disorders*, 12(3):179, 1999.

[53] A.R. Poynton and J.M. Lane. Safety profile for the clinical use of bone morphogenetic proteins in the spine. *Spine*, 27(16S):S40, 2002.

[54] G.R. Buttermann. Prospective nonrandomized comparison of an allograft with bone morphogenic protein versus an iliac-crest autograft in anterior cervical discectomy and fusion. *The Spine Journal*, 8(3):426–435, 2008.

[55] B. Perri, M. Cooper, C. Lauryssen, and N. Anand. Adverse swelling associated with use of rh-bmp-2 in anterior cervical discectomy and fusion: a case study. *The Spine Journal*, 7(2):235–239, 2007.

[56] MP Lutolf and JA Hubbell. Synthetic biomaterials as instructive extracellular microenvironments for morphogenesis in tissue engineering. *Nature biotechnology*, 23(1):47–55, 2005.

[57] D.O. Freytes, L.Q. Wan, and G. Vunjak-Novakovic. Geometry and force control of cell function. *Journal of cellular biochemistry*, 108(5):1047–1058, 2009.

[58] N. Li Jeon, H. Baskaran, S.K.W. Dertinger, G.M. Whitesides, L. Van De Water, and M. Toner. Neutrophil chemotaxis in linear and complex gradients of interleukin-8 formed in a microfabricated device. *Nature biotechnology*, 20(8):826–830, 2002.

[59] A. Shamloo, N. Ma, M. Poo, L.L. Sohn, and S.C. Heilshorn. Endothelial cell polarization and chemotaxis in a microfluidic device. *Lab Chip*, 8(8):1292–1299, 2008.

[60] B.G. Chung, L.A. Flanagan, S.W. Rhee, P.H. Schwartz, A.P. Lee, E.S. Monuki, and N.L. Jeon. Human neural stem cell growth and differentiation in a gradient-generating microfluidic device. *Lab Chip*, 5(4):401–406, 2005.

[61] J. Pihl, J. Sinclair, E. Sahlin, M. Karlsson, F. Petterson, J. Olofsson, and O. Orwar. Microfluidic gradient-generating device for pharmacological profiling. *Analytical chemistry*, 77(13):3897–3903, 2005.

[62] A. Khademhosseini, R. Langer, J. Borenstein, and J.P. Vacanti. Microscale technologies for tissue engineering and biology. *Proceedings of the National Academy of Sciences of the United States of America*, 103(8):2480–2487, 2006.

[63] J.B. Leach, K.A. Bivens, C.N. Collins, and C.E. Schmidt. Development of photocrosslinkable hyaluronic acid-polyethylene glycol-peptide composite hydrogels for soft tissue engineering. *Journal of Biomedical Materials Research Part A*, 70(1):74–82, 2004.

[64] E. Alsberg, KW Anderson, A. Albeiruti, RT Franceschi, and DJ Mooney. Cell-interactive alginate hydrogels for bone tissue engineering. *Journal of dental research*, 80(11):2025, 2001.

[65] S. Van Vlierberghe, P. Dubruel, and E. Schacht. Biopolymer-based hydrogels as scaffolds for tissue engineering applications: a review. *Biomacromolecules*, 2011.

[66] M. Qiao, D. Chen, X. Ma, and Y. Liu. Injectable biodegradable temperature-responsive plga–peg–plga copolymers: Synthesis and effect of copolymer composition on the drug release from the copolymer-based hydrogels. *International journal of pharmaceutics*, 294(1):103–112, 2005.

[67] S. Sant, M.J. Hancock, J.P. Donnelly, D. Iyer, and A. Khademhosseini. Biomimetic gradient hydrogels for tissue engineering. *The Canadian journal of chemical engineering*, 88(6):899–911, 2010.

[68] J.L. Patat and J.P. Ouhayoun. Use of a porous calcium carbonate based material as support of a growth factor in the preparation of a bioabsorbable implant, January 27 1998. US Patent 5,711,957.

[69] D. Neen, D. Noyes, M. Shaw, S. Gwilym, N. Fairlie, and N. Birch. Healos and bone marrow aspirate used for lumbar spine fusion: a case controlled study comparing healos with autograft. *Spine*, 31(18):E636, 2006.

[70] J.Z. Baskin, A. Vasanji, J. McMasters, Y. Soenjaya, A.M. Barbu, and S.J. Eppell. Nanophase bone substitute in vivo response to subcutaneous implantation. *Journal of Biomedical Materials Research Part A*, 2012.

[71] R.A. Miller, J.M. Brady, and D.E. Cutright. Degradation rates of oral resorbable implants (polylactates and polyglycolates): rate modification with changes in pla/pga copolymer ratios. *Journal of Biomedical Materials Research*, 11(5):711–719, 1977.

[72] K.A. Hing. Bioceramic bone graft substitutes: influence of porosity and chemistry. *International journal of applied ceramic technology*, 2(3):184–199, 2005.

[73] LM Mathieu, M.O. Montjovent, P.E. Bourban, D.P. Pioletti, and J.A.E. Månson. Bioresorbable composites prepared by supercritical fluid foaming. *Journal of Biomedical Materials Research Part A*, 75(1):89–97, 2005.

[74] H. Tai, M.L. Mather, D. Howard, W. Wang, L.J. White, J.A. Crowe, S.P. Morgan, A. Chandra, D.J. Williams, S.M. Howdle, et al. Control of pore size and structure of tissue engineering scaffolds produced by supercritical fluid processing. *Eur Cell Mater*, 14:64–77, 2007.

[75] I. Gibson, M.M. Savalani, C.X.F. Lam, R. Olkowski, A.K. Ekaputra, K.C. Tan, and D.W. Hutmacher. Towards a medium/high load-bearing scaffold fabrication system. *Tsinghua Science & Technology*, 14:13–19, 2009.

[76] J.C. Reichert, M.E. Wullschleger, A. Cipitria, J. Lienau, T.K. Cheng, M.A. Schütz, G.N. Duda, U. Nöth, J. Eulert, and D.W. Hutmacher. Custom-made composite scaffolds for segmental defect repair in long bones. *International Orthopaedics*, 35 (8):1229–1236, 2011.

[77] T. Ren, J. Ren, X. Jia, and K. Pan. The bone formation in vitro and mandibular defect repair using plga porous scaffolds. *Journal of Biomedical Materials Research Part A*, 74(4):562–569, 2005.

[78] S.L. Ishaug-Riley, G.M. Crane-Kruger, M.J. Yaszemski, and A.G. Mikos. Three-dimensional culture of rat calvarial osteoblasts in porous biodegradable polymers. *Biomaterials*, 19(15):1405–1412, 1998.

[79] R. Zhang and P.X. Ma. Poly (α-hydroxyl acids)/hydroxyapatite porous composites for bone-tissue engineering. i. preparation and morphology. 1999.

[80] K.S. Shakesheff, K.M. Aliasger. Porous matrix comprising cross-linked particles, 2010. US Patent 7,785,617.

[81] I. Zein, D.W. Hutmacher, K.C. Tan, and S.H. Teoh. Fused deposition modeling of novel scaffold architectures for tissue engineering applications. *Biomaterials*, 23 (4):1169–1185, 2002.

[82] M. E. Hoque, W. Y. San, F. Wei, S. Li, M. H. Huang, M. Vert, and D. W. Hutmacher. Processing of polycaprolactone and polycaprolactone-based copolymers into 3d scaffolds, and their cellular responses. *Tissue Engineering - Part A*, 15(10):3013–3024, 2009.

[83] Brian McKibbin. The biology of fracture healing in long bones. *The Journal of bone and joint surgery. British volume*, 60(2):150, 1978.

[84] Lutz Claes, Peter Augat, Gebhard Suger, and Hans-Joachim Wilke. Influence of size and stability of the osteotomy gap on the success of fracture healing. *Journal of orthopaedic research*, 15(4):577–584, 1997.

[85] Georg Matziolis, Jens Tuischer, Grit Kasper, Mark Thompson, Barbara Bartmeyer, Dörte Krocker, Carsten Perka, and Georg Duda. Simulation of cell differentiation in fracture healing: mechanically loaded composite scaffolds in a novel bioreactor system. *Tissue engineering*, 12(1):201–208, 2006.

[86] Peter Augat, Johannes Burger, Sandra Schorlemmer, Thomas Henke, Manfred Peraus, and Lutz Claes. Shear movement at the fracture site delays healing in a diaphyseal fracture model. *Journal of orthopaedic research*, 21(6):1011–1017, 2003.

[87] A. Battler, M. Scheinowitz, A. Bor, D. Hasdai, Z. Vered, E. Di Segni, N. Varda-Bloom, D. Nass, S. Engelberg, M. Eldar, et al. Intracoronary injection of basic fibroblast growth factor enhances angiogenesis in infarcted swine myocardium. *Journal of the American College of Cardiology*, 22(7):2001–2006, 1993.

[88] R.R. Chen and D.J. Mooney. Polymeric growth factor delivery strategies for tissue engineering. *Pharmaceutical research*, 20(8):1103–1112, 2003.

[89] H. Okada, H. Toguchi, et al. Biodegradable microspheres in drug delivery. *Critical reviews in therapeutic drug carrier systems*, 12(1):1, 1995.

[90] S. Li, M. Vert, et al. Biodegradation of aliphatic polyesters. *Degradable polymers: principles and applications*, pages 43–87, 1995.

[91] JM Schakenraad, MJ Hardonk, J. Feijen, I. Molenaar, and P. Nieuwenhuis. Enzymatic activity toward poly (l-lactic acid) implants. *Journal of biomedical materials research*, 24(5):529–545, 1990.

[92] L. Michlovská, L. Vojtová, L. Mravcová, S. Hermanová, J. Kučerík, and J. Jančář. Functionalization conditions of plga-peg-plga copolymer with itaconic anhydride. In *Macromolecular Symposia*, volume 295, pages 119–124. Wiley Online Library, 2010.

[93] R.A. Jain. The manufacturing techniques of various drug loaded biodegradable poly (lactide-co-glycolide)(plga) devices. *Biomaterials*, 21(23):2475–2490, 2000.

[94] D.F. Lazarous, M. Shou, M. Scheinowitz, E. Hodge, V. Thirumurti, A.N. Kitsiou, J.A. Stiber, A.D. Lobo, S. Hunsberger, E. Guetta, et al. Comparative effects of basic fibroblast growth factor and vascular endothelial growth factor on coronary collateral development and the arterial response to injury. *Circulation*, 94(5):1074–1082, 1996.

[95] D.F. Bowen-Pope, T.W. Malpass, D.M. Foster, and R. Ross. Platelet-derived growth factor in vivo: levels, activity, and rate of clearance. *Blood*, 64(2):458–469, 1984.

[96] O. Jeon, S.J. Song, S.W. Kang, A.J. Putnam, and B.S. Kim. Enhancement of ectopic bone formation by bone morphogenetic protein-2 released from a heparin-conjugated poly (l-lactic-co-glycolic acid) scaffold. *Biomaterials*, 28(17):2763–2771, 2007.

[97] B. Zhao, T. Katagiri, H. Toyoda, T. Takada, T. Yanai, T. Fukuda, U. Chung, T. Koike, K. Takaoka, and R. Kamijo. Heparin potentiates the in vivo ectopic bone formation induced by bone morphogenetic protein-2. *Journal of Biological Chemistry*, 281(32):23246–23253, 2006.

[98] VR Sinha and A. Trehan. Biodegradable microspheres for protein delivery. *Journal of Controlled Release*, 90(3):261–280, 2003.

[99] J.L. Cleland, R.S. Langer, American Chemical Society. Division of Biochemical Technology, and American Chemical Society. Meeting. *Formulation and delivery of proteins and peptides*. American Chemical Society Washington, DC, 1994.

[100] M. van de Weert, W.E. Hennink, and W. Jiskoot. Protein instability in poly (lactic-co-glycolic acid) microparticles. *Pharmaceutical research*, 17(10):1159–1167, 2000.

[101] G. Jiang, B.H. Woo, F. Kang, J. Singh, and P.P. DeLuca. Assessment of protein release kinetics, stability and protein polymer interaction of lysozyme encapsulated poly (d, l-lactide-co-glycolide) microspheres. *Journal of controlled release*, 79(1):137–145, 2002.

[102] M. van de Weert, J. Hoechstetter, W.E. Hennink, and D.J.A. Crommelin. The effect of a water/organic solvent interface on the structural stability of lysozyme. *Journal of controlled release*, 68(3):351–359, 2000.

[103] C. Pérez and K. Griebenow. Improved activity and stability of lysozyme at the water/ch2ci2 interface: enzyme unfolding and aggregation and its prevention by polyols. *Journal of Pharmacy and Pharmacology*, 53(9):1217–1226, 2001.

[104] C. Srinivasan, YK Katare, T. Muthukumaran, and AK Panda. Effect of additives on encapsulation efficiency, stability and bioactivity of entrapped lysozyme from biodegradable polymer particles. *Journal of microencapsulation*, 22(2):127–138, 2005.

[105] M. Morlock, H. Koll, G. Winter, and T. Kissel. Microencapsulation of rh-erythropoietin, using biodegradable poly (,-lactide-co-glycolide): protein stability and the effects of stabilizing excipients. *European journal of pharmaceutics and biopharmaceutics*, 43(1):29–36, 1997.

[106] J.M. Péan, M.C. Venier-Julienne, F. Boury, P. Menei, B. Denizot, and J.P. Benoit. Ngf release from poly (d, l-lactide-co-glycolide) microspheres. effect of some formulation parameters on encapsulated ngf stability. *Journal of controlled release*, 56(1):175–187, 1998.

[107] J.F. Carpenter, M.J. Pikal, B.S. Chang, and T.W. Randolph. Rational design of stable lyophilized protein formulations: some practical advice. *Pharmaceutical research*, 14(8):969–975, 1997.

[108] O.F.L. Johnson, J.L. Cleland, H.J. Lee, M. Charnis, E. Duenas, W. Jaworowicz, D. Shepard, A. Shahzamani, A.J.S. Jones, and S.D. Putney. A month–long effect

from a single injection of microencapsulated human growth hormone. *Nature medicine*, 2(7):795–799, 1996.

[109] K. Fu, AM Klibanov, and R. Langer. Protein stability in controlled-release systems. *Nature biotechnology*, 18(1):24–25, 2000.

[110] J. Kang and S.P. Schwendeman. Comparison of the effects of mg (oh) 2 and sucrose on the stability of bovine serum albumin encapsulated in injectable poly (,-lactide-co-glycolide) implants. *Biomaterials*, 23(1):239–245, 2002.

[111] G. Zhu, S.R. Mallery, and S.P. Schwendeman. Stabilization of proteins encapsulated in injectable poly (lactide-co-glycolide). *Nature biotechnology*, 18(1): 52–57, 2000.

[112] Y. Zhang, S. Zale, L. Sawyer, and H. Bernstein. Effects of metal salts on poly (dl-lactide-co-glycolide) polymer hydrolysis. *Journal of biomedical materials research*, 34(4):531–538, 1997.

[113] T.W. Randolph. Phase separation of excipients during lyophilization: effects on protein stability. *Journal of pharmaceutical sciences*, 86(11):1198–1203, 1997.

[114] M. Vert, J. Mauduit, and S. Li. Biodegradation of pla/ga polymers: increasing complexity. *Biomaterials*, 15(15):1209–1213, 1994.

[115] I. Grizzi, H. Garreau, S. Li, and M. Vert. Hydrolytic degradation of devices based on poly (dl-lactic acid) size-dependence. *Biomaterials*, 16(4):305–311, 1995.

[116] G. Spenlehauer, M. Vert, JP Benoit, and A. Boddaert. In vitro and in vivo degradation of poly (d, l lactide/glycolide) type microspheres made by solvent evaporation method. *Biomaterials*, 10(8):557–563, 1989.

[117] T. Morita, Y. Horikiri, H. Yamahara, T. Suzuki, and H. Yoshino. Formation and isolation of spherical fine protein microparticles through lyophilization of protein-poly (ethylene glycol) aqueous mixture. *Pharmaceutical research*, 17(11): 1367–1373, 2000.

[118] T. Morita, Y. Sakamura, Y. Horikiri, T. Suzuki, and H. Yoshino. Protein encapsulation into biodegradable microspheres by a novel s/o/w emulsion method using poly (ethylene glycol) as a protein micronization adjuvant. *Journal of controlled release*, 69(3):435–444, 2000.

[119] Y.Y. Yang, T.S. Chung, and N. Ping Ng. Morphology, drug distribution, and in vitro release profiles of biodegradable polymeric microspheres containing

protein fabricated by double-emulsion solvent extraction/evaporation method. *Biomaterials*, 22(3):231–241, 2001.

[120] R. Jalil and JR Nixon. Biodegradable poly (lactic acid) and poly (lactide-co-glycolide) microcapsules: problems associated with preparative techniques and release properties. *Journal of microencapsulation*, 7(3):297–325, 1990.

[121] D. Blanco and M.J. Alonso. Protein encapsulation and release from poly (lactide-co-glycolide) microspheres: effect of the protein and polymer properties and of the co-encapsulation of surfactants. *European journal of pharmaceutics and biopharmaceutics*, 45(3):285–294, 1998.

[122] H. Sah. Stabilization of proteins against methylene chloride/water interface-induced denaturation and aggregation. *Journal of controlled release*, 58(2):143–151, 1999.

[123] C. Pérez, P. De Jesús, and K. Griebenow. Preservation of lysozyme structure and function upon encapsulation and release from poly (lactic-co-glycolic) acid microspheres prepared by the water-in-oil-in-water method. *International journal of pharmaceutics*, 248(1):193–206, 2002.

[124] C. Thomasin, H. Nam-Trân, H.P. Merkle, and B. Gander. Drug microencapsulation by pla/plga coacervation in the light of thermodynamics. 1. overview and theoretical considerations. *Journal of pharmaceutical sciences*, 87(3):259–268, 1998.

[125] S. Takada, Y. Uda, H. Toguchi, and Y. Ogawa. Application of a spray drying technique in the production of trh-containing injectable sustained-release microparticles of biodegradable polymers. *PDA Journal of Pharmaceutical Science and Technology*, 49(4):180–184, 1995.

[126] BW Wagenaar and BW Müller. Piroxicam release from spray-dried biodegradable microspheres. *Biomaterials*, 15(1):49–54, 1994.

[127] Z. Yang, P. Birkenhauer, F. Julmy, D. Chickering, J.P. Ranieri, H.P. Merkle, T.F. Lüscher, and B. Gander. Sustained release of heparin from polymeric particles for inhibition of human vascular smooth muscle cell proliferation. *Journal of controlled release*, 60(2):269–277, 1999.

[128] S.K. Lopac, M.P. Torres, J.H. Wilson-Welder, M.J. Wannemuehler, and B. Narasimhan. Effect of polymer chemistry and fabrication method on protein release and stability from polyanhydride microspheres. *Journal of Biomedical Materials Research Part B: Applied Biomaterials*, 91(2):938–947, 2009.

[129] A.S. Determan, J.R. Graham, K.A. Pfeiffer, and B. Narasimhan. The role of microsphere fabrication methods on the stability and release kinetics of ovalbumin encapsulated in polyanhydride microspheres. *Journal of microencapsulation*, 23(8):832–843, 2006.

[130] K.A. Athanasiou, G.G. Niederauer, and C. Agrawal. Sterilization, toxicity, biocompatibility and clinical applications of polylactic acid/polyglycolic acid copolymers. *Biomaterials*, 17(2):93–102, 1996.

[131] IP Matthews, C. Gibson, and AH Samuel. Enhancement of the kinetics of the aeration of ethylene oxide sterilized polymers using microwave radiation. *Journal of biomedical materials research*, 23(2):143–156, 1989.

[132] L. Montanari, M. Costantini, E.C. Signoretti, L. Valvo, M. Santucci, M. Bartolomei, P. Fattibene, S. Onori, A. Faucitano, B. Conti, et al. Gamma irradiation effects on poly (dl-lactictide-co-glycolide) microspheres. *Journal of controlled release*, 56(1-3):219–229, 1998.

[133] S. Freitas, B. Rudolf, H.P. Merkle, and B. Gander. Flow-through ultrasonic emulsification combined with static micromixing for aseptic production of microspheres by solvent extraction. *European journal of pharmaceutics and biopharmaceutics*, 61(3):181–187, 2005.

[134] A.G. Hausberger, R.A. Kenley, and P.P. DeLuca. Gamma irradiation effects on molecular weight and in vitro degradation of poly (d, l-lactide-co-glycolide) microparticles. *Pharmaceutical research*, 12(6):851–856, 1995.

[135] M.M. Bradford et al. A rapid and sensitive method for the quantitation of microgram quantities of protein utilizing the principle of protein-dye binding. *Analytical biochemistry*, 72(1-2):248–254, 1976.

[136] PK Smith, R.I. Krohn, GT Hermanson, AK Mallia, FH Gartner, M.D. Provenzano, EK Fujimoto, NM Goeke, BJ Olson, and DC Klenk. Measurement of protein using bicinchoninic acid. *Analytical biochemistry*, 150(1):76–85, 1985.

[137] A. Giteau, M.C. Venier-Julienne, A. Aubert-Pouëssel, and J.P. Benoit. How to achieve sustained and complete protein release from plga-based microparticles? *International journal of pharmaceutics*, 350(1-2):14–26, 2008.

[138] R.L. Cleek, K.C. Ting, S. G Eskin, and A.G. Mikos. Microparticles of poly (dl-lactic-co-glycolic acid)/poly (ethylene glycol) blends for controlled drug delivery. *Journal of controlled release*, 48(2-3):259–268, 1997.

[139] T. Morita, Y. Horikiri, T. Suzuki, and H. Yoshino. Applicability of various amphiphilic polymers to the modification of protein release kinetics from biodegradable reservoir-type microspheres. *European journal of pharmaceutics and biopharmaceutics*, 51(1):45–53, 2001.

[140] S. Chen and J. Singh. Controlled release of growth hormone from thermosensitive triblock copolymer systems: In vitro and in vivo evaluation. *International journal of pharmaceutics*, 352(1-2):58–65, 2008.

[141] G.M. Zentner, R. Rathi, C. Shih, J.C. McRea, M.H. Seo, H. Oh, BG Rhee, J. Mestecky, Z. Moldoveanu, M. Morgan, et al. Biodegradable block copolymers for delivery of proteins and water-insoluble drugs. *Journal of controlled release*, 72 (1-3):203–215, 2001.

[142] S. Chen, R. Pieper, D.C. Webster, and J. Singh. Triblock copolymers: synthesis, characterization, and delivery of a model protein. *International journal of pharmaceutics*, 288(2):207–218, 2005.

[143] T. Kissel, YX Li, C. Volland, S. Görich, and R. Koneberg. Parenteral protein delivery systems using biodegradable polyesters of aba block structure, containing hydrophobic poly (lactide-co-glycolide) a blocks and hydrophilic poly (ethylene oxide) b blocks. *Journal of controlled release*, 39(2):315–326, 1996.

[144] J.L. Cleland and A.J.S. Jones. Stable formulations of recombinant human growth hormone and interferon-γ for microencapsulation in biodegradable mircospheres. *Pharmaceutical research*, 13(10):1464–1475, 1996.

[145] JM Pean, MC Venier-Julienne, R. Filmon, M. Sergent, R. Phan-Tan-Luu, and JP Benoit. Optimization of hsa and ngf encapsulation yields in plga microparticles. *International journal of pharmaceutics*, 166(1):105–115, 1998.

[146] D. Klose, F. Siepmann, K. Elkharraz, S. Krenzlin, and J. Siepmann. How porosity and size affect the drug release mechanisms from plga-based microparticles. *International journal of pharmaceutics*, 314(2):198–206, 2006.

[147] E. Bible, D. Chau, M.R. Alexander, J. Price, K.M. Shakesheff, and M. Modo. The support of neural stem cells transplanted into stroke-induced brain cavities by plga particles. *Biomaterials*, 30(16):2985–2994, 2009.

[148] E. Tarelli, A. Mire-Sluis, H.A. Tivnann, B. Bolgiano, D.T. Crane, C. Gee, X. Lemercinier, M.L. Athayde, N. Sutcliffe, P.H. Corran, et al. Recombinant

human albumin as a stabilizer for biological materials and for the preparation of international reference reagents. *Biologicals*, 26(4):331–346, 1998.

[149] A. Bonincontro, A. De Francesco, and G. Onori. Influence of ph on lysozyme conformation revealed by dielectric spectroscopy. *Colloids and Surfaces B: Biointerfaces*, 12(1):1–5, 1998.

[150] AJ Kirby. Hydrolysis and formation of esters of organic acids. *Comprehensive Chemical Kinetics*, 10:57–207, 1972.

[151] J. Simon, G. Carl, Y. Yang, V. Thomas, S.M. Dorsey, and A.W. Morgan. Cell interactions with biomaterials gradients and arrays. *Combinatorial Chemistry &# 38; High Throughput Screening*, 12(6):544–553, 2009.

[152] S. Chung, R. Sudo, V. Vickerman, I.K. Zervantonakis, and R.D. Kamm. Microfluidic platforms for studies of angiogenesis, cell migration, and cell–cell interactions. *Annals of biomedical engineering*, 38(3):1164–1177, 2010.

[153] V. Vickerman, J. Blundo, S. Chung, and R. Kamm. Design, fabrication and implementation of a novel multi-parameter control microfluidic platform for three-dimensional cell culture and real-time imaging. *Lab Chip*, 8(9):1468–1477, 2008.

[154] S. Chung, R. Sudo, P.J. Mack, C.R. Wan, V. Vickerman, and R.D. Kamm. Cell migration into scaffolds under co-culture conditions in a microfluidic platform. *Lab Chip*, 9(2):269–275, 2009.

[155] D. Odedra, L.L.Y. Chiu, M. Shoichet, and M. Radisic. Endothelial cells guided by immobilized gradients of vascular endothelial growth factor on porous collagen scaffolds. *Acta Biomaterialia*, 2011.

[156] J.E. Phillips, K.L. Burns, J.M. Le Doux, R.E. Guldberg, and A.J. García. Engineering graded tissue interfaces. *Proceedings of the National Academy of Sciences*, 105(34):12170, 2008.

[157] T.M. Keenan and A. Folch. Biomolecular gradients in cell culture systems. *Lab Chip*, 8(1):34–57, 2007.

[158] V.V. Abhyankar, M.A. Lokuta, A. Huttenlocher, and D.J. Beebe. Characterization of a membrane-based gradient generator for use in cell-signaling studies. *Lab Chip*, 6(3):389–393, 2006.

[159] C.T. Lo, D.J. Throckmorton, A.K. Singh, and A.E. Herr. Photopolymerized diffusion-defined polyacrylamide gradient gels for on-chip protein sizing. *Lab Chip*, 8(8):1273–1279, 2008.

[160] J. Atencia, J. Morrow, and L.E. Locascio. The microfluidic palette: A diffusive gradient generator with spatio-temporal control. *Lab Chip*, 9(18):2707–2714, 2009.

[161] X. Wang, E. Wenk, X. Zhang, L. Meinel, G. Vunjak-Novakovic, and D.L. Kaplan. Growth factor gradients via microsphere delivery in biopolymer scaffolds for osteochondral tissue engineering. *Journal of Controlled Release*, 134(2):81–90, 2009.

[162] M. Singh, C.P. Morris, R.J. Ellis, M.S. Detamore, and C. Berkland. Microsphere-based seamless scaffolds containing macroscopic gradients of encapsulated factors for tissue engineering. *Tissue Engineering Part C: Methods*, 14(4):299–309, 2008.

[163] Q. Hou, D. Chau, C. Pratoomsoot, P.J. Tighe, H.S. Dua, K.M. Shakesheff, and F.R.A.J. Rose. In situ gelling hydrogels incorporating microparticles as drug delivery carriers for regenerative medicine. *Journal of pharmaceutical sciences*, 97 (9):3972–3980, 2008.

[164] H. Sah. A new strategy to determine the actual protein content of poly (lactide-co-glycolide) microspheres. *Journal of pharmaceutical sciences*, 86(11):1315–1318, 1997.

[165] A. Fleming. On a remarkable bacteriolytic element found in tissues and secretions. *Proceedings of the Royal Society of London. Series B, Containing Papers of a Biological Character*, 93(653):306–317, 1922.

[166] JM Bezemer, R. Radersma, DW Grijpma, PJ Dijkstra, J. Feijen, and CA Van Blitterswijk. Zero-order release of lysozyme from poly (ethylene glycol)/poly (butylene terephthalate) matrices. *Journal of controlled release*, 64(1-3):179–192, 2000.

[167] J. Sohier, RE Haan, K. De Groot, and JM Bezemer. A novel method to obtain protein release from porous polymer scaffolds: emulsion coating. *Journal of controlled release*, 87(1-3):57–68, 2003.

[168] R. Ihaka and R. Gentleman. R: A language for data analysis and graphics. *Journal of computational and graphical statistics*, pages 299–314, 1996.

[169] R Development Core Team. *R: A Language and Environment for Statistical Computing*. R Foundation for Statistical Computing, Vienna, Austria, 2009. URL `http://www.R-project.org`. ISBN 3-900051-07-0.

[170] M. Lee, T.T. Chen, M.L. Iruela-Arispe, B.M. Wu, and J.C.Y. Dunn. Modulation of protein delivery from modular polymer scaffolds. *Biomaterials*, 28(10):1862–1870, 2007.

[171] J. Saif, T.M. Schwarz, D.Y.S. Chau, J. Henstock, P. Sami, S.F. Leicht, P.C. Hermann, S. Alcala, F. Mulero, K.M. Shakesheff, et al. Combination of injectable multiple growth factor–releasing scaffolds and cell therapy as an advanced modality to enhance tissue neovascularization. *Arteriosclerosis, thrombosis, and vascular biology*, 30(10):1897–1904, 2010.

[172] Z.S. Patel, M. Yamamoto, H. Ueda, Y. Tabata, and A.G. Mikos. Biodegradable gelatin microparticles as delivery systems for the controlled release of bone morphogenetic protein-2. *Acta biomaterialia*, 4(5):1126–1138, 2008.

[173] K. Langer, S. Balthasar, V. Vogel, N. Dinauer, H. Von Briesen, and D. Schubert. Optimization of the preparation process for human serum albumin (hsa) nanoparticles. *International journal of pharmaceutics*, 257(1):169–180, 2003.

[174] R.E. Canfield. The amino acid sequence of egg white lysozyme. *Journal of Biological Chemistry*, 238(8):2698–2707, 1963.

[175] LR Wetter and HF Deutsch. Immunological studies on egg white proteins. *Journal of Biological Chemistry*, 192(1):237–242, 1951.

[176] N. Ferrara, K.A. Houck, L.B. Jakeman, J. Winer, and D.W. Leung. The vascular endothelial growth factor family of polypeptides. *Journal of cellular biochemistry*, 47(3):211–218, 1991.

[177] Y.J. Park, Y.M. Lee, J.Y. Lee, Y.J. Seol, C.P. Chung, and S.J. Lee. Controlled release of platelet-derived growth factor-bb from chondroitin sulfate–chitosan sponge for guided bone regeneration. *Journal of controlled release*, 67(2):385–394, 2000.

[178] Evonik. Bioresorbable polymer tg and melting point data. `www.surmodicsbiomaterials.com/pdf/lakeshore-melting-point.pdf`.

[179] X.M. Lam, E.T. Duenas, A.L. Daugherty, N. Levin, and J.L. Cleland. Sustained release of recombinant human insulin-like growth factor-i for treatment of diabetes. *Journal of controlled release*, 67(2):281–292, 2000.

[180] J. Yang and J.L. Cleland. Factors affecting the in vitro release of recombinant human interferon-γ (rhifn-γ) from plga microspheres. *Journal of pharmaceutical sciences*, 86(8):908–914, 1997.

[181] RC Davies, A. Neuberger, and BM Wilson. The dependence of lysozyme activity on ph and ionic strength. *Biochimica et Biophysica Acta (BBA)-Enzymology*, 178(2): 294–305, 1969.

[182] S. Spinella-Jaegle, S. Roman-Roman, C. Faucheu, F.W. Dunn, S. Kawai, S. Gallea, V. Stiot, AM Blanchet, B. Courtois, R. Baron, et al. Opposite effects of bone morphogenetic protein-2 and transforming growth factor-[beta] 1 on osteoblast differentiation. *Bone*, 29(4):323–330, 2001.

[183] K. Hanada, J.E. Dennis, and A.I. Caplan. Stimulatory effects of basic fibroblast growth factor and bone morphogenetic protein-2 on osteogenic differentiation of rat bone marrow-derived mesenchymal stem cells. *Journal of bone and Mineral Research*, 12(10):1606–1614, 1997.

[184] T. Nakase, K. Takaoka, K. Masuhara, K. Shimizu, H. Yoshikawa, and T. Ochi. Interleukin-1 [beta] enhance and tumor necrosis factor-[alpha] inhibits bone morphogenetic protein-2-induced alkaline phosphatase activity in mc3t3-e1 osteoblastic cells. *Bone*, 21(1):17–21, 1997.

[185] G. Rawadi, B. Vayssière, F. Dunn, R. Baron, and S. Roman-Roman. Bmp-2 controls alkaline phosphatase expression and osteoblast mineralization by a wnt autocrine loop. *Journal of Bone and Mineral Research*, 18(10):1842–1853, 2003.

[186] B. Han, B. Tang, and M.E. Nimni. Quantitative and sensitive in vitro assay for osteoinductive activity of demineralized bone matrix. *Journal of orthopaedic research*, 21(4):648–654, 2003.

[187] T. Katagiri, A. Yamaguchi, M. Komaki, E. Abe, N. Takahashi, T. Ikeda, V. Rosen, J.M. Wozney, A. Fujisawa-Sehara, and T. Suda. Bone morphogenetic protein-2 converts the differentiation pathway of c2c12 myoblasts into the osteoblast lineage. *The Journal of cell biology*, 127(6):1755–1766, 1994.

[188] Jiongyu Ren, Keith A Blackwood, Amir Doustgani, Patrina P Poh, Roland Steck, Molly M Stevens, and Maria A Woodruff. Melt-electrospun polycaprolactone strontium-substituted bioactive glass scaffolds for bone regeneration. *Journal of Biomedical Materials Research Part A*, 2013.

[189] MPharm Andrew Olaye. *Differentiation of embryonic stem cells throughcontrolled release of growth factors from microspheres*. Univesity of Nottingham, 2006.

[190] A. Ravaglioli, A. Krajewski, GC Celotti, A. Piancastelli, B. Bacchini, L. Montanari,

G. Zama, and L. Piombi. Mineral evolution of bone. *Biomaterials*, 17(6):617–622, 1996.

[191] M.L.C. Anderson, W.J.A. Dhert, J.D. de Bruijn, R.A.J. Dalmeijer, H. Leenders, C.A. van Blitterswijk, and A.J. Verbout. Critical size defect in the goat's os ilium: A model to evaluate bone grafts and substitutes. *Clinical orthopaedics and related research*, 364:231, 1999.

[192] F.C. den Boer, P. Patka, F.C. Bakker, B.W. Wippermann, A. van Lingen, G.Q.M. Vink, K. Boshuizen, and H.J.T.M. Haarman. New segmental long bone defect model in sheep: Quantitative analysis of healing with dual energy x-ray absorptiometry. *Journal of orthopaedic research*, 17(5):654–660, 1999.

[193] E. Newman, AS Turner, and JD Wark. The potential of sheep for the study of osteopenia: current status and comparison with other animal models. *Bone*, 16 (4):S277–S284, 1995.

[194] A. Nafei, J. Kabel, A. Odgaard, F. Linde, and I. Hvid. Properties of growing trabecular ovine bone: part ii: architectural and mechanical properties. *Journal of Bone and Joint Surgery-British Volume*, 82(6):921, 2000.

[195] T.A. Einhorn. Clinically applied models of bone regeneration in tissue engineering research. *Clinical orthopaedics and related research*, 367:S59, 1999.

[196] L. Rimondini, N. Nicoli-Aldini, M. Fini, G. Guzzardella, M. Tschon, and R. Giardino. In vivo experimental study on bone regeneration in critical bone defects using an injectable biodegradable pla/pga copolymer. *Oral Surgery, Oral Medicine, Oral Pathology, Oral Radiology, and Endodontology*, 99(2):148–154, 2005.

[197] Z. Gugala and S. Gogolewski. Regeneration of segmental diaphyseal defects in sheep tibiae using resorbable polymeric membranes: a preliminary study. *Journal of orthopaedic trauma*, 13(3):187, 1999.

[198] R.W. Lindsey, Z. Gugala, E. Milne, M. Sun, F.H. Gannon, and L.L. Latta. The efficacy of cylindrical titanium mesh cage for the reconstruction of a critical-size canine segmental femoral diaphyseal defect. *Journal of orthopaedic research*, 24(7): 1438–1453, 2006.

[199] Z. Gugala, R.W. Lindsey, and S. Gogolewski. New approaches in the treatment of critical-size segmental defects in long bones. In *Macromolecular Symposia*, volume 253, pages 147–161. Wiley Online Library, 2007.

[200] B. Rai, S.H. Teoh, DW Hutmacher, T. Cao, and KH Ho. Novel pcl-based honeycomb scaffolds as drug delivery systems for rhbmp-2. *Biomaterials*, 26(17): 3739–3748, 2005.

[201] JJ Blaker, JE Gough, V. Maquet, I. Notingher, and AR Boccaccini. In vitro evaluation of novel bioactive composites based on bioglass®-filled polylactide foams for bone tissue engineering scaffolds. *Journal of Biomedical Materials Research Part A*, 67(4):1401–1411, 2003.

[202] V. Maquet, A.R. Boccaccini, L. Pravata, I. Notingher, and R. Jérôme. Porous poly (α-hydroxyacid)/bioglass® composite scaffolds for bone tissue engineering. i: preparation and in vitro characterisation. *Biomaterials*, 25(18):4185–4194, 2004.

[203] DW Hutmacher and S. Cool. Concepts of scaffold-based tissue engineeringâĂŤthe rationale to use solid free-form fabrication techniques. *Journal of cellular and molecular medicine*, 11(4):654–669, 2007.

[204] A.R. Boccaccini, J.A. Roelher, L.L. Hench, V. Maquet, and R. JérÇŠme. A composites approach to tissue engineering. In *26th Annual Conference on Composites, Advanced Ceramics, Materials, and Structures: B: Ceramic Engineering and Science Proceedings*, pages 805–816. Wiley Online Library, 2002.

[205] Y. Zhou, D.W. Hutmacher, S.L. Varawan, and T.M. Lim. In vitro bone engineering based on polycaprolactone and polycaprolactone–tricalcium phosphate composites. *Polymer international*, 56(3):333–342, 2007.

[206] B. Rai, S.H. Teoh, KH Ho, DW Hutmacher, T. Cao, F. Chen, and K. Yacob. The effect of rhbmp-2 on canine osteoblasts seeded onto 3d bioactive polycaprolactone scaffolds. *Biomaterials*, 25(24):5499–5506, 2004.

[207] S.H. Teoh, D.W. Hutmacher, K.C. Tan, K.F. Tam, and I. Zein. Methods for fabricating a filament for use in tissue engineering, May 4 2004. US Patent 6,730,252.

[208] H. Hosseinkhani, M. Hosseinkhani, A. Khademhosseini, and H. Kobayashi. Bone regeneration through controlled release of bone morphogenetic protein-2 from 3-d tissue engineered nano-scaffold. *Journal of controlled release*, 117(3):380–386, 2007.

[209] S. Young, Z.S. Patel, J.D. Kretlow, M.B. Murphy, P.M. Mountziaris, L.S. Baggett, H. Ueda, Y. Tabata, J.A. Jansen, M. Wong, et al. Dose effect of dual delivery of vascular endothelial growth factor and bone morphogenetic protein-2 on bone

regeneration in a rat critical-size defect model. *Tissue Engineering Part A*, 15(9): 2347–2362, 2009.

[210] H. Peng, V. Wright, A. Usas, B. Gearhart, H.C. Shen, J. Cummins, J. Huard, et al. Synergistic enhancement of bone formation and healing by stem cell-expressed vegf and bone morphogenetic protein-4. *Journal of Clinical Investigation*, 110(6): 751–760, 2002.

[211] H. Peng, A. Usas, A. Olshanski, A.M. Ho, B. Gearhart, G.M. Cooper, and J. Huard. Vegf improves, whereas sflt1 inhibits, bmp2-induced bone formation and bone healing through modulation of angiogenesis. *Journal of Bone and Mineral Research*, 20(11):2017–2027, 2005.

[212] F. Berthod, J. Symes, N. Tremblay, J.A. Medin, and F.A. Auger. Spontaneous fibroblast-derived pericyte recruitment in a human tissue-engineered angiogenesis model in vitro. *Journal of Cellular Physiology*, 227(5):2130–2137, 2012.

[213] WL Murphy, CA Simmons, D. Kaigler, and DJ Mooney. Bone regeneration via a mineral substrate and induced angiogenesis. *Journal of dental research*, 83(3): 204–210, 2004.

[214] JM Kanczler, RO Oreffo, et al. Osteogenesis and angiogenesis: the potential for engineering bone. *Eur Cell Mater*, 15(2):100–114, 2008.

[215] J. Kleinheinz, U. Stratmann, U. Joos, and H.P. Wiesmann. Vegf-activated angiogenesis during bone regeneration. *Journal of oral and maxillofacial surgery*, 63(9):1310–1316, 2005.

[216] F. Geiger, H. Bertram, I. Berger, H. Lorenz, O. Wall, C. Eckhardt, H.G. Simank, and W. Richter. Vascular endothelial growth factor gene-activated matrix (vegf165-gam) enhances osteogenesis and angiogenesis in large segmental bone defects. *Journal of Bone and Mineral Research*, 20(11):2028–2035, 2005.

[217] M. Lind et al. Growth factor stimulation of bone healing. effects on osteoblasts, osteomies, and implants fixation. *Acta Orthopaedica Scandinavica. Supplementum*, 283:2, 1998.

[218] S. Sakai, I. Hashimoto, and K. Kawakami. Synthesis of an agarose-gelatin conjugate for use as a tissue engineering scaffold. *Journal of bioscience and bioengineering*, 103(1):22–26, 2007.